AN ANALYSIS OF CATALOGED DECEMBER 2020 LANDSLIDES NEAR HAINES, ALASKA

By

Victoria A. Nelson, B.S.

A Thesis Submitted in Partial Fulfillment of the Requirements

For the Degree of

Master of Science

In

Geological Engineering

University of Alaska Fairbanks

May 2023

APPROVED:

Margaret Darrow, Committee Chair
De Anne Stevens, Committee Member
Shishay Kidanu, Committee Member
Margaret Darrow, Chair
Department of Civil, Geological, and Environmental Engineering
William Schnabel, Dean
College of Engineering and Mines
Richard Collins, Director
Graduate School

ABSTRACT

From November 30 to December 2, 2020, an atmospheric river event brought high winds, heavy precipitation, and unseasonably warm temperatures to Southeast Alaska. In a 48-hour period, weather stations located in the Haines, Alaska, area recorded record-breaking amounts of precipitation. This resulted in 160 landslides around the community, some of which cut off evacuation routes and access to the community's fuel supply, and caused power outages and evacuations. The largest of the landslides occurred along Beach Road on December 2, 2020; it destroyed or severely damaged four residences and killed two occupants. This report focuses on 58 of the landslides, chosen based on their proximity and impact to road corridors or private property. During field investigations in 2021 and 2022, I observed and described landslides, took *in situ* strength measurements, and sampled soils that I subsequently tested in the laboratory for engineering index properties such as soil classification, moisture content, and organic content. I mapped landslide extents and evidence of previous landslides using high-resolution lidar data. Using all of these data, I developed a landslide catalog of the 58 landslides, which contains information about location, impact on the road system in 2020, field observations, stratigraphy, laboratory test results, landslide classification, maps, and relevant photographs. Analysis of the collected data suggests that the most significant factor that contributed to the December 2020 landslides was the amount and intensity of precipitation. This precipitation exacerbated the preexisting condition of high slope angles in the surrounding area, and resulted in excess pore pressure in soil types that usually drain well. Anthropogenic factors, such as removal of vegetation and the toe of slopes, also likely played a role in the distribution of the landslides. Recommendations for further study based on results in this report are: 1) to date previous landslides in the study area to determine the frequency of these events; 2) to install additional weather stations in the Haines area for widespread real-time weather monitoring and studying effects of localized high precipitation and/or wind on landslide occurrence; and 3) to conduct additional strength testing on soil and bedrock within the failed areas.

TABLE OF CONTENTS

PAGE

LIST OF FIGURES

PAGE

LIST OF TABLES

PAGE

ACKNOWLEDGMENTS

I'd like to thank the residents of Haines, Alaska, specifically C. Buxton, J. Norton, T. Ganner, M. and M. Belize, R. White, A. Myren, and J. McDonough for their generosity of time and information. A special thanks to "The Fellowship" for their contributions as guides and as bear deterrents. Additional thanks to the Andriesen family for their kindness and internet connection. Thanks to T. Eckhoff, M. Larsen, and E. Stevens for creating and providing the data from ADOT&PF that became a major support for the landslide catalog. To Haines residents and business owners allowing us to access landslides on their private property, thank you. And finally, my thanks to M. Darrow, for reminding me to "never forget the water!"

This material is based upon work supported by the National Science Foundation (NSF) under Grant No. 2114015, and in fulfillment of FEMA Cooperating Technical Partners (CTP) Grant No. EMS-2021-CA-00013. Any opinions, findings, and conclusions or recommendations expressed in this material are those of the author and do not necessarily reflect the views of the NSF or FEMA.

DEDICATION

To my mother and father, for always believing in me, even when I didn't believe in myself.

To the community of Haines, Alaska, for their resilience in the face of disaster.

To D. Simmons and J. Larson. Rest in peace.

CHAPTER 1: INTRODUCTION

On November 30, 2020, a storm-force low pressure system moved into the Gulf of Alaska, bringing with it strong winds and heavy precipitation (Cravens, 2021). From November 30 to December 2, 2020, the system remained stationary over the region, causing record-breaking amounts of precipitation, as well as unseasonably warm temperatures. The storm event resulted in a disaster declaration by the State of Alaska (SOA, 2020). Haines, Alaska, was hit particularly hard by this storm. There were road washouts throughout the downtown area, with whole sections being undercut and washed away, as well as reports of holes half a meter or more in depth opening in the pavement (Haines Police Department, written comm., 2020). These washouts—as well as reports of standing water at least 15 cm deep—hindered emergency response and evacuation efforts for the duration of the storm and for several weeks afterward. More than 50 reported landslides along Lutak Road temporarily severed the community's connection to the Haines Ferry Terminal and to the community's main fuel storage area. Residents along Lutak Road and Lutak Spur were cut off from downtown Haines for two days, and 46 homes along the road lost power for up to five days (Clayton, 2020). Sand flows along Lutak Spur caused substantial property damage. The largest of the landslides occurred on North Riley Ridge on December 2, 2020, at 1:17 pm, severing Beach Road, destroying or severely damaging four residences, and resulting in the deaths of two residents (Darrow and others, 2022). Though not covered in this report, there were several landslides that impacted the Haines Highway and Mosquito Lake Road to the northwest of Haines, and Mud Bay Road to the southwest. Overall, the Alaska Department of Transportation and Public Facilities (ADOT&PF) reported 160 instances of landslides throughout the Haines Borough as a result of the December 2020 storm.

I initially took part in a research project funded by the National Science Foundation (NSF; Grant No. 2114015), which focused on understanding why the Beach Road Landslide (BRLS) occurred. I participated in field work conducted in June 2021 and July 2022. While the research was primarily focused on investigating the BRLS, the research team quickly learned that dozens of landslides all around the Haines area had a tremendous impact on the residents. Subsequent research for studying other affected areas, such as Lutak Road, was funded by FEMA for the Grant "Landslide Resiliency Project for Haines, Alaska" (CTP Grant No. EMS-2021-CA-00013). This grant was obtained by the Alaska Division of Geological & Geophysical Surveys (DGGS) in the immediate aftermath of the December 2020 storm event. Work conducted for this report is

also part of a thesis submitted by V. Nelson in partial fulfillment of requirements for a Master's of Science degree in Geological Engineering, from the University of Alaska Fairbanks.

My research question is: What factors contributed to the widespread landslides in December 2020? To help answer this, I observed and described landslides, took *in situ* strength measurements, and sampled soils that I subsequently tested in the laboratory for engineering index properties. Once back from the field, I mapped landslide features using high-resolution (1-m) lidar data. I used all of these data to develop a landslide catalog of the observed December 2020 landslides. In this thesis, I analyze these data to find commonalities in landslide occurrence, investigating factors such as soil type and depositional environment, slope angle, potential anthropogenic influences, and geomorphic evidence of previous landslide events.

Chapter 2 of this document details the regional geology of the Haines area, and discusses the climate and history of atmospheric rivers in Southeast Alaska. Chapter 3 discusses the methodology for the field investigations and the desktop analyses. Chapter 4 is the landslide catalog, which is a repository for field observations, laboratory results, landslide event classifications, and other relevant information about landslides occurring along Lutak Spur and Lutak Road, and near Piedad Road and Beach Road. The catalog will serve as a companion to a landslide inventory map of the Haines area (being developed separately). Chapter 5 is an analysis of the accrued data and observations with the goal of answering the research question. Chapter 6 contains conclusions and suggestions for future study.

Some of this research was previously presented at the 65th Annual Meeting of the Association of Environmental and Engineering Geologists (Nelson, 2022). Some of the data within this report with a focus on the BRLS was previously published by Darrow and others (2022).

CHAPTER 2: REGIONAL SETTING AND CLIMATE

The community of Haines is located between the Chilkoot and Chilkat River valleys, approximately 129 air kilometers northwest of Juneau, and 64 kilometers by road from the border between Alaska and British Columbia, Canada (fig. 1). The Haines area was originally inhabited by the Tlingit peoples. White settlers came to the area in the 1880s and 1890s as part of the Gold Rush, and the first U.S. military installation in Alaska—Fort William H. Seward—was established in Haines in 1904 (ADCRA, 2021). This part of Southeast Alaska is well-known for its fishing, canning, and timber industries (ADCRA, 2021). As of 2020, Haines and the surrounding communities within the Haines Borough (606,935.2 hectares) had a population of around 2,600 (United States Census Bureau, 2022).

BEDROCK GEOLOGY

Brew and Ford (1994) provide an overview of the tectonic and geologic character of the study area; unless otherwise noted, the contents of this paragraph are paraphrased from their publication. The Haines area is part of the Wrangellia terrane, consisting of Upper Paleozoic volcanic breccias, flows, and volcaniclastic rocks that are intruded locally by Late Paleozoic granitic rocks (Skolai Group). Permian limestone, pelitic rocks, chert, and argillite overlie the Paleozoic assemblage. There are several thousand meters of subaerial to pillowed massive tholeiitic basalts with intrusions of gabbro (as sills, dikes, and plutons), overlain by Upper Triassic limestone that grades into Upper Triassic argillaceous and calcareous rocks. Finally, the terrane is overlain by the Gravina overlap assemblage and the post-amalgamation Wrangell Lava. Davis and Plafker (1985) dated two Upper Triassic rock units—the Chilkat metabasalt and Nikolai greenstone—to determine the potential ages of the eruption events that generated those rock units. These authors concluded that the Chilkat metabasalts are part of a younger unit that represents a marine environment, while the Nikolai greenstone is an older, subaerial to restricted marine environment unit (Davis and Plafker, 1985).

There are three significant faults in the Haines area: the Chatham Strait fault, the Chilkat River fault, and the Lutak Inlet-Chilkoot River fault. All three of these faults are part of the Denali fault system, which extends from Southeast to Interior Alaska (Brothers and others, 2018). The Chatham Strait fault is a 400-km long strike-slip fault that demonstrated no significant signs of activity for the last 13,000 years (Brothers and others, 2018). The Chilkat River fault was active from at least the middle Tertiary to almost the present day, and is estimated to have 150 km of

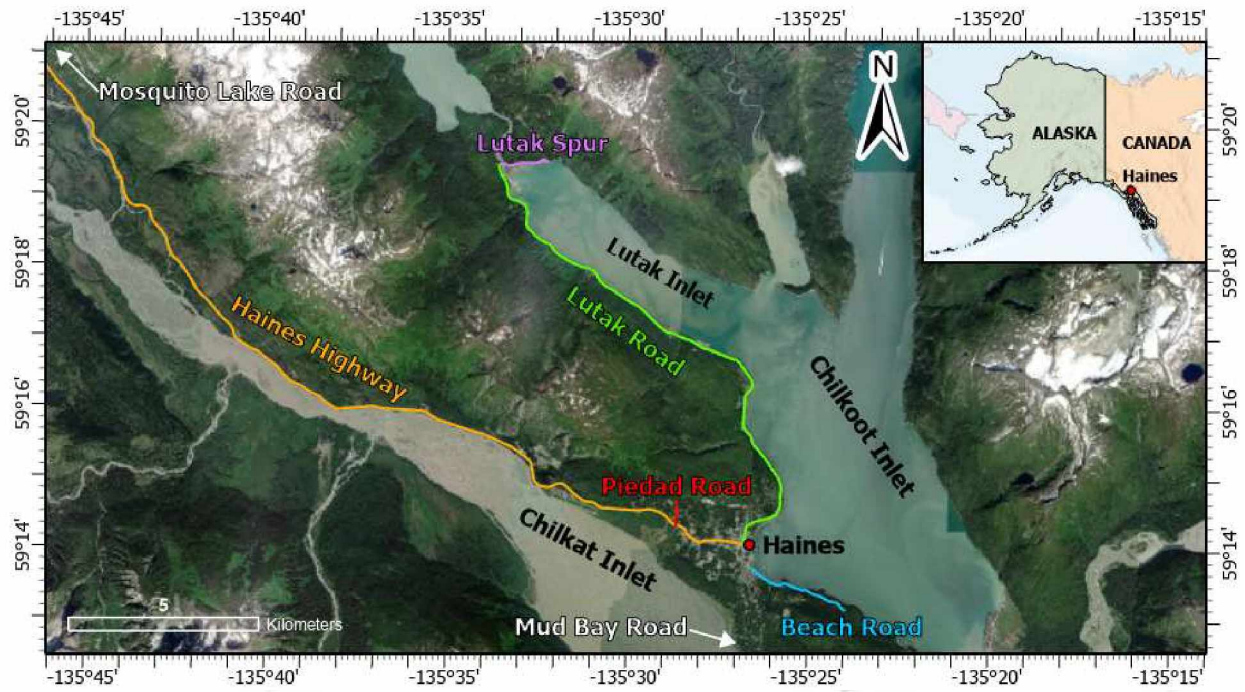

Figure 1. Location of the project area, including the community of Haines with roadways of interest (colored and labeled); map inset is the location of Haines relative to Alaska and Canada (map data from ADOT&PF, 2023; ADNR, 2020; State of Alaska Open Data Geoportal, accessed 2023).

right-lateral separation (Brew and Ford, 1994). Not much information is available on the activity of the Lutak Inlet-Chilkoot Inlet fault, but it is thought that only minor separation has occurred (Brew and Ford, 1994).

GLACIATION AND SURFICIAL GEOLOGY

During the Last Glacial Maximum (LGM), which occurred between 26,000 and 19,000 years ago (Lesnek and others, 2020), Chatham Strait and Lynn Canal were filled completely by a large valley glacier (Brothers and others, 2018). This valley glacier was likely a part of the Cordilleran Ice Sheet (CIS), which covered the majority of Southeast Alaska for thousands of years, reaching its maximum extent between 20,000 and 17,000 years ago (Lesnek and others, 2020). The CIS retreated from the Pacific coast in two pulses: one from 17,000 to 15,000 years ago, when it retreated through the fjords, and a second from 15,000 to 11,000 years ago, which left only localized ice caps (Lesnek and others, 2020; Baichtal and others, 2021). The retreat was enhanced by rising sea levels, which induced calving of the CIS, and a forebulge formed as a result of the weight of glaciers in the area (Baichtal and others, 2021). This forebulge collapsed around 12,000 years ago.

The effects of glaciation are still present in the area in the form of glacial isostatic adjustment (GIA), or the process of the Earth's crust rebounding after glacial melt. GIA has been variable in the area, since the growth and retreat of the CIS (Baichtal and others, 2021). The current uplift observed in the Haines area is a result of glacial advance and retreat during the Little Ice Age (LIA), a climate interval affecting localized areas around the world from the early 14th century into the 19th century (Jackson and Rafferty, 2023). GIA resulting from the retreat of LIA glaciers began around 1770 AD (±20 yrs), and the Haines area has risen 4-4.5 m since then (Larsen and others, 2005). Currently, the rate of uplift for the area is around 20 mm/year, as measured with a regional global positioning system (GPS) deformation array with sites across Southeast Alaska (Motyka and others, 2007). Glaciation is also the reason for the steep slopes in the study area (some as steep as 88°). It is natural for glaciers to create valleys and other landforms through erosion; after the glaciers retreat, these valley walls are too steep to remain stable for long periods (Evans and Clague, 1999).

There are several different types of surficial deposits present in the study area, including aeolian and fluvial deposits, beach and elevated shore deposits, and floodplain deposits (Lemke and Yehle, 1972). A few of the landslides with sources at elevations of approximately 130–250 m upslope along Lutak Road originated in areas mapped as diorite (Lemke and Yehle, 1972; Brew and Ford, 1994). The majority of the landslides within the extent of the Lemke and Yehle (1972) map occurred within colluvial deposits, elevated fine-grained marine deposits, and elevated shore and delta deposits. These units are largely composed of non-plastic silty gravel and sand (Lemke and Yehle, 1972).

CLIMATE IN SOUTHEAST ALASKA

The Haines Borough lies within the southeast marine climate zone (ADCRA, 2021). This zone experiences cool summers, mild winters, and heavy precipitation throughout the year (Lemke and Yehle, 1972). It lacks prolonged periods of freezing temperatures at low altitudes; however, freezing temperatures are prevalent at high altitudes, resulting in extensive snowpack development and glaciers. At the Haines Downtown Cooperative Observer Program (COOP) station (HAXA2, elev. 7.6 m), located near the boat harbor, the average annual temperature is 5.1°C, with a record high of 31.7°C and a record low of -24.4°C; the average annual total precipitation is approximately 157 cm, and the average annual snowfall amount is approximately 465 cm (NWS, 2023b).

Defining atmospheric rivers and their impact on Alaska

An atmospheric river (AR) is defined as: "[a] long, narrow region in the atmosphere—like rivers in the sky—that transport water vapor outside of the tropics (NOAA, 2023a)." ARs are "characterized by their plumelike structure of focused tropospheric water vapor content and intense low-level winds (Mundhenk and others, 2016a)"; this water vapor content is "roughly equivalent to the average flow of water at the mouth of the Mississippi River (NOAA, 2023a)." ARs are considered responsible for most of the moisture flux into the Arctic, which also may be contributing to the amplification of warming in this region (Mundhenk and others, 2016a). Alaska, particularly the Southeast region, has a history of ARs generating significant amounts of rainfall that result in flooding and infrastructure damage (Jacobs and others, 2016). In January 2014, an AR over the region resulted in extensive flooding and debris flows in Sitka and on Prince of Wales Island (Ralph and Jacobs, 2019); in August 2015 another significant rain event in Sitka caused several landslides that resulted in three deaths (Waldholz and Woosley, 2015).

Data provided by Mundhenk and others (2016a) suggest that, for Southeast Alaska and Northwest British Columbia, there was an increased AR occurrence frequency above the annual mean for the months of December through February between 1979 and 2014. These authors also noted a link between the location and intensity of ARs and the weather events known as *El Niño* and *La Niña* (Mundhenk and others, 2016b). These events are climate patterns in the Pacific Ocean that have a global impact, with *La Niña* events commonly resulting in heavy rain and flooding along the west coast of North America (NOAA, 2023b). A *La Niña* event was occurring during December 2020. *La Niña* events result in a poleward shift of AR occurrence (Mundhenk and others, 2016b), meaning that ARs are more frequently impacting Southeast Alaska instead of normally-impacted areas such as the western U.S. and British Columbia.

Characterizing the December 2020 storm event

The December 2020 storm event was the result of an AR (Jacobs, unpublished data, 2020). Over the duration of the storm—from November 30 to December 2—the average daily temperature rose above freezing. Thus, most of the precipitation generated by the AR at low elevations was rain instead of snow. The start of the 2020 winter had a greater-than-average snowpack (60 cm of snow in the week preceding the storm, compared to the 2019–2020 average depth of approximately 10 cm; NWS, 2023b). Local residents reported that this snow pack completely melted in some areas during the storm event. Weather stations on Flower

Mountain (SNTL 1285, elev. 765.0 m) and Ripinsky Ridge (RRWA2, elev. 792.5 m) reported significant accumulations of snow between December 1 and 2. Rainfall totals at HAXA2 and the Haines Airport weather station (PAHN, elev. 14.9 m) exceeded established records (NWS 2023b) The precipitation averages for the months of November and December for the years 2000–2016 (2000 being the first year of record for HAXA2) compared to the amount of precipitation recorded in 2020 are shown graphically in figures 2 and 3. Additionally, residents from Beach Road and Lutak Spur reported that the ground was not frozen during the storm event (Balise and Grubb, pers. comm., 2021). Between the rainfall and the liquid water coming from the melting snowpack, it is estimated that nearly 17 inches (73 cm) of water was released in the Haines area over the span of 48 hours (Cravens, 2021). The rainfall amounts correspond to a return interval of between 200 and 500 years (NWS, 2023a).

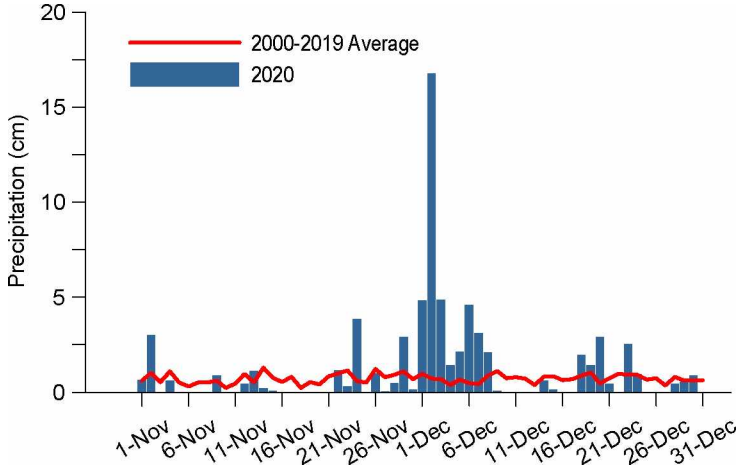

Figure 2. Daily precipitation values in 2020 compared to average values for November and December at HAXA2. Data from NWS (2023b).

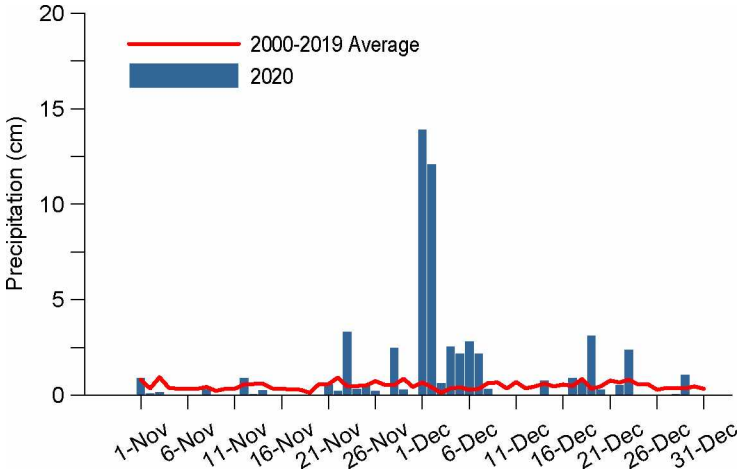

Figure 3. Daily precipitation values in 2020 compared to average values for November and December at PAHN. Data from NWS (2023b).

CHAPTER 3: METHODOLOGY

FIELD INVESTIGATIONS

My advisor, Dr. Margaret M. Darrow, and I conducted two field investigations in June 2021 and July 2022 (additional crew members from organizations such as DGGS and from the Haines area are listed in Chapter 4). The June 2021 trip was focused mostly on the landslide that occurred along Beach Road, and included site investigations, collecting high-resolution lidar data, and collecting the soil matrix and bedrock samples for later laboratory testing (Darrow and others, 2022). We also visited sites along Lutak Road and Lutak Spur in 2021. Those sites became the main focus of the 2022 field visit as we sought to fill the knowledge gaps between data collected in 2021 and data provided to us by ADOT&PF in 2020, through more extensive site observations (such as walking up channels into catchment areas) and additional soil sample collection for laboratory testing.

Most of the landslides we investigated corresponded to a list of sites provided by the ADOT&PF, where state roads were impacted during the December 2020 weather event. We also investigated landslides that impacted private property, such as locations along Lutak Spur and Piedad Road. During the field investigation of each site, we identified the type of mass movement, described exposed stratigraphy, and estimated overall soil thickness. We sampled representative soils, which we transported to the University of Alaska Fairbanks (UAF) for laboratory testing (see “Laboratory Testing” for more details). Chapter 4 contains descriptions for each site.

For two sites along Lutak Road, we measured the *in situ* shear strength of soils using a field vane shear device (Humboldt vane inspection kit, H-4227) in accordance with the American Society for Testing and Materials (ASTM) D2573 standard (ASTM, 2018). The shear strength is the maximum amount of shear stress a soil can experience before it fails. For most soils, the addition of water results in an overall reduction of shear strength, increasing the failure potential (Abdulkareem, 2019). Due to the fragility of the vanes, it is not recommended to use the vane shear device in soils that contain coarse fragments such as gravel. Because of the overall coarse-grained soils in the Haines area, we were limited in where we could conduct strength tests.

At the BRLS, we collected 16 samples of bedrock from around the landslide body to evaluate the strength of bedrock. The testing was done using a point-load tester (Wille Geotechnik, LP

4500/LP 4600) and followed the ASTM D5731 standard (ASTM, 2017b), in which pressure is applied to a rock sample to determine rock strength. Weak bedrock is recognized as a common trigger for landslides (AGI, 2023). A more in-depth analysis of the bedrock in relation to the BRLS can be found in Darrow and others (2022).

LABORATORY TESTING

I tested the sampled soils to determine their engineering index properties, such as moisture content, grain-size distribution, plasticity, specific gravity, and organic content. Laboratory testing followed ASTM standard procedures, as indicated in table 1. Test results are listed in Chapter 4 for corresponding sites. If dry sieve and sedimentation analyses were conducted on samples from a specific site, the graphical results also are contained in that site's entry.

Appendices A and B contain comprehensive laboratory test results for 2021 and 2022, respectively, including results for soil samples that do not directly correspond to a catalog site. Results are presented in the seven-column sheet format used by the ADOT&PF Northern Region Materials Section, which includes numerical values for gradation, plasticity, and specific gravity, as well as sample location information.

MAPPING USING GEOGRAPHIC INFORMATION SYSTEM (GIS)

To map geomorphic evidence of landslides, I used two lidar data sets. The first lidar data set was collected in 2020 in the days immediately following the storm (Daanen and others, 2021). The second lidar data set (Zechmann, in press) was collected in the fall of 2021 with the goal of

Table 1. *Summary of laboratory testing.*

Test Name	ASTM Designation	Reference	No. Samples Tested
Dry sieve analysis (gradation)	D6913	ASTM (2017d)	41
Soil classification (USCS)	D2487	ASTM (2017a)	41
Water content	D2216	ASTM (2019)	34
Specific gravity	D854	ASTM (2014)	21
Sedimentation analysis (hydrometer)	D7928	ASTM (2021b)	20
Atterberg limits	D4318	ASTM (2017c)	17
Point load testing	D5731	ASTM (2017b)	16
Organic material of organic soils	D2974	ASTM (2020)	14
Field vane shear test	D2573	ASTM (2018)	2

collecting data at higher elevations that were missed in 2020 due to weather. I produced lidar derivatives such as slope maps, hillshades, and contours (with 1-m and 2-m intervals) from each data set. The hillshades I produced from the 2020 and 2021 data each had a sun angle of 315° and an azimuth of 45°. I followed the landslide mapping protocol outlined by Slaughter and others (2017), with a few modifications to adapt the protocol to the Alaska landscape in the Haines area, the most obvious being the lack of mappable deposits.

I mapped all scarps in my area of interest, including those adjacent to landslides that occurred in December 2020, along Lutak Spur and Lutak Road, and within stream channels leading to these roads. I identified scarps based on their visual appearance (i.e., arcuate, concave shape) in the slope map and using contour lines (e.g., clusters of lines at the head scarp, v-shaped lines on flanks). I also mapped landslide extents for areas classified as debris slides or sand flows for which the head scarp and flanks could be verified in the field. Most of these landslides lacked mappable deposits due to cleanup efforts by ADOT&PF after the storm. As a result, while I could delineate the scarps and flanks of these landslides, I arbitrarily terminated each landslide extent in a straight line at the road. I measured the length, width, and area of each mapped extent. Because of the arbitrary termination at the road, however, the resulting length and area are likely underestimates. I used elevations from the lidar data to verify soil thickness estimates determined in the field. If I could not verify the head scarp of a 2020 landslide, such as with a debris flow with multiple potential head scarps, I did not map the extent.

CHAPTER 4: LANDSLIDE CATALOG

This catalog is a collection of landslide field observations and measurements, laboratory testing results, landslide classifications, and other relevant information for the December 2020 landslide events. Landslides are presented based on location following specific roads in the Haines area. Catalog entries start at the far (east) end of Lutak Spur, work back toward Haines along Lutak Road, and then include three sites on Piedad Road and Beach Road. Figure 4 shows the extent of six index maps (figs. 5–10), which can be used to locate specific landslide locations along these roads. The following is a description of the formatting used within the catalog, including explanations of each category and abbreviations.

Site #: Number corresponding to site location in index maps (figs. 5–10)

Date(s) Visited: Date(s) of site visit(s)

FEMA DOT#: Identification number given by ADOT&PF and the Federal Emergency Management Agency (FEMA) in December 2020. This number is used in official references. Sites without this identifier are listed as "N/A" for not applicable.

Field Crew: Names of field investigators. Names have been abbreviated to: VN–Victoria Nelson (UAF), MD–Margaret Darrow (UAF), JW–Joseph Wartman (University of Washington (UW)), MG–Michael Grilliot (UW), AL–Andrew Lyda (UW), KB–Kate Bull (DGGS), RD–Ronald Daanen (DGGS), CB–Cindy Buxton (Haines), RW–Russ White (Haines)

Field Name: Unofficial name of location or property on which the slide occurred, including adjacent road name

GPS Coordinates: Coordinates provided in Universal Transverse Mercator format (UTM; NAD 83, Zone 8), taken either with a handheld GPS unit or determined in a GIS environment

Samples Taken: Sample location (in UTM), identification number, type of sample, and laboratory testing results. All soil classifications are presented using the Unified Soil Classification System (USCS) according to ASTM D2847 (ASTM, 2017a). Graphs of grain-size distributions, conducted according to ASTM D6913 and D7928 (ASTM, 2017d; 2021b; respectively), are included after the entry. For selected sites, we conducted vane shear tests to measure *in situ* undrained shear strength in fine-grained soils (ASTM, 2018); we also collected rock samples from Beach Road for point load testing (ASTM, 2017b). Results of those field strength tests are included in this section. Abbreviations: MC – moisture content; Org – organic; DSA – dry sieve analysis; H – sedimentation analysis (hydrometer); TOS – top of slope

***Landslide Classification (and Dimensions)*:** We classified each landslide based on criteria provided by Hungr and others (2001; 2014). For certain sites, we measured

landslide length, width, length-to-width ratio (L/W), and overall affected area using lidar data (Daanen and others, 2021; Zechmann, in press).

Site Description: This general site summary includes observations of the landslide characteristics, soil stratigraphy (where exposed), and the surrounding area. This section includes descriptions of impacted structures and utilities as provided by ADOT&PF or residents, and any notes on ADOT&PF's response, including volume of material removed if the mass movement impacted a road. Any debris removal volumes or lengths provided are estimates obtained from ADOT&PF (2020).
Abbreviations: Bn – brown; Bk – black; Gy – gray; Or – orange; Rd – red; Wh – white; Dk – dark; Org – organic; Org mat - organic mat; PG – poorly-graded; Gr – gravel; Sa – sand; Si – silt; Cl – clay; Bx – bedrock

Additional Notes: This category is a repository for miscellaneous notes relevant to the site.

To help orient users of this catalog by providing additional context, each site entry is accompanied by a set of two maps. The first provides the location of the landslide relative to other landslides in the immediate area at scales ranging from 1:7,000 to 1:27,000, and uses high-resolution (50 cm) optical imagery (ADNR, 2020) as the map background. The scale of the second map varies according to landslide extent, and includes head scarps and landslide extents that I interpreted from the lidar-based slope maps derived from Daanen and others (2021) and Zechmann (in press). Both maps include site identification numbers (Site ID#) located as points on the road with access to the landslide, with the exception of the Beach Road Minor landslide, which did not impact a roadway. Photographs were taken by VN or MD unless otherwise noted.

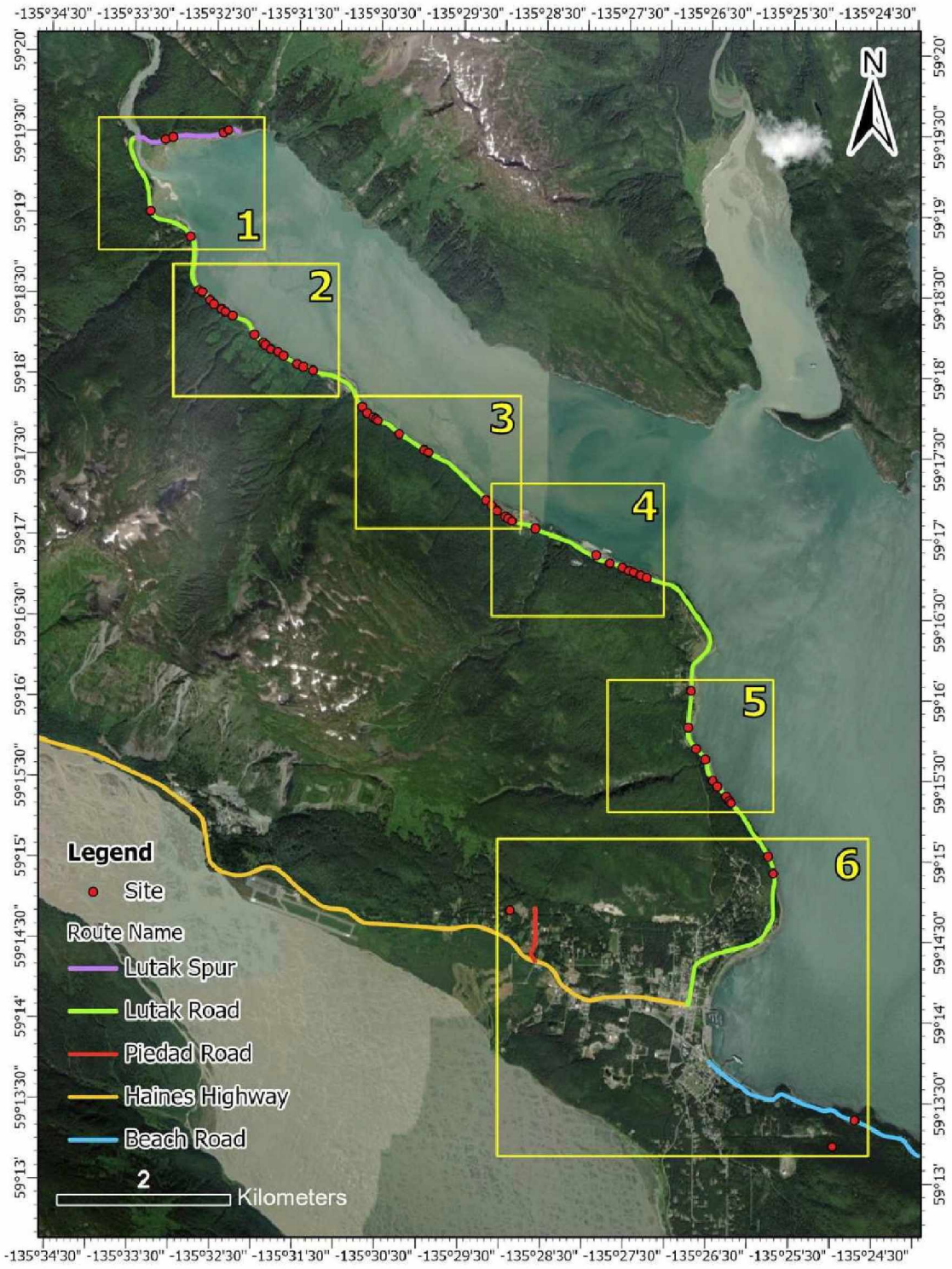

Figure 4. Location map of investigated landslides. The six insets correspond to index maps (see figs. 5–10) (basemap from ADNR, 2020).

Figure 5. Index map 1, showing sites 1 through 6; scale: 1:12,000 (basemap from ADNR, 2020).

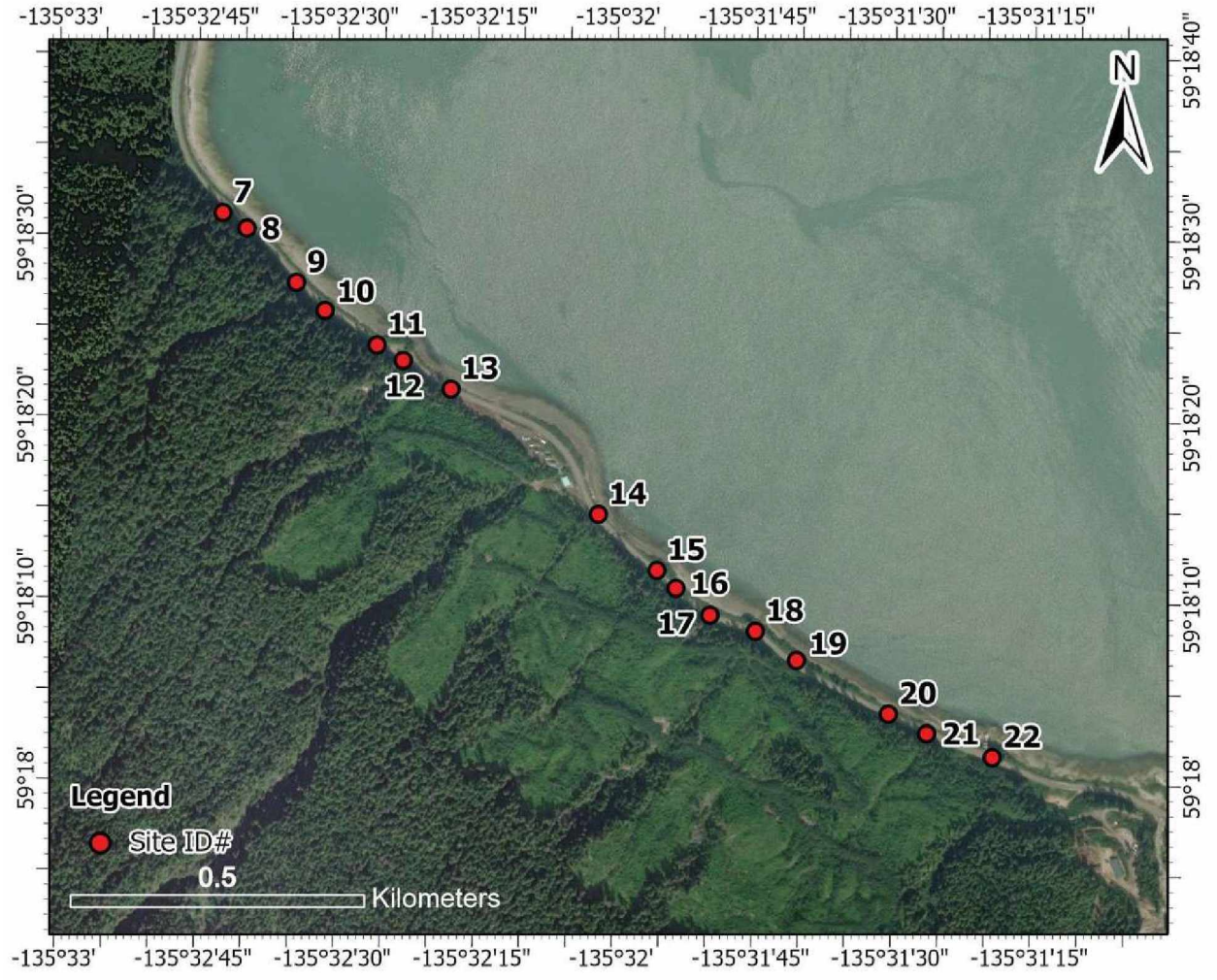

Figure 6. Index map 2, showing sites 7 through 22; scale: 1:12,000 (basemap from ADNR, 2020).

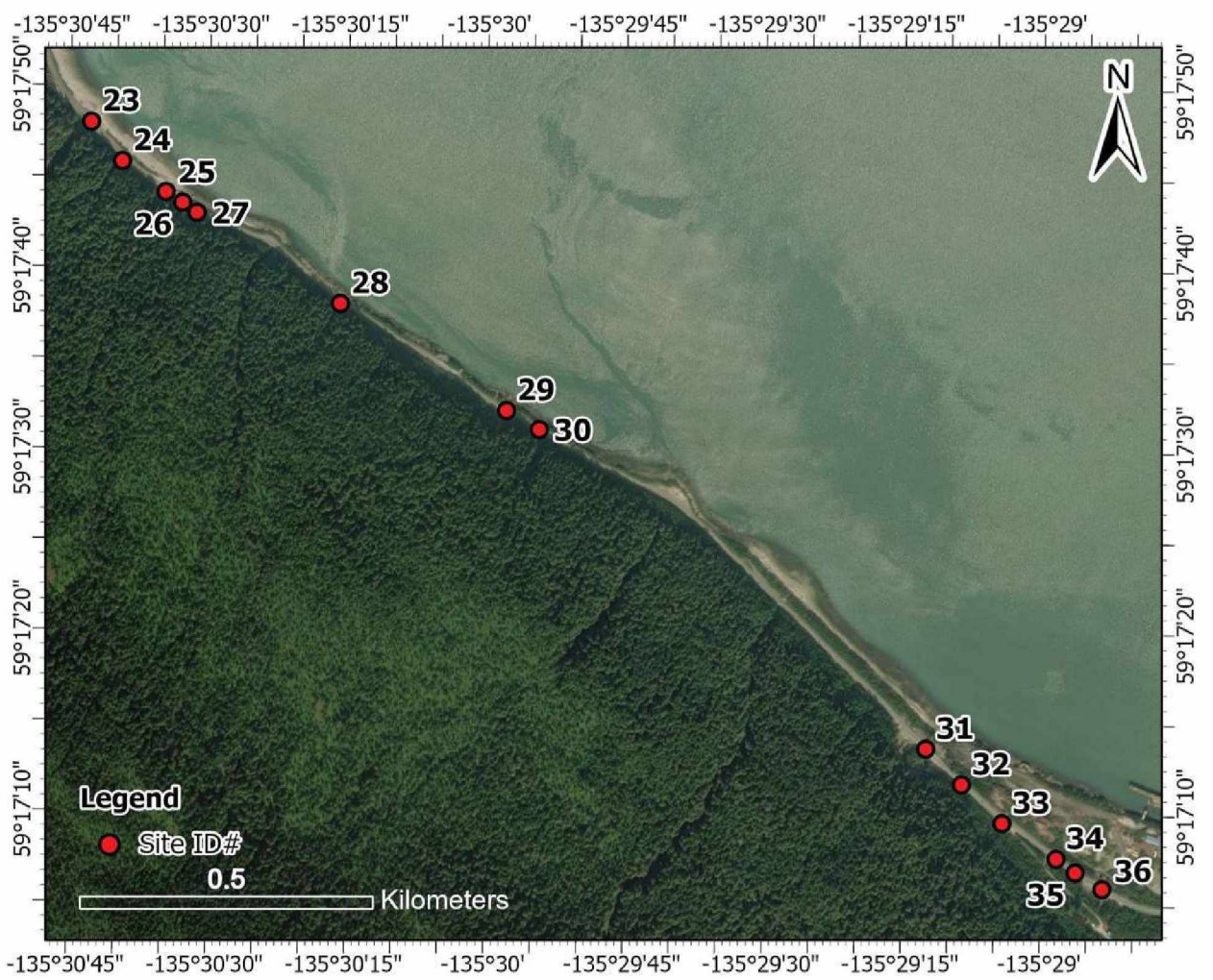

Figure 7. Index map 3, showing sites 23 through 37; scale: 1:12,000 (basemap from ADNR, 2020).

Figure 8. Index map 4, showing sites 38 through 44 (sites in gray are detailed in index map 3); scale: 1:12,000 (basemap from ADNR, 2020).

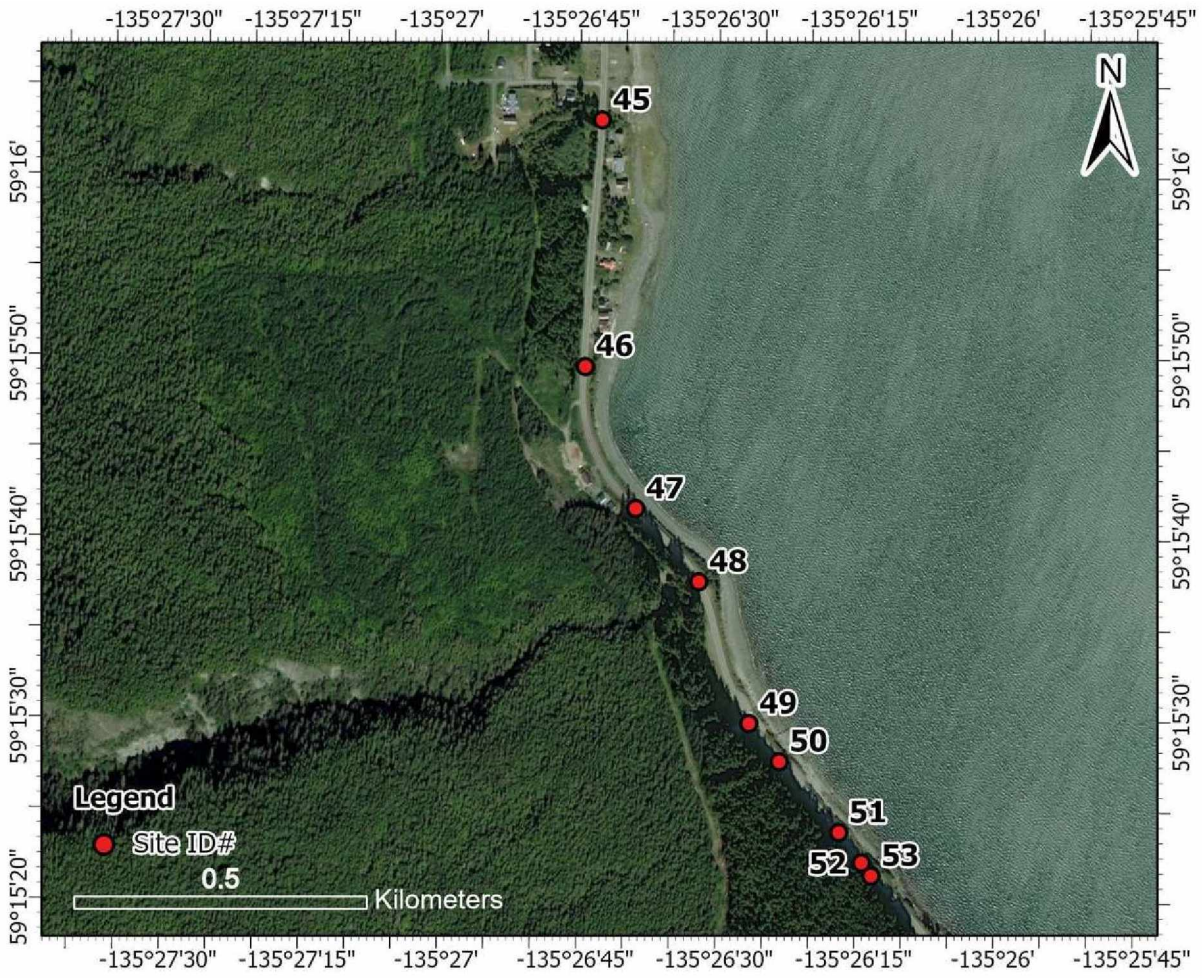

Figure 9. Index map 5, showing sites 45 through 53; scale: 1:12,000 (basemap from ADNR, 2020).

Figure 10. Index map 6, showing sites 54 through 58; scale: 1:24,000 (basemap from ADNR, 2020).

Site ID#: 1 **Date Visited:** 6/21/2021
FEMA DOT#: N/A **Field Crew:** VN, MD, JW
Field Name: GP sand flow, Lutak Spur
GPS Coordinates: UTM Z8 469285 6576400 (fig. 11)

Samples Taken: Samples were collected from the toe of the sand flow, close to the property owner's home.

UTM Z8 469285 6576400:
21-15 (tin) ***MC 3.6%***
21-16 (plastic bag) ***poorly-graded sand with gravel (SP)*** (fig. 12)
UTM Z8 469299 6576410:
21-17 (tin) ***MC 5.0%***
21-18 (plastic bag) ***poorly-graded sand (SP)*** (fig. 12)

Landslide Classification and Dimensions: *Sand flow slide*; length 32 m, width 16 m, L/W 2.0, aerial extent 426.2 m^2

Site Description: A sand flow occurred in a ~40° slope composed mostly of sand with gravel (lithology: tonalite) and forested with hemlock, impacting the back corner of the house (fig. 13). During the December 2020 event, this flow broke through the basement wall of the structure. The deposits reflect pulses of flow with fine layers 20-40-cm thick separated by coarse sand ~2-cm thick. Gullies were observed on the slope on either side of the failure area.

Soil Stratigraphy: (head scarp)

0 – 10 cm	Org mat
>10 cm	Gy PG Sa w/ cobbles, alternating coarse and fine layers; cross-bedding present; magnetic content; iron-cemented sand in upper 1 m

Additional notes: As per the property owner, there is a steady flow of fresh water near the road elevation that flows to the beach. Property owner did not observe any sliding events before December 2020. The ground was not frozen at the time of the December 2020 landslide.

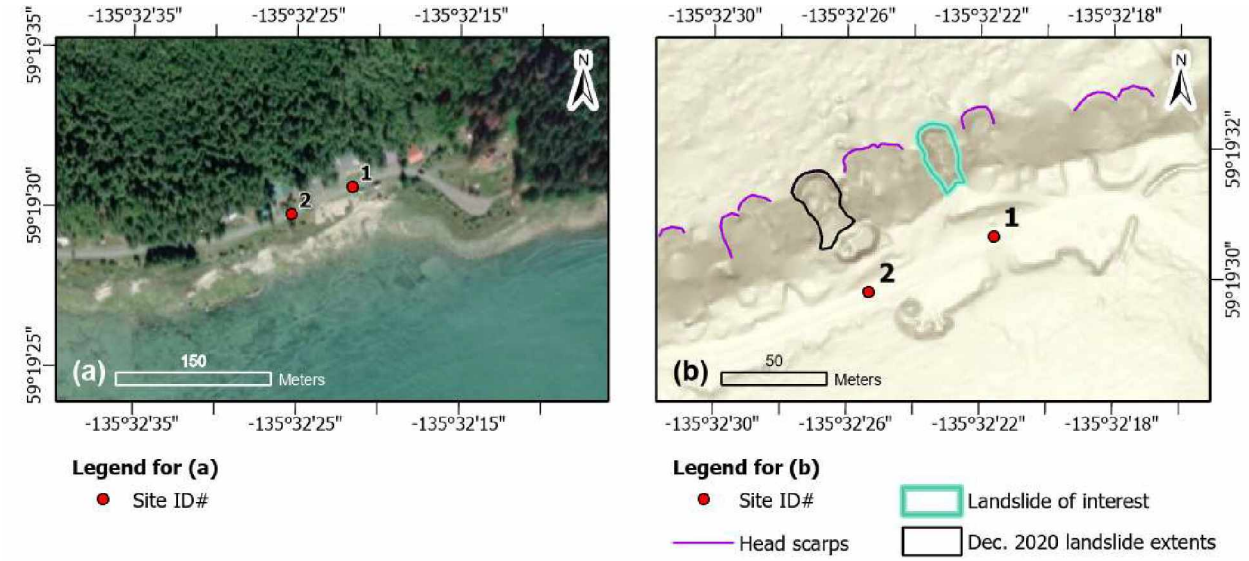

Figure 11. Maps showing location of the GP sand flow (site 1): (a) 50-cm resolution RGB imagery (basemap from ADNR, 2020); (b) slope map derived from 2020 lidar (Daanen and others, 2021). ***NOTE:*** *the legend is standard for all maps; not all items may be present in (b).*

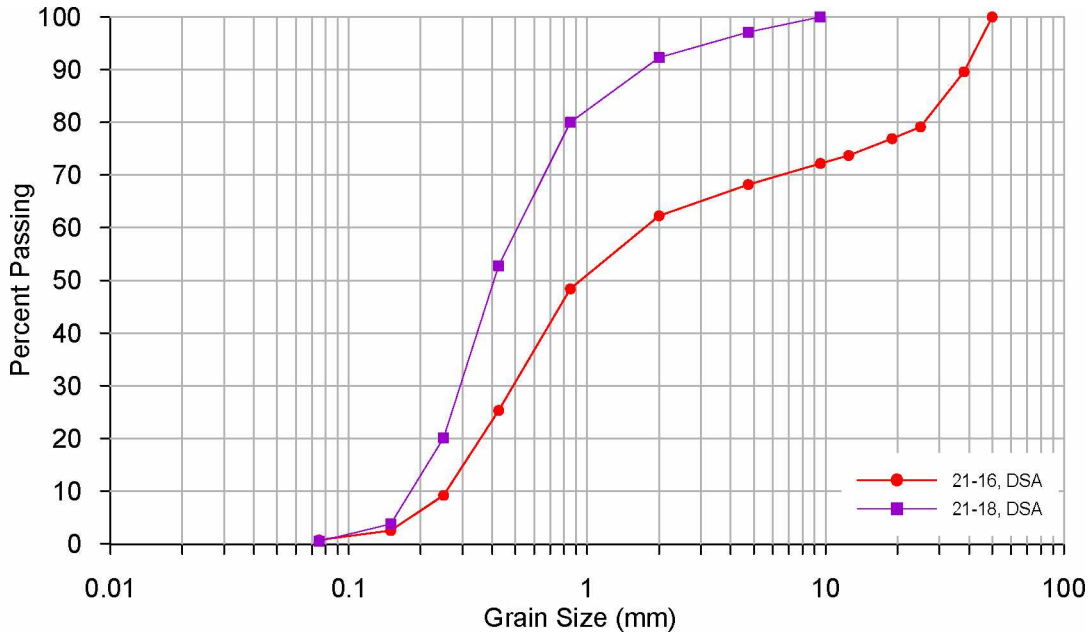

Figure 12. Grain-size distributions for samples 21-16 and 21-18.

Figure 13. Photographs of the GP sand flow (June 2021 after some clearing efforts) showing: (a) alternating coarse and fine layers exposed in the left flank adjacent to the impacted corner of the house; (b) sampling location (shovel for scale).

Site ID#: 2 **Date Visited:** 6/21/2021
FEMA DOT#: N/A **Field Crew:** VN, MD, JW
Field Name: VP sand flow, Lutak Spur
GPS Coordinates: UTM Z8 469246 6576359 (fig. 14)

Samples Taken:

Samples from the head scarp area (*UTM Z8 469239 6576407):*
- 21-11 (plastic bag) ***poorly-graded sand (SP)*** (fig. 15)
- 21-12 (tin) ***MC 8.0%***

Samples from the toe of the VP sand flow (*UTM Z8 469236 6576369)*:
- 21-13 (tin) ***MC 4.7%***
- 21-14 (plastic bag) ***poorly-graded sand (SP)*** (fig. 15)

Landslide Classification and Dimensions: *Sand flow slide*; length 33 m, width 18 m, L/W 1.8, aerial extent 549.9 m^2

Site Description: The sand flow occurred on a ~40° slope composed mostly of sand, with some gravel layers. The slope and surrounding areas are forested with hemlock. The sand flow destroyed a house on the property.

Soil Stratigraphy: (at head scarp)

0 – 10 cm	Org mat
>10 cm	Gy PG Sa [21-11, 21-12], alternating dark and light sand layers of varying thicknesses; cross-bedding present; magnetic content; iron-cemented Sa in upper 1 m (fig. 16)

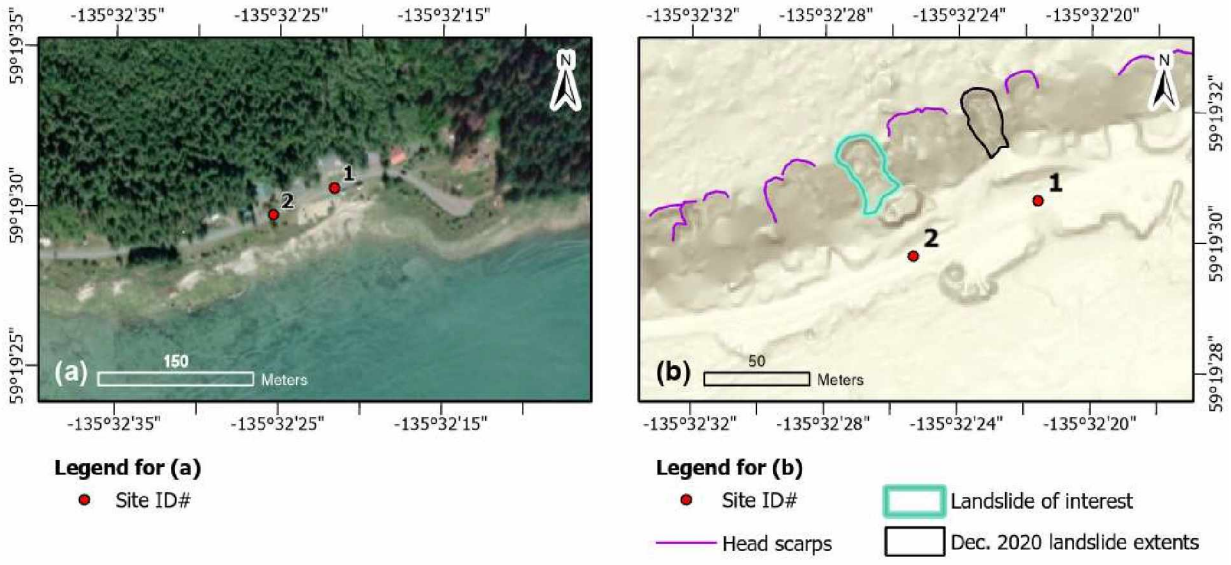

Figure 14. Maps showing location of the VP sand flow (site 2): (a) 50-cm resolution RGB imagery (basemap from ADNR, 2020); (b) slope map derived from 2020 lidar (Daanen and others, 2021). ***NOTE:*** *the legend is standard for all maps; not all items may be present in (b).*

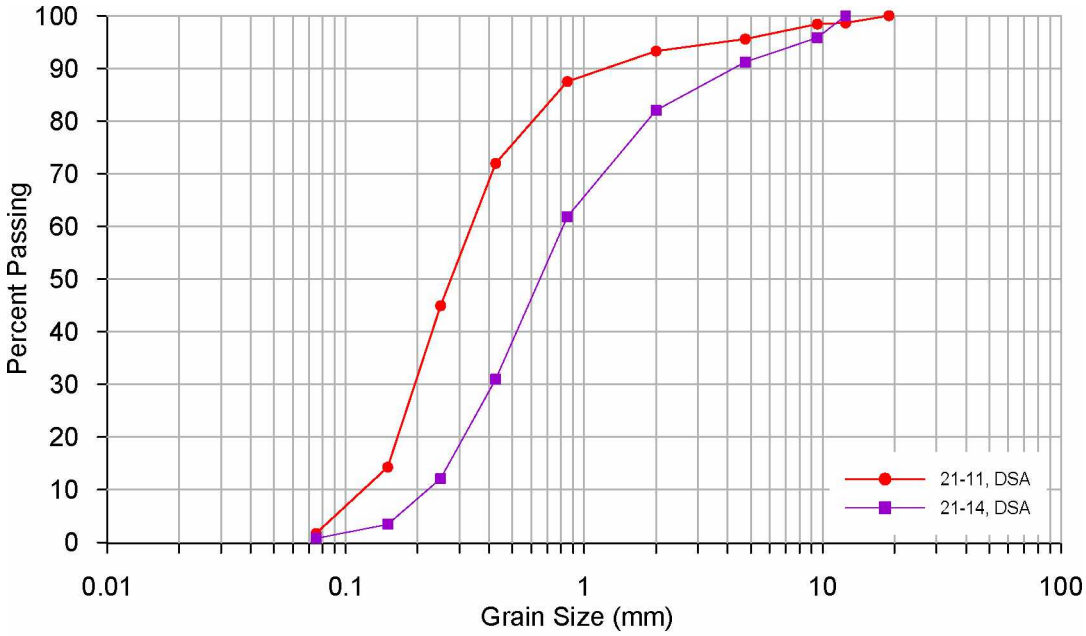

Figure 15. Grain-size distributions for samples 21-11 and 21-14.

Figure 16. Photographs of the VP sand flow slide (June 2021) showing: (a) stratigraphy exposed in the left flank at the slope base, showing alternating fine and coarse sand layers with interspersed gravel and cobbles; (b) the head scarp, as seen from the left flank, with iron-cemented sand both intact beneath the organic mat and loose on the slope.

Site ID#:	3	**Date Visited:**	7/22/2022
FEMA DOT#:	N/A	**Field Crew:**	VN, MD, KB, CB
Field Name:	FP sand flow, Lutak Spur		
GPS Coordinates:	UTM Z8 468662 6576363 (fig. 17)		

Samples Taken: Samples were collected from the head scarp and near the left flank (*UTM Z8 468662 6576363*). Figure 18 is a graph containing all grain-size distributions.

22-29 (bag)	***poorly-graded sand (SP)*** coarse- to fine-sand layer sequence, 10-cm thick
22-30 (bag)	***poorly-graded sand (SP)*** coarse- to fine-sand layer sequence, 20-cm thick
22-31 (bag)	***poorly-graded sand (SP)*** coarse- to fine-sand layer sequence, 10-cm thick
22-32 (tin)	***MC 0.9%***, only coarse sand layer, 5-cm thick
22-33 (tin)	***MC 6.6%***, only fine sand layer, 6-cm thick
22-34 (bag)	***poorly-graded sand (SP)***, only coarse layer, 25-cm thick
22-35 (bag)	***poorly-graded sand (SP)***, only fine sand layer, 5-cm thick
22-36 (bag)	***poorly-graded sand with gravel (SP)*** mostly coarse sand layer with cobbles, 5 m from TOS

Landslide Classification and Dimensions: *Sand flow slide*; length 13 m, width 27 m, L/W 0.5, aerial extent 302.7 m^2

Site Description: The slope failure at this location occurred along the left bank of a deeply-incised channel within the bluff (fig. 17b). Approximately 5 m of stratigraphy was exposed. We carefully measured the thicknesses of the alternating fine- and coarse-grained layers, collecting representative samples.

Soil Stratigraphy: Refer to figure 19 for photographs illustrating the overall stratigraphy; the average thicknesses were 5 cm for the fine-grained layers and 10 cm for the coarse observed throughout the deposit. We also observed coarse-grained layers with gravel and cobbles throughout the deposit.

Additional notes: The samples collected from this site were reserved to determine magnetic content. Some of the fine-grained sand sequences contained rootlets. ADOT&PF personnel walked the base of the slope in this area post-failure and described it as “spongy, almost liquefied (Eckhoff, pers. comm., June 2021),” which is notable for sand.

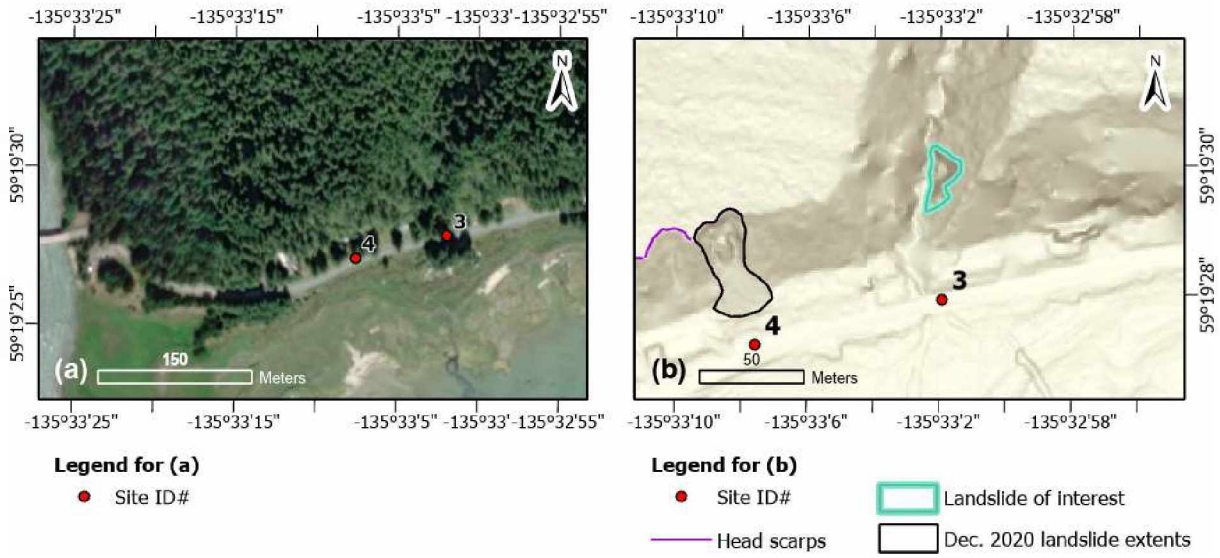

Figure 17. Maps showing location of the FP sand flow (site 3): (a) 50-cm resolution RGB imagery (basemap from ADNR, 2020); (b) slope map derived from 2020 lidar (Daanen and others, 2021). ***NOTE:*** *the legend is standard for all maps; not all items may be present in (b).*

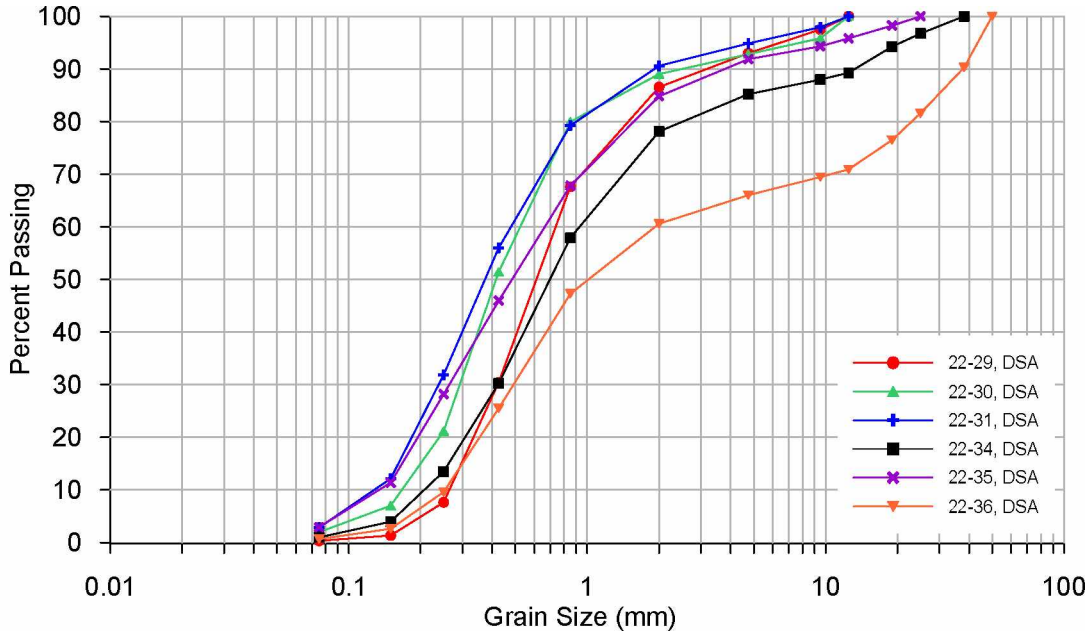

Figure 18. Grain-size distributions for the samples collected from the FP sand flow.

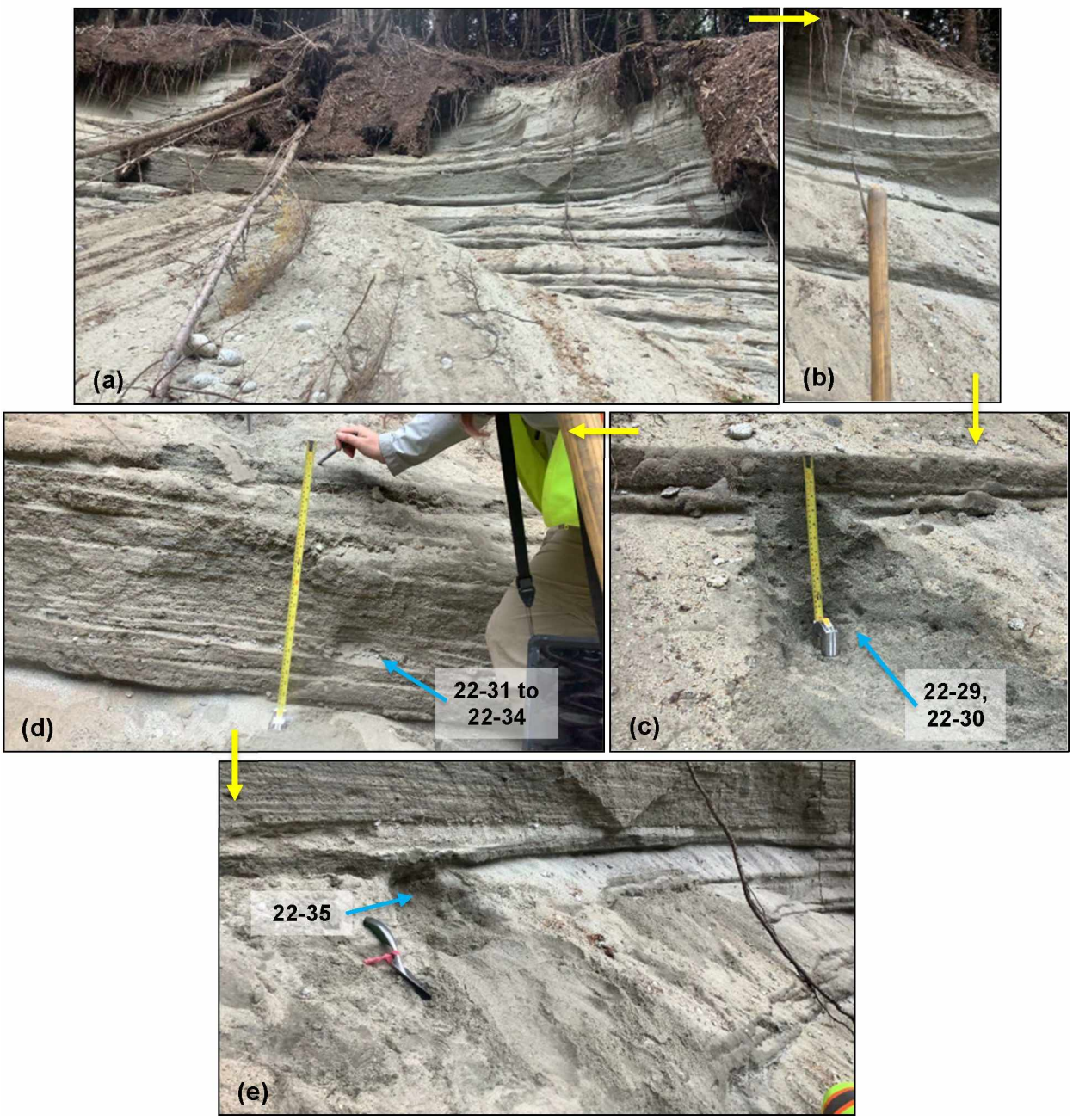

Figure 19. Photographs of the FP sand flow, taken in sequential order (see yellow arrows) starting from the head scarp and moving downslope (July 2022): (a) head scarp area near the left flank, with fine-grained and coarse-grained sand; (b) continuation of stratigraphy directly below the extent of (a), illustrating the coarse-grained sand as a "slope-forming unit" and the fine-grained sand as a "cliff-forming unit;" (c) approximately 0.5 m below the extent of (b), we sampled a 6.5-cm thick fine-grained / 30-cm thick coarse-grained sequence (samples 22-29 and 22-30); (d) directly beneath (c), a 58-cm thick sequence of fine-grained (avg. thickness 3.0 cm) and coarse-grained (avg. thickness 1.5 cm) sand, from which samples 22-31 through 22-34 were taken; (e) 1.5 m to the right of (d) was a less-disturbed exposure of fine-grained sand layers (each approximately 5-cm thick), from which we sampled 22-35; sample 22-36 was collected from a coarse-grained layer just below the extent of (e).

Site ID#: 4 **Date Visited:** 6/17/2021
FEMA DOT#: N/A **Field Crew:** VN, MD
Field Name: MP sand flow, Lutak Spur
GPS Coordinates: UTM Z8 468553 6576317 (fig. 20)

Samples Taken: Samples were collected from the landslide body approximately mid-slope.
UTM Z8 468559 6576320:
21-03 (tin) ***MC 5.6%***
21-04 (Ziploc bag) ***poorly-graded sand with gravel (SP)*** (fig. 21)

Landslide Classification and Dimensions: *Sand flow slide*; length 48 m, width 20 m, L/W 2.4, aerial extent 998.8 m^2

Site Description: Residential structures are at the base of a ~40° slope composed mostly of sand; the above bluff and adjacent slopes are forested with hemlock. The exposed stratigraphy (fig. 22) alternates between fine-grained and coarse-grained sand with gravel clasts (tonalite with 30% amphibole, 40% quartz, 30% plagioclase feldspar). We observed iron-cemented sand in the head scarp, but not in soil pits dug in the bluff above the landslide.

Soil Stratigraphy: (head scarp towards right flank)
0 – 20 cm Org mat with roots
20 – 25 cm Gy PG Sa, w/ iron oxidation
>25 cm Gy PG Sa w/ rounded granitic clasts up to 10 cm, cross-bedding

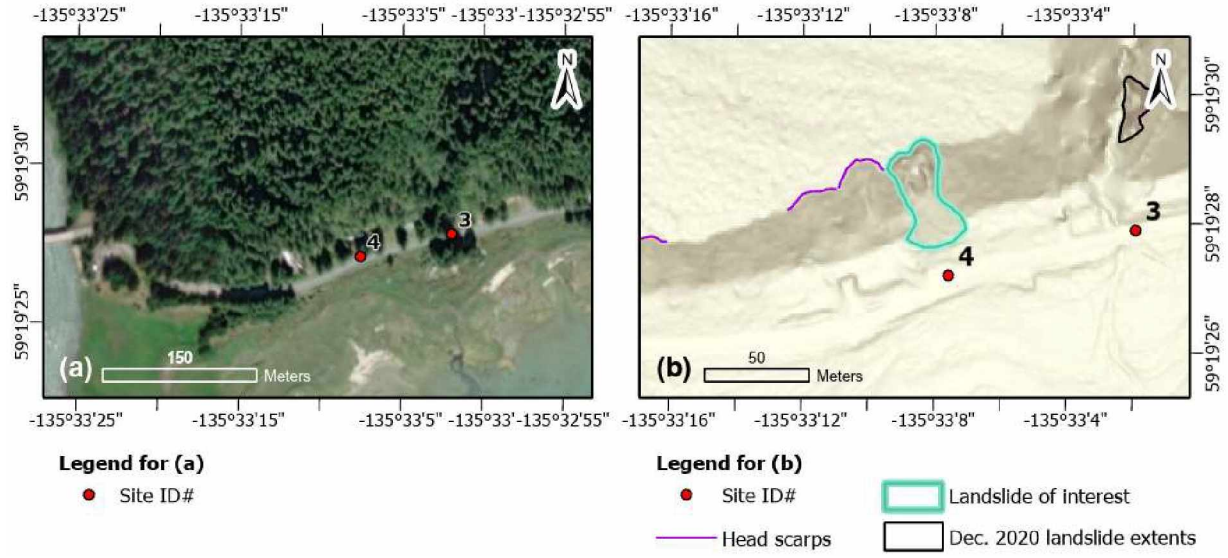

*Figure 20. Maps showing location of the MP sand flow (site 4): (a) 50-cm resolution RGB imagery (basemap from ADNR, 2020); (b) slope map derived from 2020 lidar (Daanen and others, 2021). **NOTE:** the legend is standard for all maps; not all items may be present in (b).*

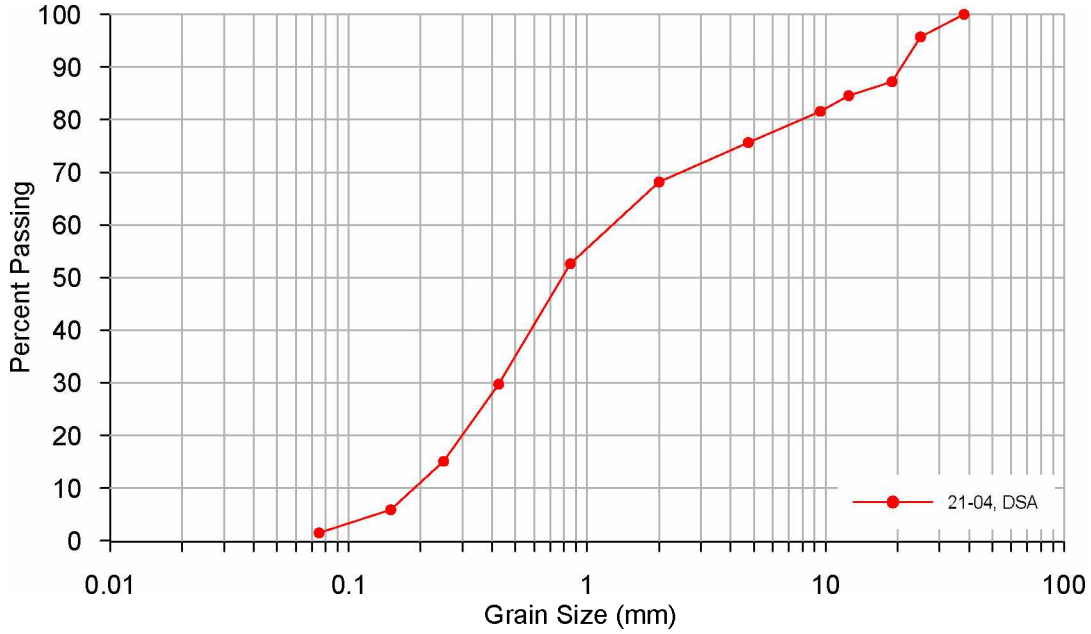

Figure 21. Grain-size distribution for sample 21-04.

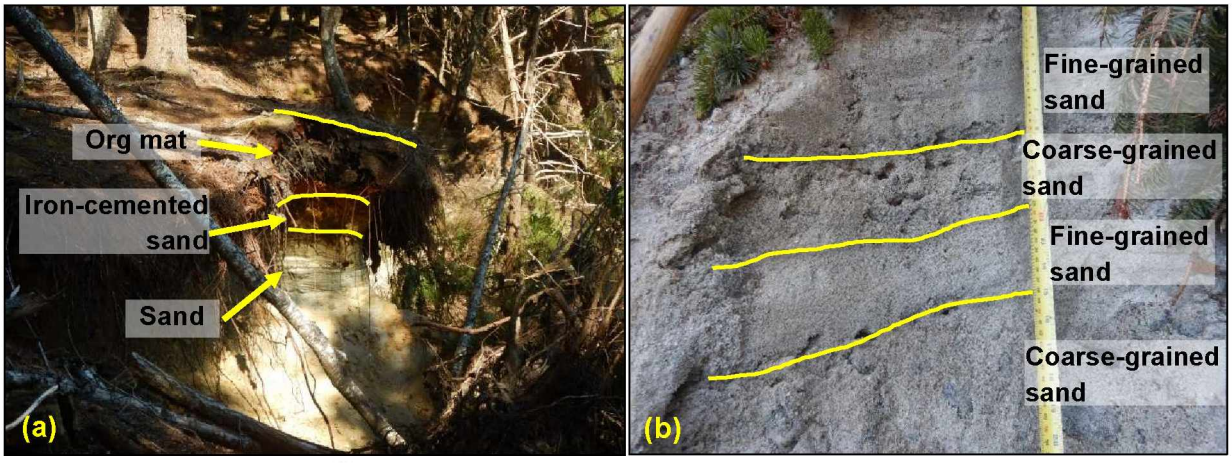

Figure 22. Photographs of the MP sand flow (June 2021): (a) head scarp area with annotated stratigraphy; (b) annotated view of stratigraphy along right flank.

Site ID#: 5 **Date Visited:** 6/17/2021
FEMA DOT#: 12 **Field Crew:** VN, MD
Field Name: Lutak Road
GPS Coordinates: UTM Z8 468408 6575461 (fig. 23)

Samples Taken: No samples were taken at this location.

Landslide Classification: *Debris flow*

Site Description: Remnant debris from this channel was visible from the road in June 2021 (fig. 24). ADOT&PF (2020) marked this site as having a major impact on Lutak Road, blocking both lanes and requiring permanent repair. The length of highway impacted was between 20 and 100 ft (6 – 30 m). ADOT&PF additionally noted that the channel is now in a different location than before the event.

Soil Stratigraphy: Not described; source area not investigated

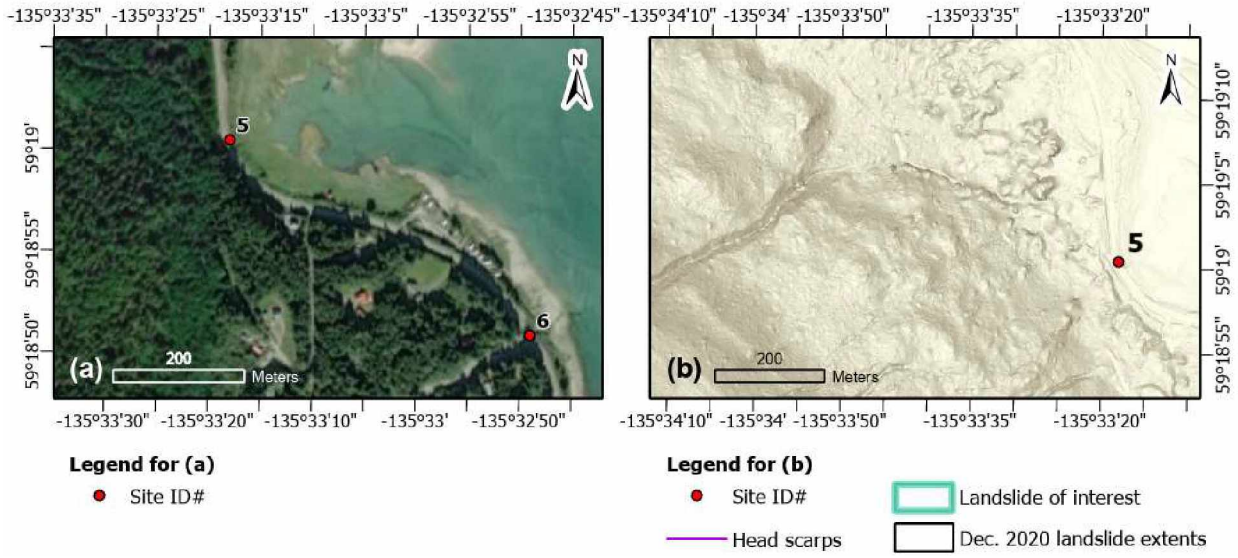

*Figure 23. Maps showing location of FEMA DOT#12 (site 5): (a) 50-cm resolution RGB imagery (basemap from ADNR, 2020); (b) slope map derived from 2020 lidar (Daanen and others, 2021). **NOTE:** the legend is standard for all maps; not all items may be present in (b).*

Figure 24. Photograph of the channel at FEMA DOT#12 taken from Lutak Road, with remnant debris in the foreground (June 2021).

Site ID#: 6 **Date Visited:** 6/17/2021
FEMA DOT#: 15 **Field Crew:** VN, MD
Field Name: Lutak Road
GPS Coordinates: UTM Z8 468872 6575166 (fig. 25)

Samples Taken: No samples were taken at this location.

Landslide Classification: *Debris flow*

Site Description: This is an established river channel (i.e. Shakuseyi Creek) containing large cobbles (fig. 26). During the December 2020 storm event, debris came up to the top of the culvert on the upstream side, but did not overtop the road. ADOT&PF removed the debris with an excavator (Eckhoff, pers. comm., June 2021).

Soil Stratigraphy: Not described; source area not investigated

Additional notes: ADOT&PF routinely removes debris from this area and has built berms to constrain the channel (Eckhoff, pers. comm., June 2021). We observed sediment deposited downstream of the culvert outlet; this is potentially indicative of past debris flows going out of the channel and over the road.

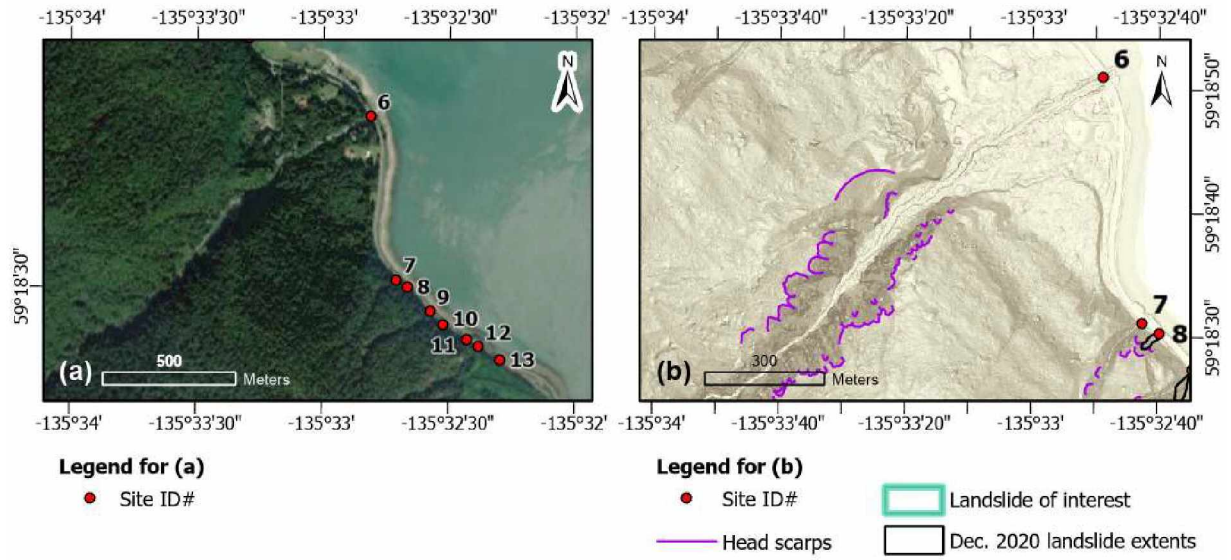

Figure 25. Maps showing location of FEMA DOT#15 (site 6): (a) 50-cm resolution RGB imagery (basemap from ADNR, 2020); (b) slope map derived from 2020 lidar (Daanen and others, 2021). ***NOTE:*** *the legend is standard for all maps; not all items may be present in (b).*

Figure 26. Photograph of FEMA DOT#15 channel upstream from Lutak Road (June 2021).

Site ID#: 7 **Date Visited:** 6/17/2021
FEMA DOT#: 18 **Field Crew:** VN, MD
Field Name: Lutak Road
GPS Coordinates: UTM Z8 468976 6574565 (fig. 27)

Samples Taken: No samples were taken at this location.

Landslide Classification: *Debris flow*

Site Description: At this site, debris coming from a steep channel (fig. 28) blocked both travel lanes and impacted a length of road greater than 100 ft (30 m) (ADOT&PF, 2020). It was flagged as a major source of debris, with several hundred cubic yards/meters requiring removal. An earth berm was constructed to contain potential future deposits.

Soil Stratigraphy: Not described; source area not investigated

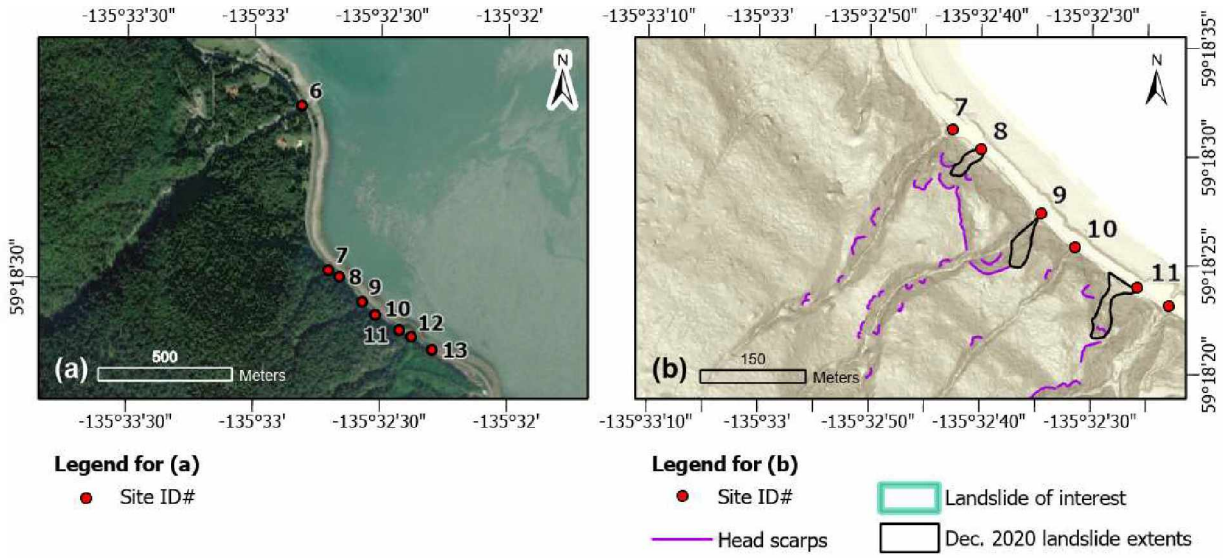

Figure 27. Maps showing location of FEMA DOT#18 (site 7): (a) 50-cm resolution RGB imagery (basemap from ADNR, 2020); (b) slope map derived from 2020 lidar (Daanen and others, 2021). ***NOTE:*** *the legend is standard for all maps; not all items may be present in (b).*

Figure 28. Photograph of FEMA DOT#18 channel from Lutak Road (June 2021).

Site ID#: 8 **Dates Visited:** 6/17, 6/23/2021
FEMA DOT#: 19 **Field Crew:** VN, MD
Field Name: Lutak Road
GPS Coordinates: UTM Z8 469011 6574530 (fig. 29)

Samples Taken: No samples were taken at this location.

Landslide Classification and Dimensions: *Debris slide*; length 53 m, width 16 m, L/W 3.3, aerial extent 775.9 m^2

Site Description: This was the site of a landslide occurring in colluvium over diorite bedrock (fig. 30). Several downed trees spanned the slide area. This site was described by ADOT&PF (2020) as a major impact, blocking the full width of the road and depositing several hundred cubic yards/meters of debris.

Soil Stratigraphy: (in head scarp, observed from mid-slope)

0 – 15 cm	Org mat
15 – 200 cm	Bn Si w/ Sa (colluvium)
>200 cm	Diorite Bx

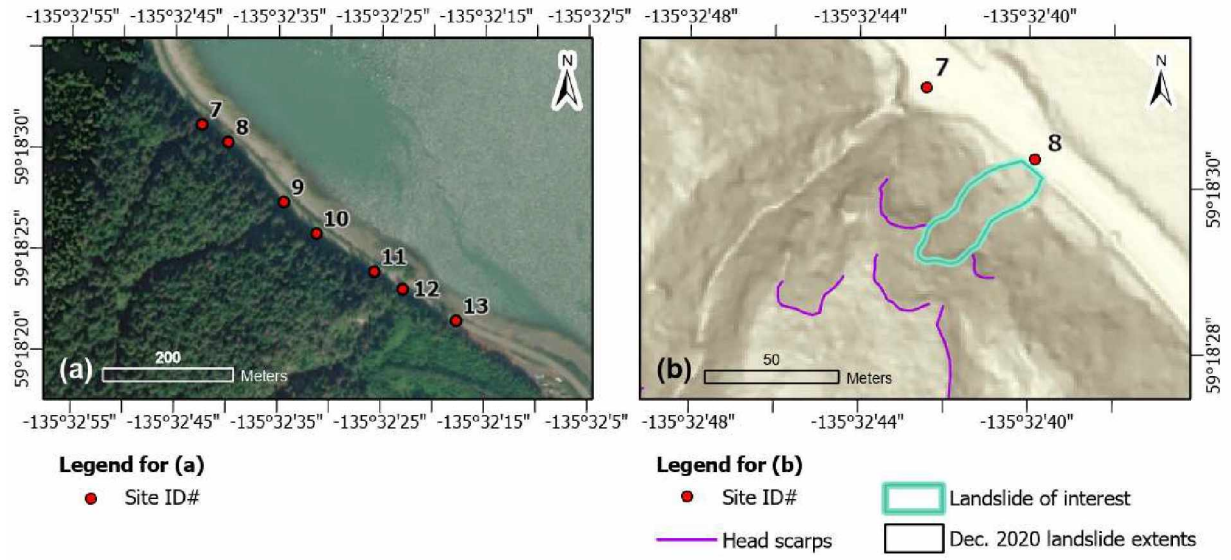

*Figure 29. Maps showing location of FEMA DOT#19 (site 8): (a) 50-cm resolution RGB imagery (basemap from ADNR, 2020); (b) slope map derived from 2020 lidar (Daanen and others, 2021). **NOTE:** the legend is standard for all maps; not all items may be present in (b).*

Figure 30. Photographs of FEMA DOT#19 (June 2021): (a) view of head scarp from road level; (b) left flank showing approximately 2 m of brown colluvial material; the diorite bedrock exposed near the head scarp was mostly covered by debris at this location.

Site ID#: 9 **Date Visited:** 6/17/2021, 7/25/2022
FEMA DOT#: 20 **Field Crew:** VN, MD
Field Name: Lutak Road
GPS Coordinates: UTM Z8 469096 6574436 (fig. 31)

Samples Taken: No samples were taken at this location.

Landslide Classification and Dimensions: *Debris slide*; length 52 m, width 31 m, L/W 1.7, aerial extent 1,320.2 m^2

Site Description: At this site, there was a significant buildup of debris that blocked both lanes of Lutak Road for at least 100 ft (30 m). ADOT&PF (2020) estimated that "several hundred cubic yards of material if not thousands" were deposited on the road and within the right-of-way (fig. 32). The channel at this location was scoured to bedrock.

Soil Stratigraphy: Close to the road, diorite bedrock is exposed in the creek channel; to the sides of this exposure, there are 2–3 m of colluvium overlying bedrock. Closer to the head scarp, the colluvium layer is thinner (<1 m), and bedrock is exposed intermittently.

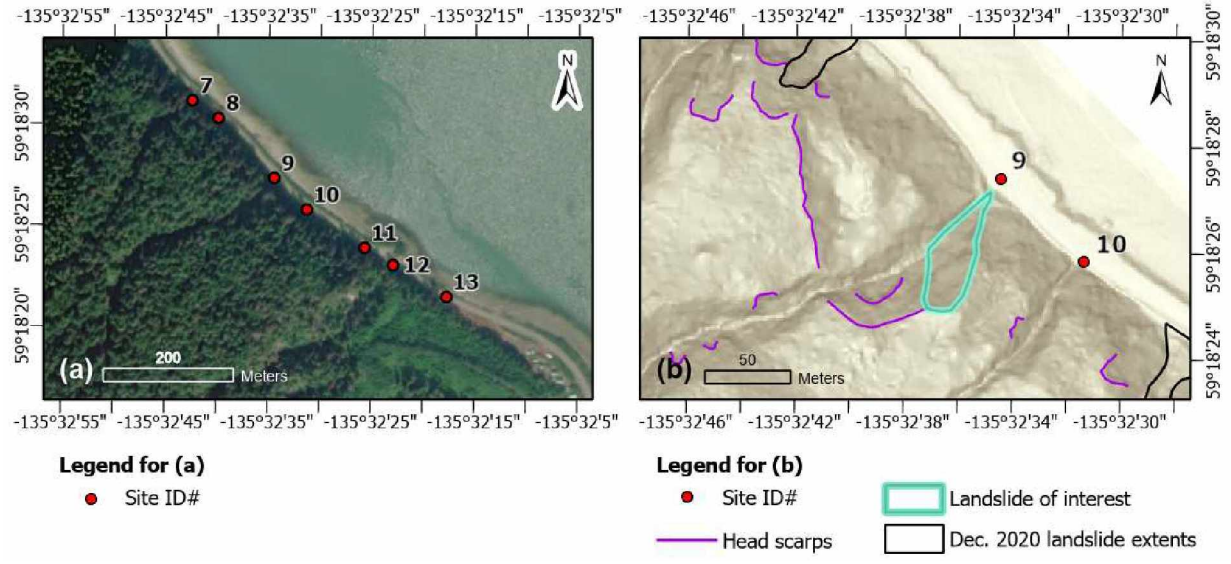

Figure 31. Maps showing location of FEMA DOT#20 (site 9): (a) 50-cm resolution RGB imagery (basemap from ADNR, 2020); (b) slope map derived from 2020 lidar (Daanen and others, 2021). ***NOTE:*** *the legend is standard for all maps; not all items may be present in (b).*

Figure 32. Photographs of the landslide area at FEMA DOT#20: (a) view up the channel in December 2020 (photograph courtesy of ADOT&PF); (b) diorite bedrock exposed in the channel (July 2022).

Site ID#: 10 **Date Visited:** 6/17/2021
FEMA DOT#: 21 **Field Crew:** VN, MD
Field Name: Lutak Road
GPS Coordinates: UTM Z8 469145 6574396 (fig. 33)

Samples Taken: No samples were taken at this location.

Landslide Classification: *Debris flow*

Site Description: The landslide at this site deposited several hundred cubic yards/meters of material onto the roadway (fig. 34), blocking both lanes (ADOT&PF, 2020). The channel was scoured to bedrock.

Soil Stratigraphy: Not described; source area not investigated

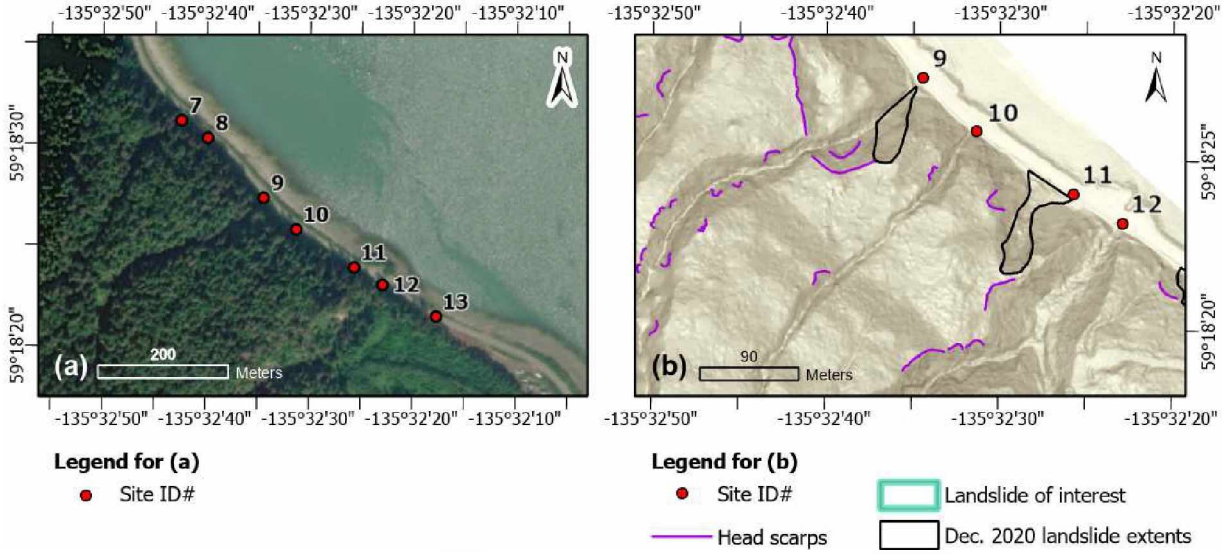

*Figure 33. Maps showing location of FEMA DOT#21 (site 10): (a) 50-cm resolution RGB imagery (basemap from ADNR, 2020); (b) slope map derived from 2020 lidar (Daanen and others, 2021). **NOTE:** the legend is standard for all maps; not all items may be present in (b).*

Figure 34. View up the channel at FEMA DOT#21 from Lutak Road in December 2020 (photograph courtesy of ADOT&PF).

Site ID#: 11 **Date Visited:** 6/17/2021, 7/25/2022
FEMA DOT#: 22 **Field Crew:** VN, MD
Field Name: Lutak Road
GPS Coordinates: UTM Z8 469218 6574342 (fig. 35)

Samples Taken: No samples were taken at this location.

Landslide Classification and Dimensions: *Debris slide*; length 93 m, width 21 m, L/W 4.4, aerial extent 1,946.4 m^2

Site Description: This landslide occurred in colluvium and scoured to bedrock (fig. 36), blocking the entire width of the road (ADOT&PF, 2020).

Soil Stratigraphy:

0 – 10 cm	Org mat
10 – 80 cm	Gy-Bn Si w/ Sa and cobbles (colluvium)
> 80 cm	Diorite Bx

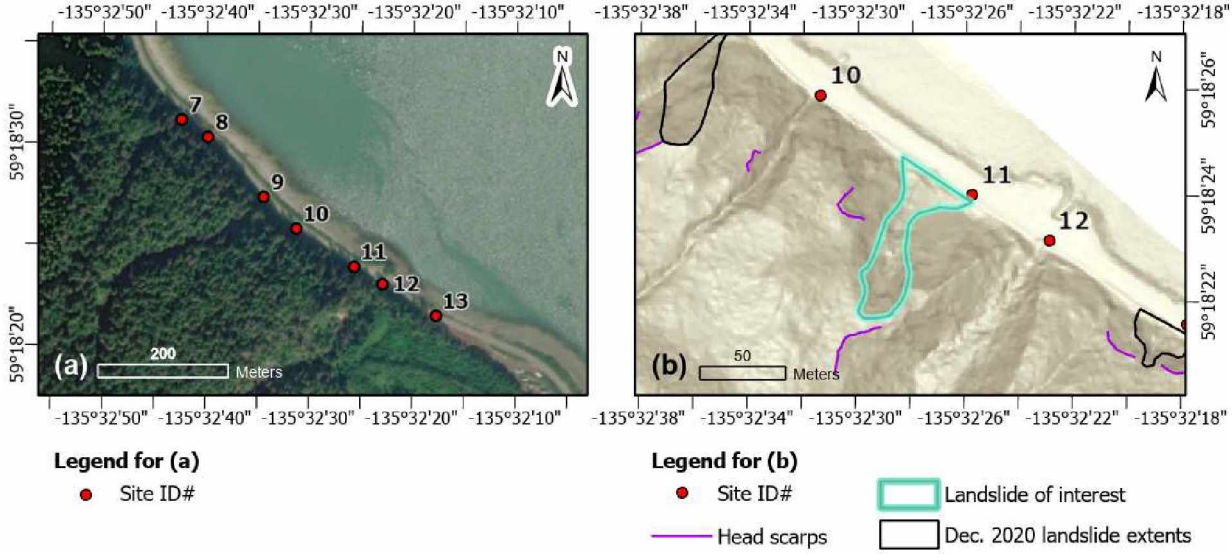

Figure 35. Maps showing location of FEMA DOT#22 (site 11): (a) 50-cm resolution RGB imagery (basemap from ADNR, 2020); (b) slope map derived from 2020 lidar (Daanen and others, 2021). ***NOTE:*** *the legend is standard for all maps; not all items may be present in (b).*

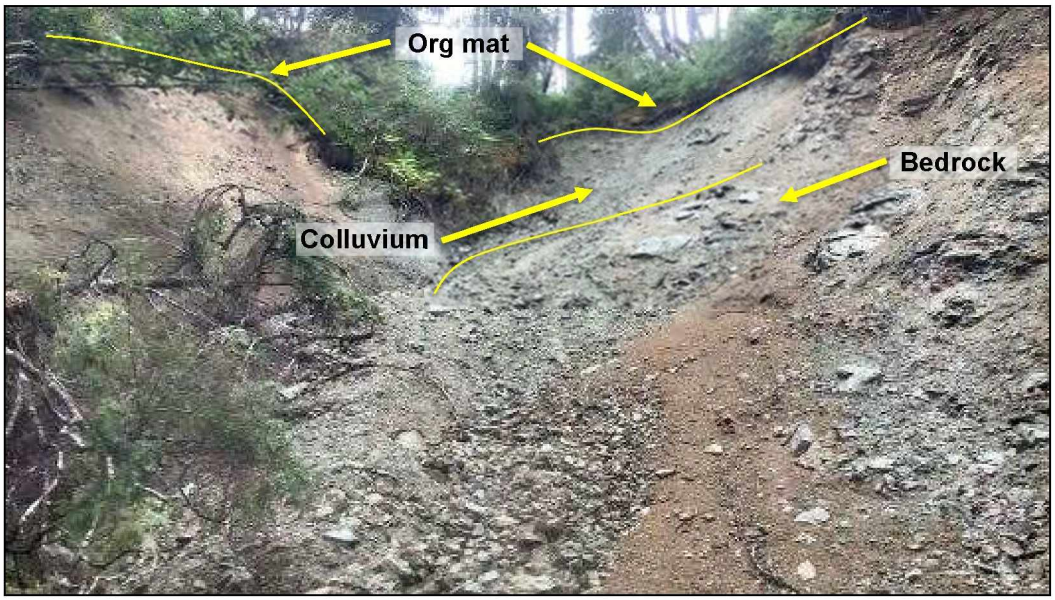

Figure 36. Annotated view of the head scarp of FEMA DOT#22 (July 2022), illustrating colluvium overlying bedrock (covered by slope wash in places).

Site ID#: 12 **Date Visited:** 6/17/2021
FEMA DOT#: 23 **Field Crew:** VN, MD
Field Name: Lutak Road
GPS Coordinates: UTM Z8 469269 6574299 (fig. 37)

Samples Taken: No samples were taken at this location.

Landslide Classification: *Debris flow*

Site Description: ADOT&PF (2020) noted that this debris flow blocked both lanes of Lutak Road for more than 100 ft (30 m), with several hundred cubic yards/meters of material (fig. 38).

Soil Stratigraphy: Not described; source area not investigated

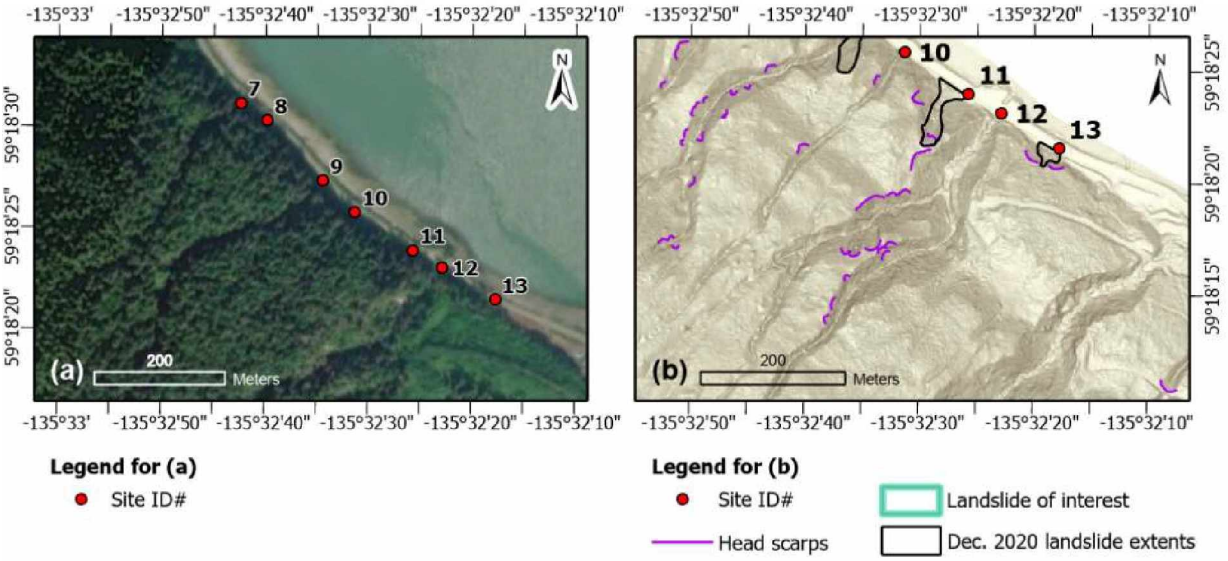

*Figure 37. Maps showing location of FEMA DOT#23 (site 12): (a) 50-cm resolution RGB imagery (basemap from ADNR, 2020); (b) slope map derived from 2020 lidar (Daanen and others, 2021). **NOTE:** the legend is standard for all maps; not all items may be present in (b).*

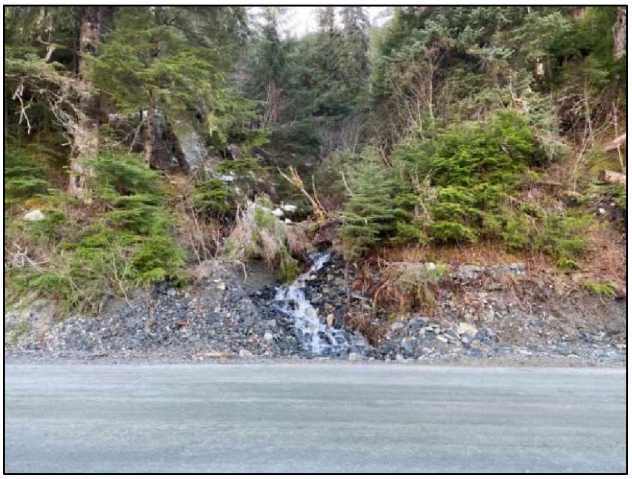

Figure 38. The channel of FEMA DOT#23 from Lutak Road in December 2020, after clean-up occurred (photograph courtesy of ADOT&PF).

Site ID#: 13 **Date Visited:** 6/17/2021
FEMA DOT#: 24 **Field Crew:** VN, MD
Field Name: Lutak Road
GPS Coordinates: UTM Z8 469354 6574256 (fig. 39)

Samples Taken: No samples were taken at this location.

Landslide Classification and Dimensions: *Debris slide*; length 20 m, width 33 m, L/W 0.6, aerial extent 603.2 m^2

Site Description: ADOT&PF (2020) reported a full blockage of Lutak Road in December 2020 and noted that the landslide had exposed the rock face (fig. 40). Between 100 and 200 cubic yards (70–150 cubic meters) of debris moved as part of this landslide (ADOT&PF, 2020).

Soil Stratigraphy:

0 – 10 cm	Org mat
10 – 50 cm	Gy Si Sa Gr (angular, colluvium; thickness varies, up to 2 m)
>50 cm	Diorite Bx

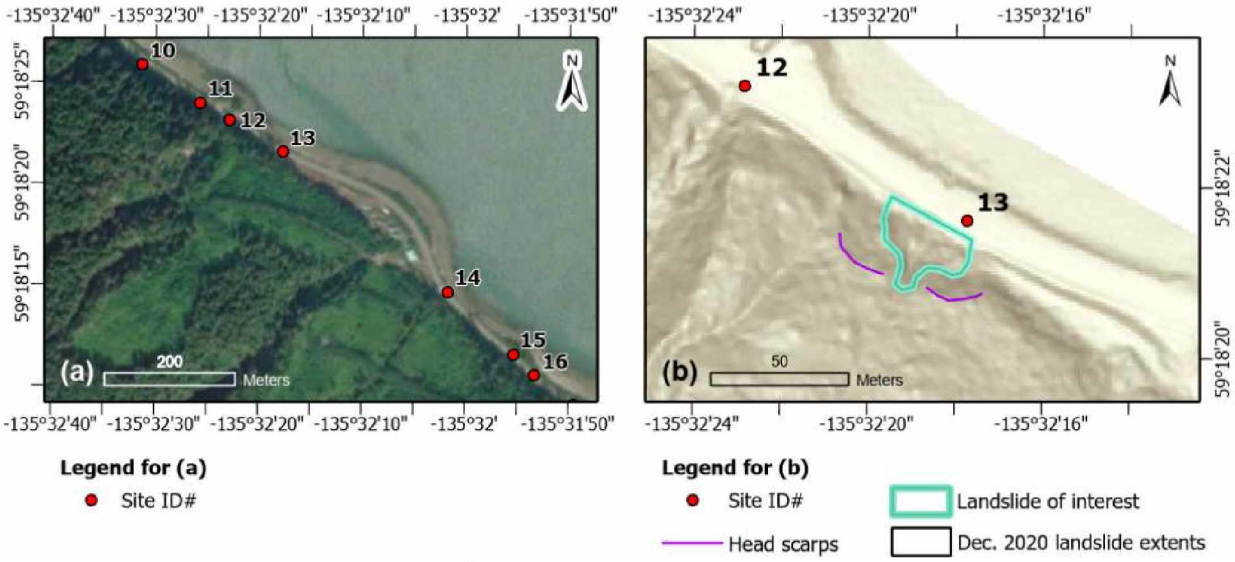

Figure 39. Maps showing location of FEMA DOT#24 (site 13): (a) 50-cm resolution RGB imagery (basemap from ADNR, 2020); (b) slope map derived from 2020 lidar (Daanen and others, 2021). ***NOTE:*** *the legend is standard for all maps; not all items may be present in (b).*

Figure 40. View of slope failure at FEMA DOT#24 from Lutak Road in December 2020, post clean-up (photograph courtesy of ADOT&PF).

Site ID#: 14 **Date Visited:** 6/17/2021
FEMA DOT#: 25 **Field Crew:** VN, MD
Field Name: Lutak Road
GPS Coordinates: UTM Z8 469604 6574034 (fig. 41)

Samples Taken: No samples were taken at this location.

Landslide Classification: *Debris flow*

Site Description: ADOT&PF (2020) reported a full blockage of Lutak Road. In the week following the storm events, ADOT&PF conducted further repairs as a result of piping through the embankment (when the culvert was plugged by debris) that caused road settlement. Figure 42 illustrates the site after clean-up.

Soil Stratigraphy: Not described; source area not investigated

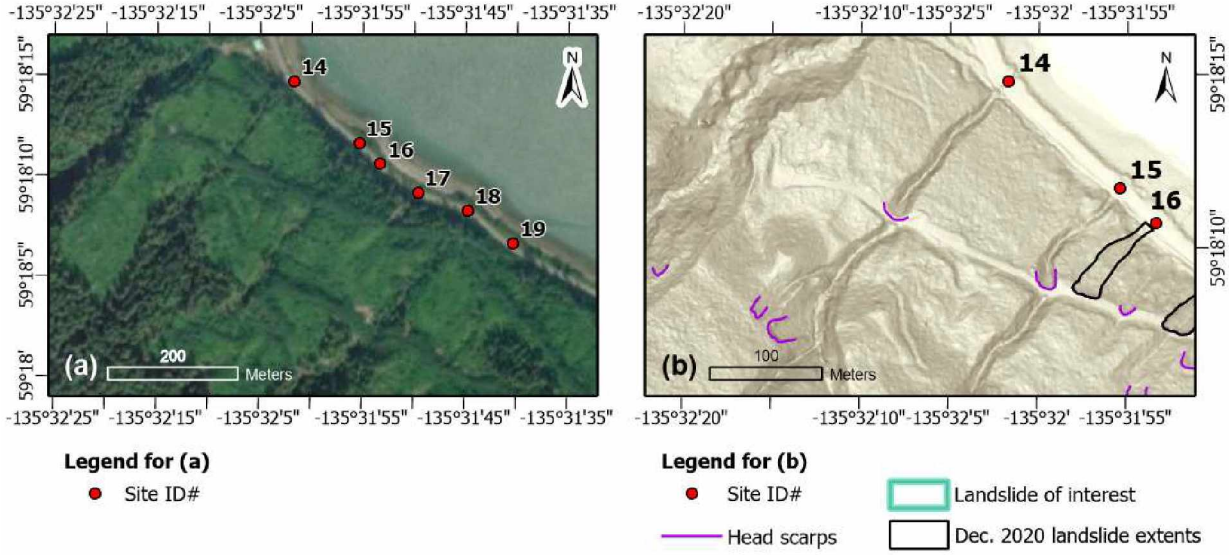

*Figure 41. Maps showing location of FEMA DOT#25 (site 14): (a) 50-cm resolution RGB imagery (basemap from ADNR, 2020); (b) slope map derived from 2020 lidar (Daanen and others, 2021). **NOTE:** the legend is standard for all maps; not all items may be present in (b).*

Figure 42. FEMA DOT#25 area in December 2020, following road clean-up (photograph courtesy of ADOT&PF).

Site ID#: 15 **Date Visited:** 6/18/2021
FEMA DOT#: 26 **Field Crew:** VN, MD
Field Name: Lutak Road
GPS Coordinates: UTM Z8 469704 6573945 (fig. 43)

Samples Taken: No samples were taken at this location.

Landslide Classification: *Debris flow*

Site Description: ADOT&PF (2020) reported that debris from this site was mostly contained within the ditch (fig. 44).

Soil Stratigraphy: Not described; source area not investigated

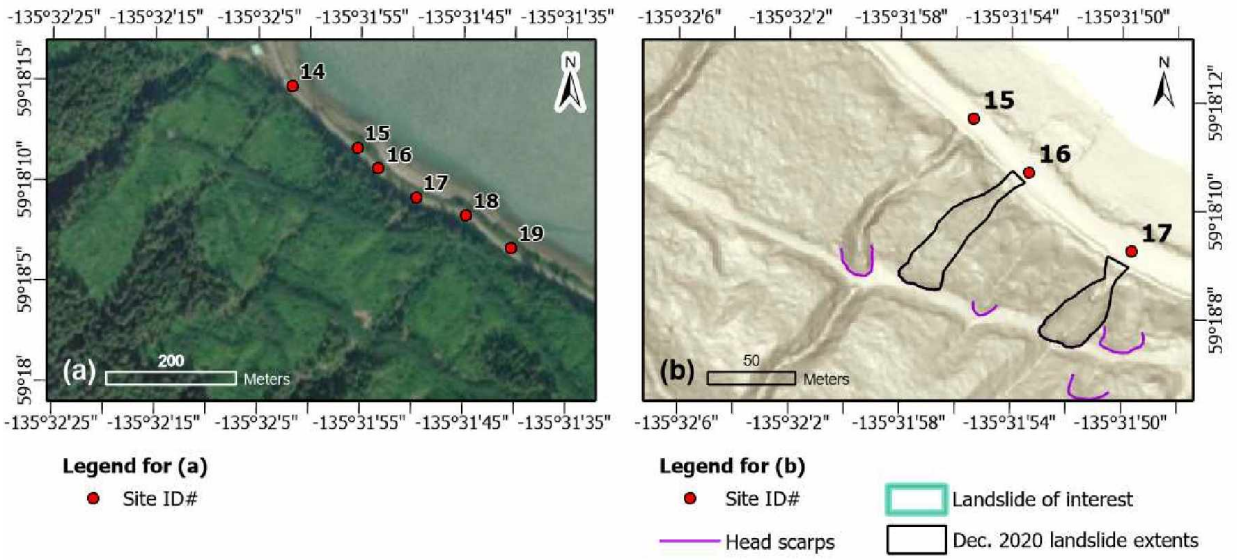

Figure 43. Maps showing location of FEMA DOT#26 (site 15): (a) 50-cm resolution RGB imagery (basemap from ADNR, 2020); (b) slope map derived from 2020 lidar (Daanen and others, 2021). ***NOTE:*** *the legend is standard for all maps; not all items may be present in (b).*

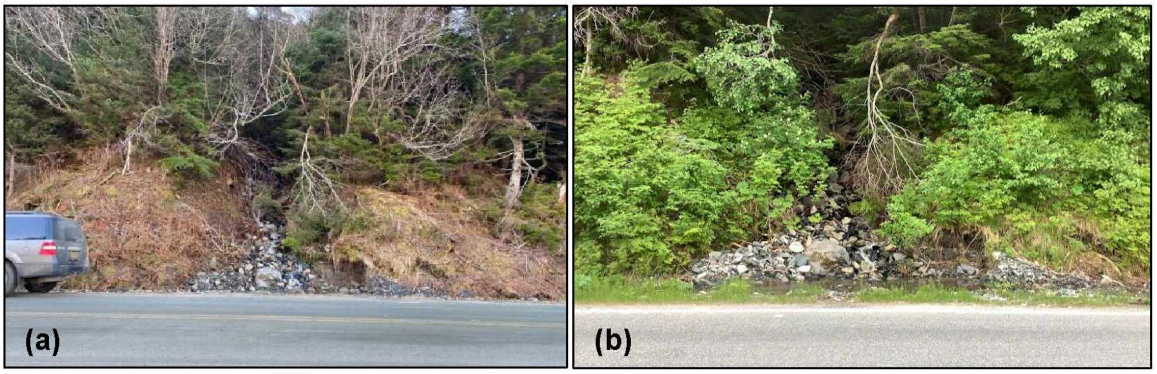

Figure 44. Photographs of FEMA DOT#26 channel in (a) December 2020 (photograph courtesy of ADOT&PF) and (b) June 2021.

Site ID#: 16 **Dates Visited:** 6/18, 6/21/2021; 7/21/2022
FEMA DOT#: 27 **Field Crew:** VN, MD, JW, MG
Field Name: Lutak Road
GPS Coordinates: UTM Z8 469702 6573888 (fig. 45)

Samples Taken: Samples were collected from the center of the landslide body, ~20 cm below the surface (*UTM Z8 469702 6573889*):

21-09 (bag) ***silty sand with gravel (SM)*** (fig. 46)
21-10 (tin) ***MC 14.3%***

Landslide Classification and Dimensions: *Debris slide*; length 96 m, width 33 m, L/W 2.9, aerial extent 603.2 m^2

Site Description: At this site, a landslide initiated below a logging road, occurring in colluvium and elevated shore and delta deposits (Lemke and Yehle, 1972; fig. 47). This landslide blocked both lanes of Lutak Road (ADOT&PF, 2020). We observed layering in the silty soil, expressed both as alternating light and dark layers and as coarse- and fine-grained textures. This layering may represent seasonal deposition.

Soil Stratigraphy: (Left flank)

0 – 10 cm	Bn Org mat
10 – 40 cm	Bn-Or Si Sa w/ Gr (colluvium)
> 40 cm	Gy Si Sa w/ Gr, cobbles, boulders (elevated shore and delta deposits)

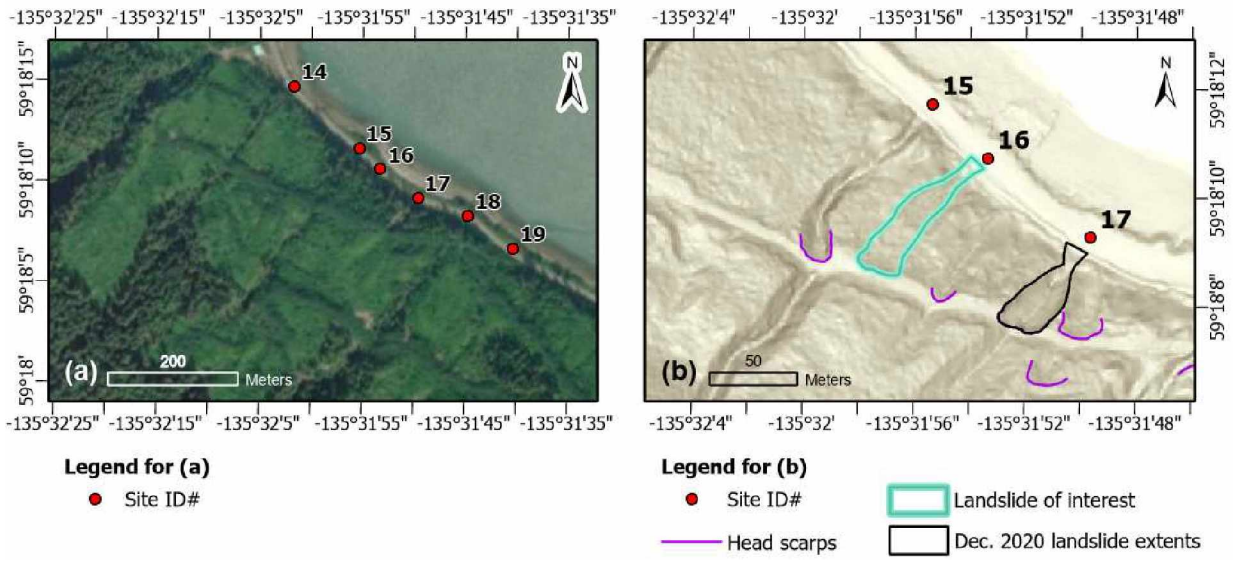

*Figure 45. Maps showing location of FEMA DOT#27 (site 16): (a) 50-cm resolution RGB imagery (basemap from ADNR, 2020); (b) slope map derived from 2020 lidar (Daanen and others, 2021). **NOTE:** the legend is standard for all maps; not all items may be present in (b).*

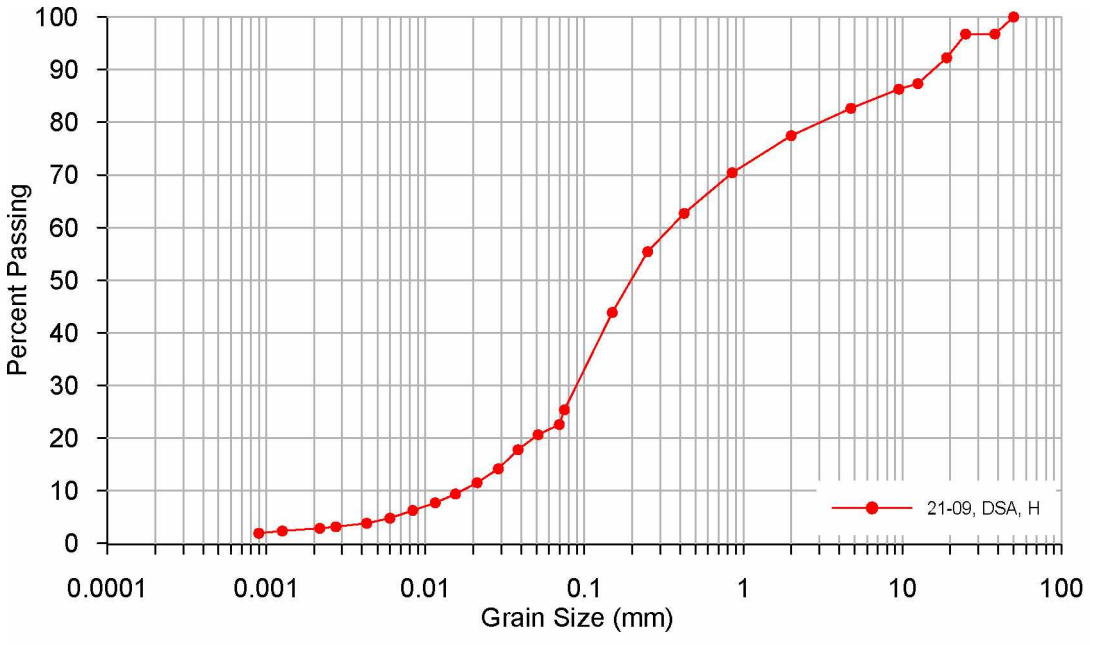

Figure 46. Grain-size distribution for sample 21-09.

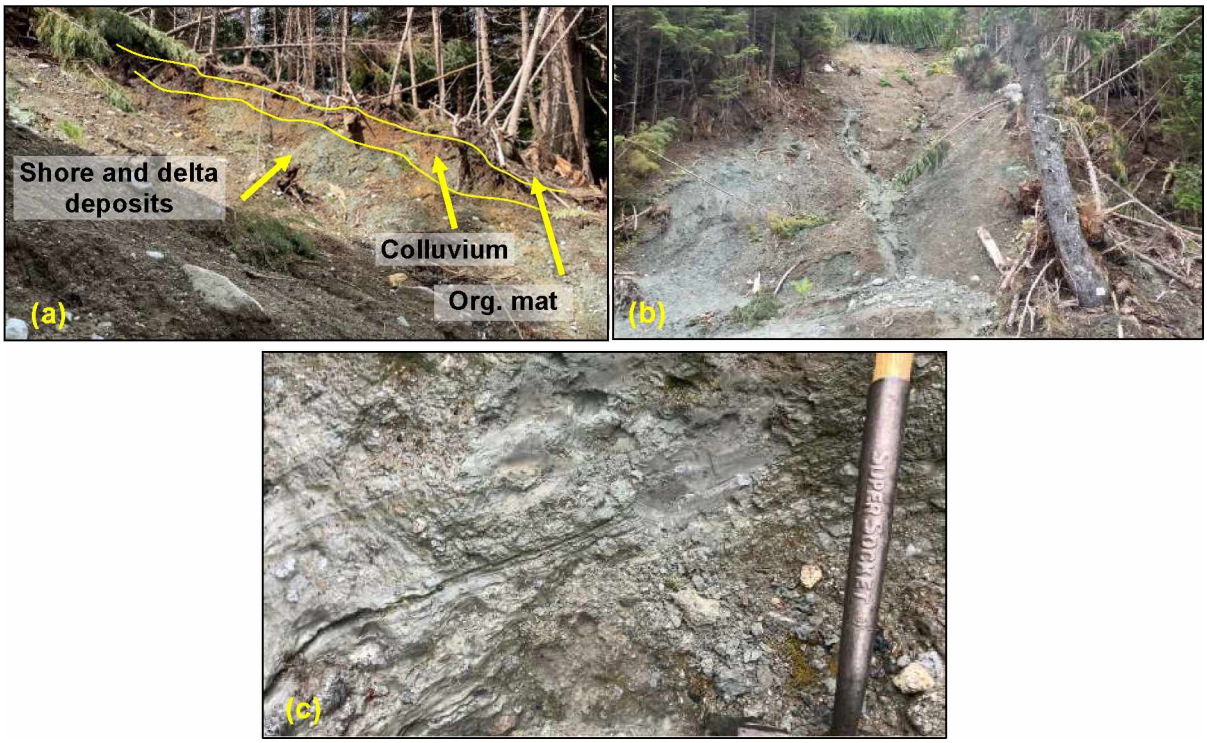

Figure 47. Photographs of FEMA DOT#27 slide area: (a) the left flank with annotated stratigraphy (June 2021); (b) looking up to the head scarp from Lutak Road (June 2021); (c) stratigraphy in the creek flowing down the slide path, showing light and dark layers (July 2022).

Site ID#: 17 **Dates Visited:** 6/18, 6/21/2021; 7/25/2022
FEMA DOT#: 28 **Field Crew:** VN, MD
Field Name: Lutak Road
GPS Coordinates: UTM Z8 469757 6573833 (fig. 48)

Samples Taken: Samples were collected from the landslide body, approximately mid-slope.
UTM Z8 469757 6573833:
21-07 (tin) ***MC 16.5%, Org 0.3%***
21-08 (bag) ***silty sand with gravel (SM)*** (fig. 49)

Landslide Classification and Dimensions: *Debris slide*; length 117 m, width 43 m, L/W 2.7, aerial extent 1,045.3 m^2

Site Description: The landslide at this site initiated below a logging road; a culvert outlet is exposed in the head scarp. The landslide occurred in colluvium and elevated beach and delta deposits (Lemke and Yehle 1972; fig. 50), and deposited several hundred cubic yards/meters of debris, blocking Lutak Road (ADOT&PF, 2020). We observed stratified silty sand with gravel in the slide area, along with cobbles and boulders up to 1 m in diameter. We also observed slabs of intrusive igneous rock (diorite, approx. 1 m by 0.1 m by 0.6 m) in the debris along the small drainage running through the landslide.

Soil Stratigraphy: (head scarp and along left flank)
0 – 50 cm Bn Org Si Sa w/ Gr (colluvium)
> 50 cm Gy Si Sa w/ Gr, stratified (elevated shore and delta deposits)

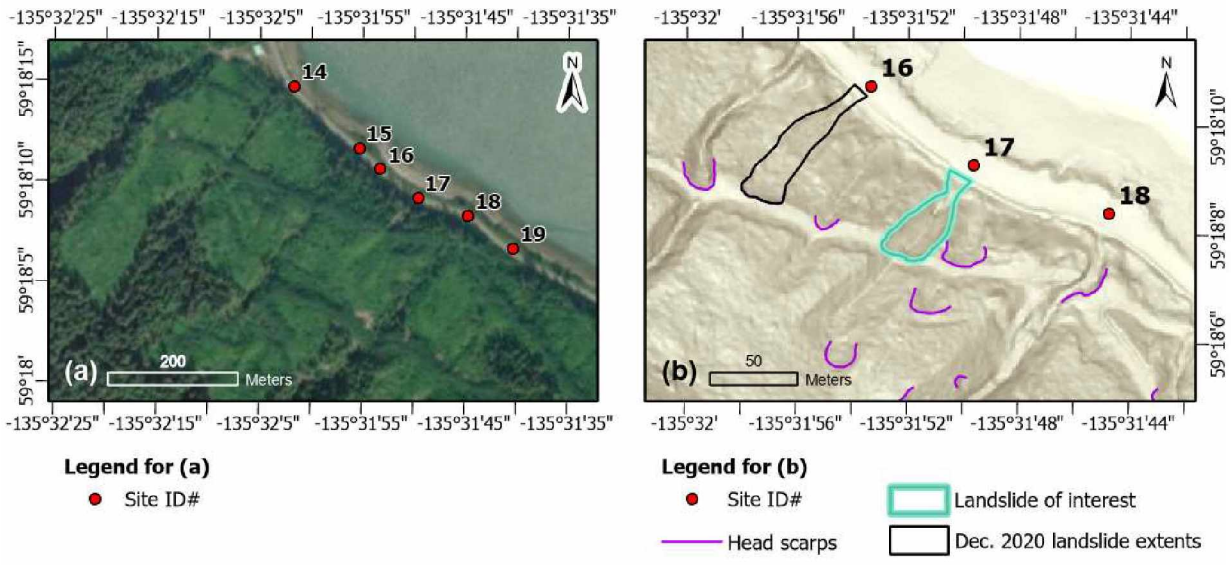

*Figure 48. Maps showing location of FEMA DOT#28 (site 17): (a) 50-cm resolution RGB imagery (basemap from ADNR, 2020); (b) slope map derived from 2020 lidar (Daanen and others, 2021). **NOTE:** the legend is standard for all maps; not all items may be present in (b).*

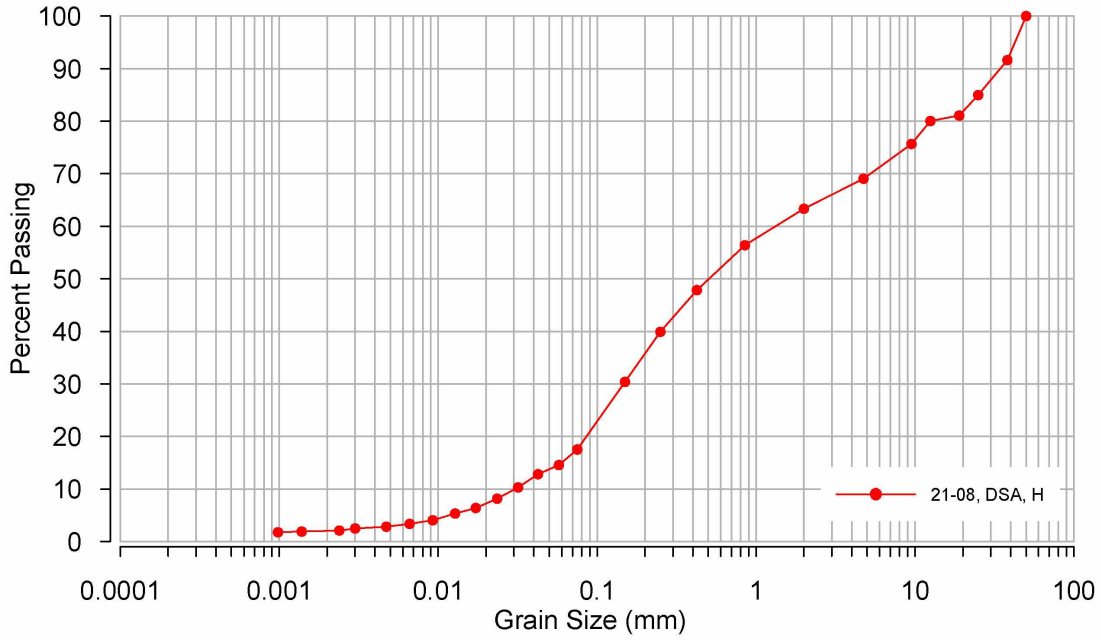

Figure 49. Grain-size distribution for sample 21-08.

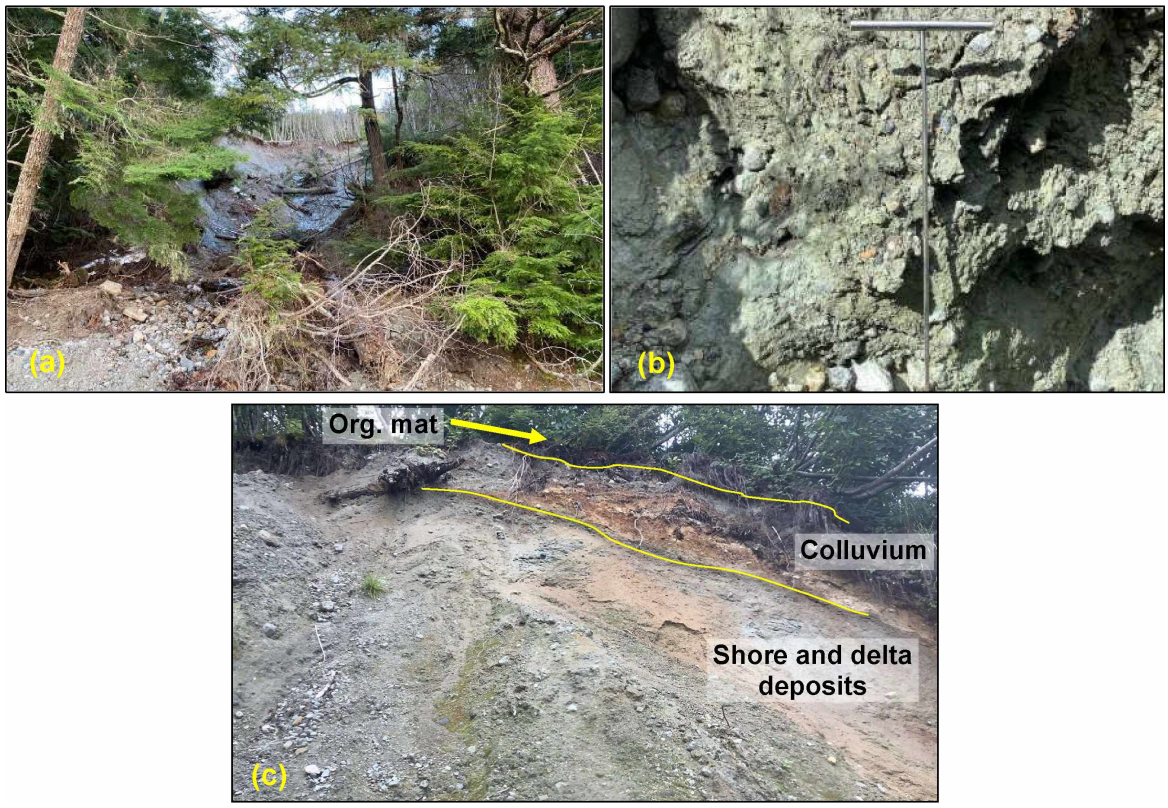

Figure 50. The FEMA DOT#28 landslide along Lutak Road: (a) view up to the head scarp in December 2020 (photograph courtesy of ADOT&PF); (b) silty sand with gravel exposed beneath the colluvium layer (June 2021); (c) sharp contact visible on left flank between colluvium and the underlying beach and delta deposits (July 2022).

Site ID#: 18 **Date Visited:** 6/18/2021
FEMA DOT#: 29 **Field Crew:** VN, MD
Field Name: Lutak Road
GPS Coordinates: UTM Z8 469875 6573842 (fig. 51)

Samples Taken: No samples were taken at this location.

Landslide Classification: *Debris flow*

Site Description: ADOT&PF (2020) marked this as a major impact, blocking both lanes of Lutak Road with several hundred cubic yards/meters of material (fig. 52).

Soil Stratigraphy: Not described; source area not investigated

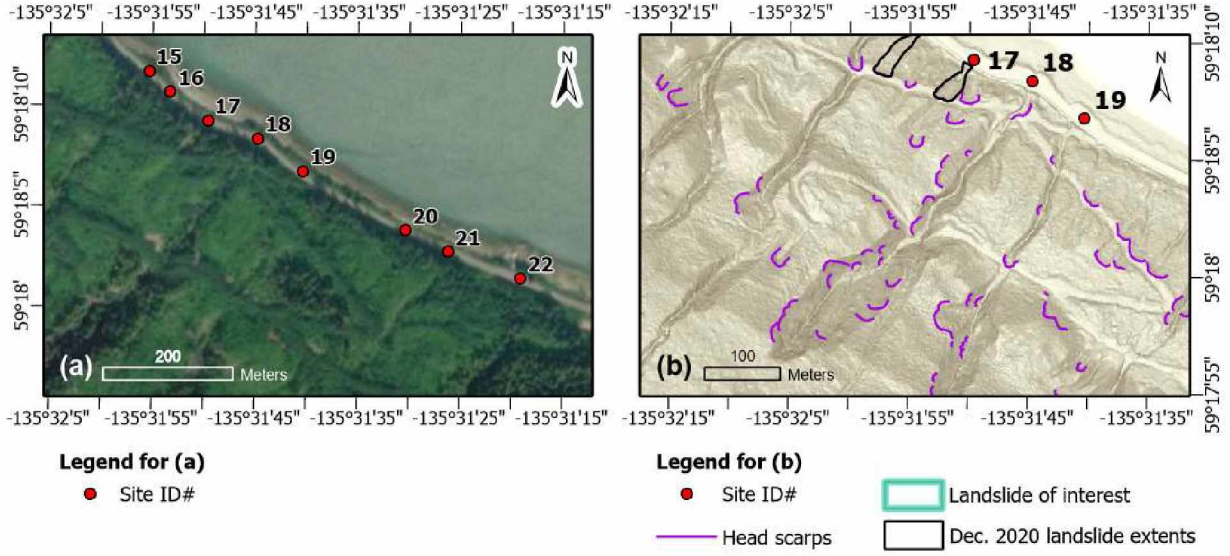

*Figure 51. Maps showing location of FEMA DOT#29 (site 18): (a) 50-cm resolution RGB imagery (basemap from ADNR, 2020); (b) slope map derived from 2020 lidar (Daanen and others, 2021). **NOTE:** the legend is standard for all maps; not all items may be present in (b).*

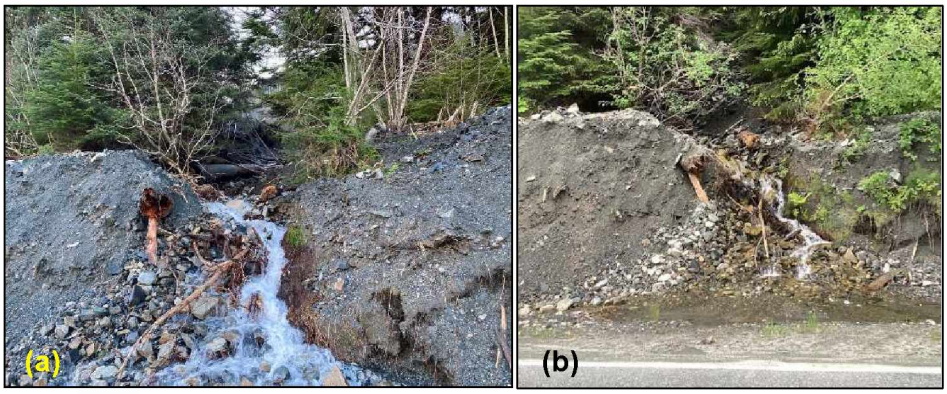

Figure 52. Views of the FEMA DOT#29 channel: (a) in December 2020 (photograph courtesy of ADOT&PF) and (b) in June 2021.

Site ID#: 19 **Date Visited:** 6/18/2021
FEMA DOT#: 30 **Field Crew:** VN, MD
Field Name: Lutak Road
GPS Coordinates: UTM Z8 469937 6573787 (fig. 53)

Samples Taken: No samples were taken at this location.

Landslide Classification: *Debris flow*

Site Description: ADOT&PF (2020) noted that the source of this debris flow was in the uphill logging area. Several hundred cubic yards/meters of debris had to be removed from both lanes of Lutak Road (fig. 54).

Soil Stratigraphy: Not described; source area not investigated

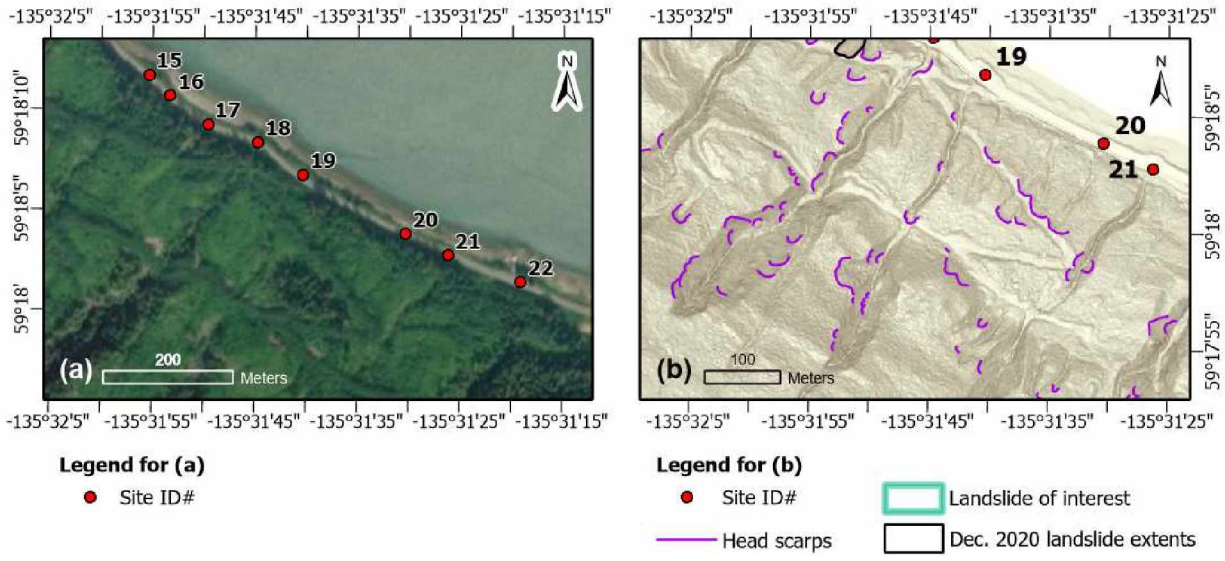

Figure 53. Maps showing location of FEMA DOT#30 (site 19): (a) 50-cm resolution RGB imagery (basemap from ADNR, 2020); (b) slope map derived from 2020 lidar (Daanen and others, 2021). ***NOTE:*** *the legend is standard for all maps; not all items may be present in (b).*

Figure 54. View of the FEMA DOT#30 channel mouth from Lutak Road in June 2021.

Site ID#: 20 **Date Visited:** 6/18/2021
FEMA DOT#: 31 **Field Crew:** VN, MD
Field Name: Lutak Road
GPS Coordinates: UTM Z8 470100 6573703 (fig. 55)

Samples Taken: No samples were taken at this location.

Landslide Classification: *Debris flow*

Site Description: ADOT&PF (2020) considered this site to be a minor deposit (less than 50 cubic yards (~30 m^3) of material deposited; fig. 56).

Soil Stratigraphy: Not described; source area not investigated

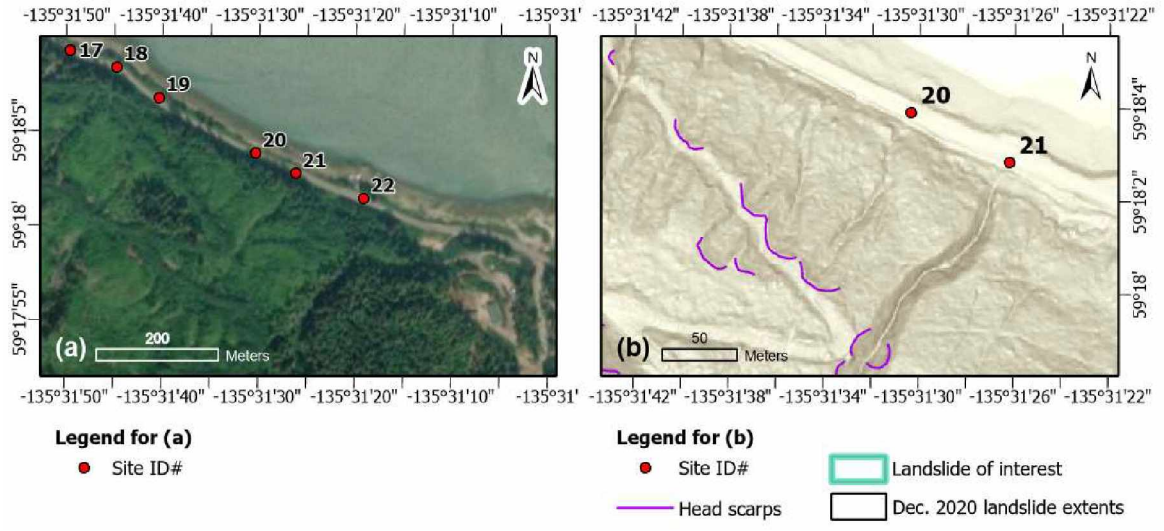

*Figure 55. Maps showing location of FEMA DOT#31 (site 20): (a) 50-cm resolution RGB imagery (basemap from ADNR, 2020); (b) slope map derived from 2020 lidar (Daanen and others, 2021). **NOTE:** the legend is standard for all maps; not all items may be present in (b).*

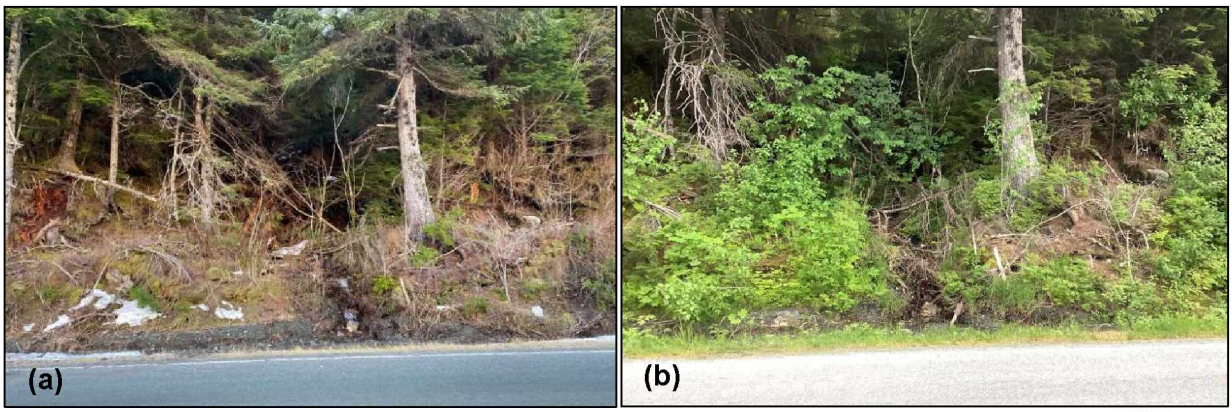

Figure 56. The channel at FEMA DOT#31 in (a) December 2020 (photograph courtesy of ADOT&PF) and (b) June 2021.

Site ID#: 21 **Date Visited:** 6/18/2021
FEMA DOT#: 32 **Field Crew:** VN, MD
Field Name: Lutak Road
GPS Coordinates: UTM Z8 470164 6573678 (fig. 57)

Samples Taken: No samples were taken at this location.

Landslide Classification: *Debris flow*

Site Description: From the road, we observed deeply-incised (~1–3 m), near-vertical walls of the drainage channel (fig. 58).

Soil Stratigraphy: Not described; source area not investigated

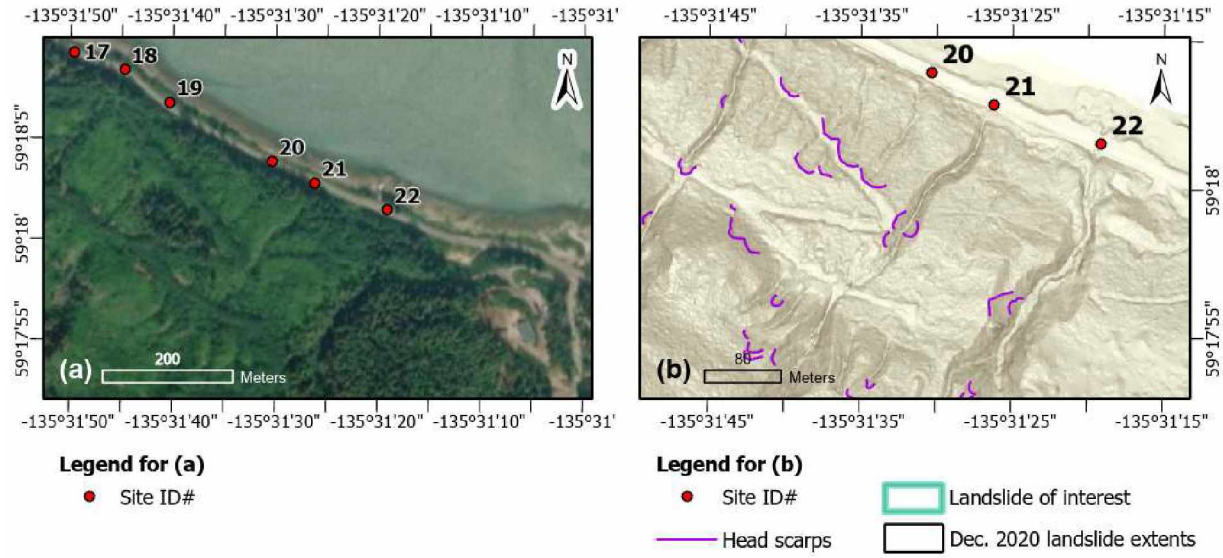

Figure 57. Maps showing location of FEMA DOT#32 (site 21): (a) 50-cm resolution RGB imagery (basemap from ADNR, 2020); (b) slope map derived from 2020 lidar (Daanen and others, 2021). ***NOTE:*** *the legend is standard for all maps; not all items may be present in (b).*

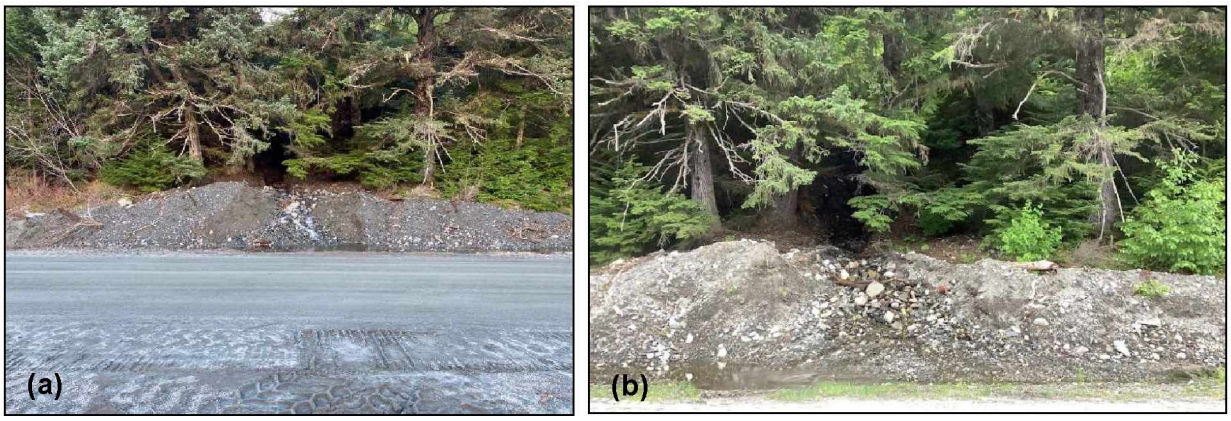

Figure 58. The channel at FEMA DOT#32 in (a) December 2020 (photograph courtesy of ADOT&PF) and (b) June 2021.

Site ID#: 22 **Date Visited:** 6/18/2021
FEMA DOT#: 33 **Field Crew:** VN, MD
Field Name: Lutak Road
GPS Coordinates: UTM Z8 470271 6573622 (fig. 59)

Samples Taken: No samples were taken at this location.

Landslide Classification: *Debris flow*

Site Description: This site is associated with a major channel having a significant source area. ADOT&PF (2020) reported between 750 and 1,000 cubic yards (570 – 760 cubic meters) of material removed from the site. Deposits of cobbles and boulders (< 0.6 m) were present along the road in June 2021 (fig. 60), as well as two vehicles buried by the deposits. This debris flow also impacted a cabin.

Soil Stratigraphy: Not described; source area not investigated

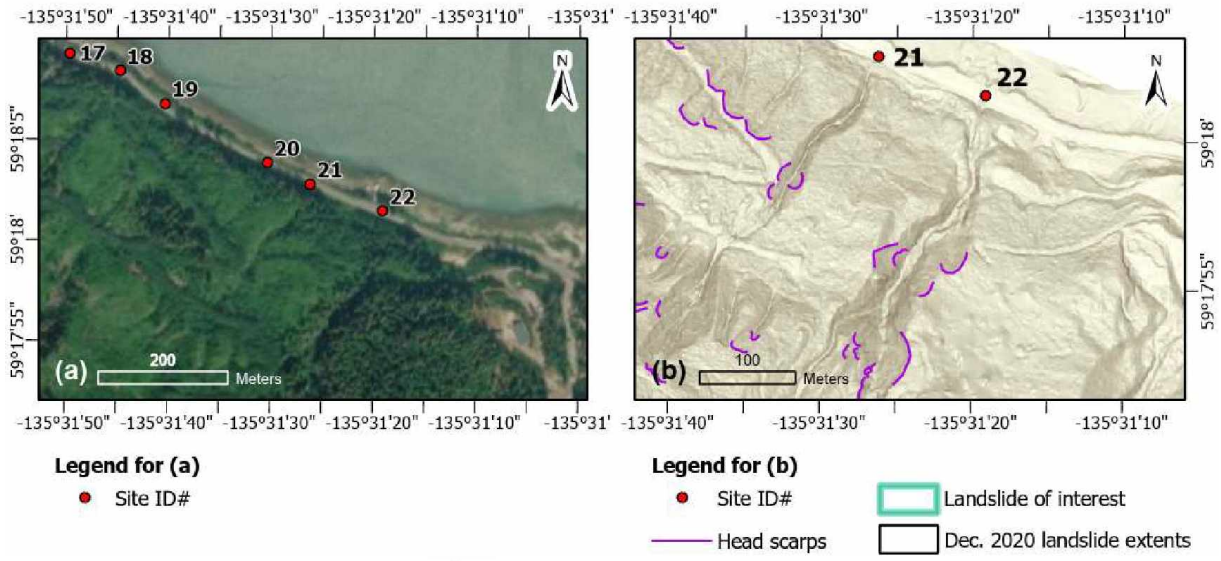

Figure 59. Maps showing location of FEMA DOT#33 (site 22): (a) 50-cm resolution RGB imagery (basemap from ADNR, 2020); (b) slope map derived from 2020 lidar (Daanen and others, 2021). ***NOTE:*** *the legend is standard for all maps; not all items may be present in (b).*

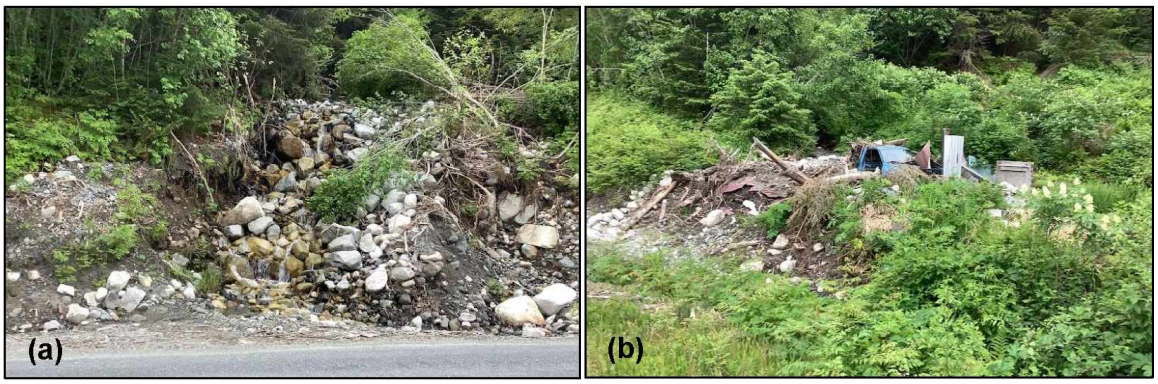

Figure 60. Photographs of FEMA DOT#33 (June 2021): (a) channel area; (b) a vehicle adjacent to the channel that was buried by debris.

Site ID#: 23 **Dates Visited:** 6/17, 6/18/2021
FEMA DOT#: 34 **Field Crew:** VN, MD
Field Name: Lutak Road
GPS Coordinates: UTM Z8 470842 6573204 (fig. 61)

Samples Taken: No samples were taken at this location.

Landslide Classification: *Debris flow*

Site Description: ADOT&PF (2020) reported removing between 500 and 750 cubic yards (380 – 570 cubic meters) of material from Lutak Road as a result of this debris flow. Several undercut trees were still in place at the top of the bank edges in June 2021 (fig. 62). We observed sub-horizontal stratigraphy in the right bank of the channel.

Soil Stratigraphy: Not described; source area not investigated

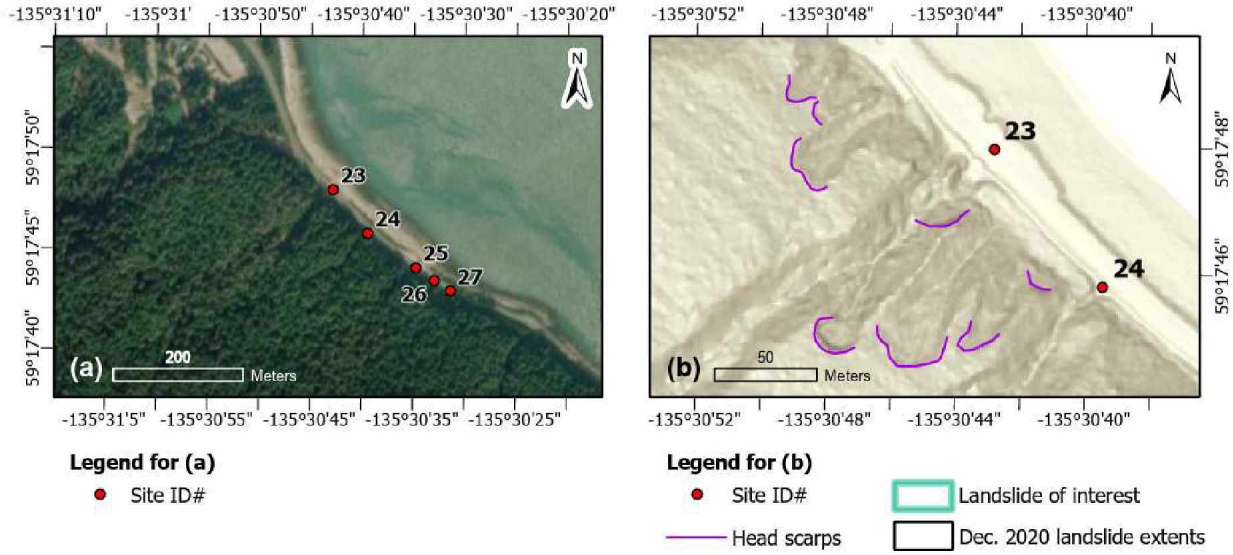

Figure 61. Maps showing location of FEMA DOT#34 (site 23): (a) 50-cm resolution RGB imagery (basemap from ADNR, 2020); (b) slope map derived from 2020 lidar (Daanen and others, 2021). ***NOTE:*** *the legend is standard for all maps; not all items may be present in (b).*

Figure 62. View of the FEMA DOT#34 channel from Lutak Road in June 2021.

Site ID#: 24 **Date Visited:** 6/18/2021
FEMA DOT#: 35 **Field Crew:** VN, MD
Field Name: Lutak Road
GPS Coordinates: UTM Z8 470900 6573142 (fig. 63)

Samples Taken: No samples were taken at this location.

Landslide Classification: *Debris flow*

Site Description: Less than 50 cubic yards (38 cubic meters) were deposited by this flow, and the deposit was mostly contained within the uphill ditch (fig. 64; ADOT&PF 2020).

Soil Stratigraphy: Not described; source area not investigated

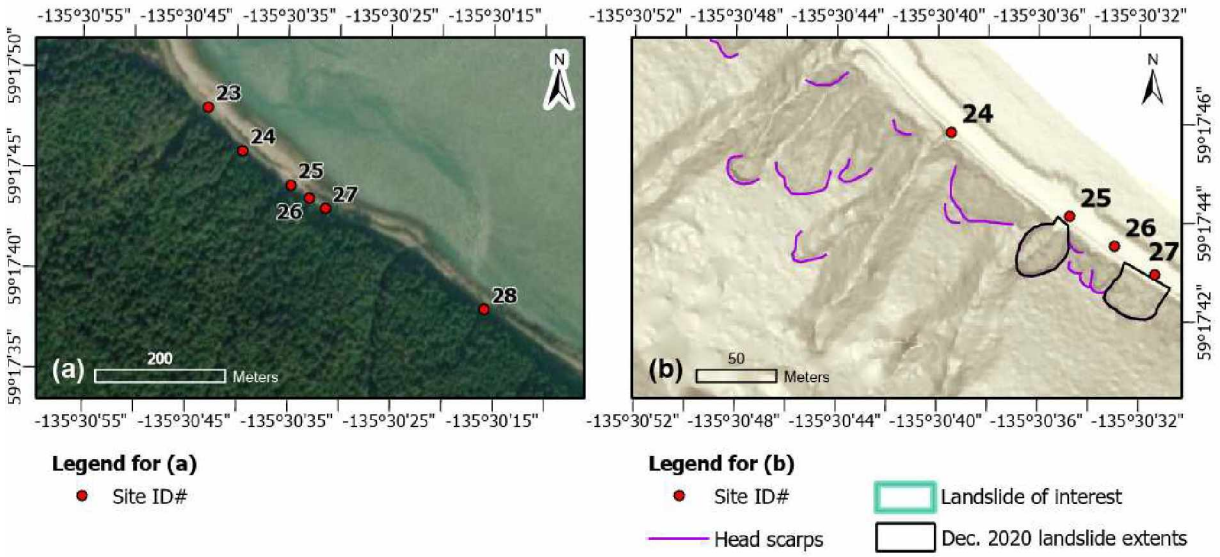

Figure 63. Maps showing location of FEMA DOT#35 (site 24): (a) 50-cm resolution RGB imagery (basemap from ADNR, 2020); (b) slope map derived from 2020 lidar (Daanen and others, 2021). ***NOTE:*** *the legend is standard for all maps; not all items may be present in (b).*

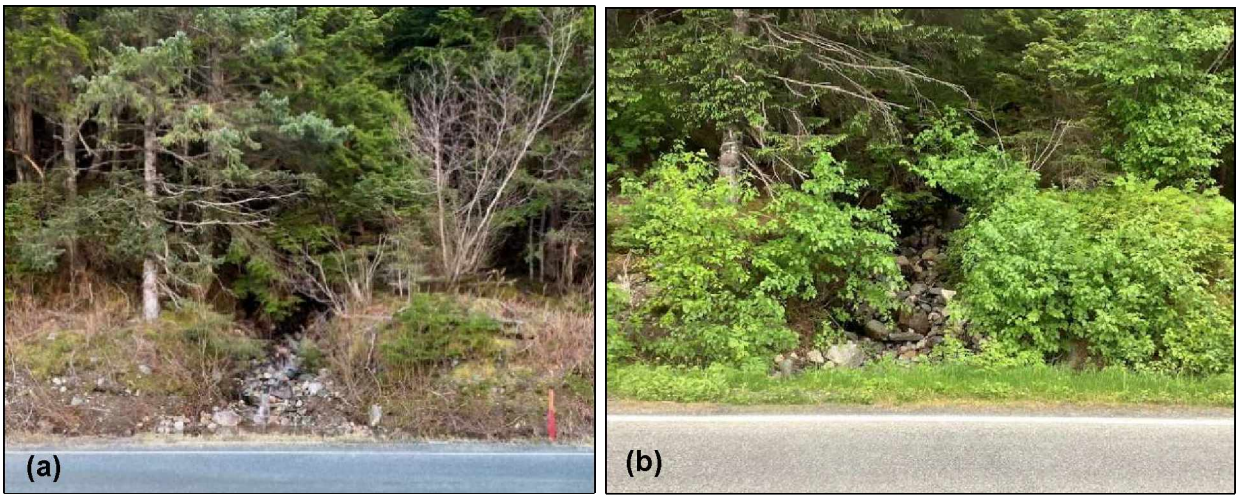

Figure 64. FEMA DOT#35 channel in (a) December 2020 (photograph courtesy of ADOT&PF) and (b) June 2021.

Site ID#: 25 **Date Visited:** 6/23/2021, 7/20/2022
FEMA DOT#: 36 **Field Crew:** VN, MD, RW
Field Name: Rubble Gulch, Lutak Road
GPS Coordinates: UTM Z8 470973 6573084 (fig. 65)

Samples Taken: Samples collected from the right flank *(UTM Z8 470968 6573056):*

21-28 (tin) ***MC 4.1%***
21-29 (bag) ***poorly-graded gravel with sand (GP)*** (fig. 66)

Samples collected from channel area uphill of debris slide (elev. ~230 m):

UTM Z8 470857 6572525:

22-14 (bag) ***poorly-graded sand (SP)*** (fig. 66)

UTM Z8 470870 6572565:

22-15 (tin) ***MC 8.5%***
22-16 (bag) ***silty sand (SM)*** (fig. 66)

Landslide Classification and Dimensions: *Debris slide*; length 16 m, width 39 m, L/W 0.4, aerial extent 578.3 m^2

Site Description: ADOT&PF (2020) estimated removing several hundred cubic yards/meters of material from this area, and that the slope failure likely occurred on the right steam bank. Observations made during the 2022 site visit also support this conclusion (fig. 67).

Soil Stratigraphy: (Right flank of debris slide; location of 2021 samples)

0 – 30 cm	Dk Bn Org mat
30 – 60 cm	Rd-Bn Org Gr Sa (colluvium)
>60 cm	Gy Gr w/ Sa, sub-horizontal stratification w/ cobbles (elevated beach deposits); Bn-Rd oxidation/cement present in upper 1 m [21-28, 21-29]

(Along right bank of channel uphill of debris slide; approximate location of 2022 samples)

0 – 27 cm	Org mat
27 – 31 cm	Gy-Wh Si Sa [22-15, 22-16]
31 – 43 cm	Bn-Or Si Sa (iron oxidized)

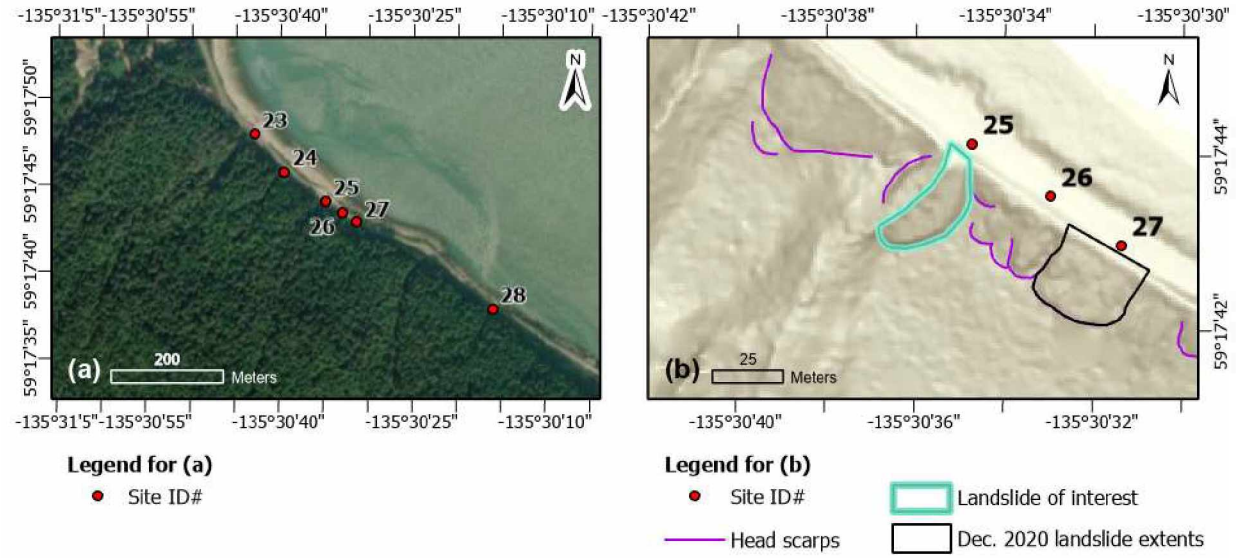

*Figure 65. Maps showing location of FEMA DOT#36 (site 25): (a) 50-cm resolution RGB imagery (basemap from ADNR, 2020); (b) slope map derived from 2020 lidar (Daanen and others, 2021). **NOTE:** the legend is standard for all maps; not all items may be present in (b).*

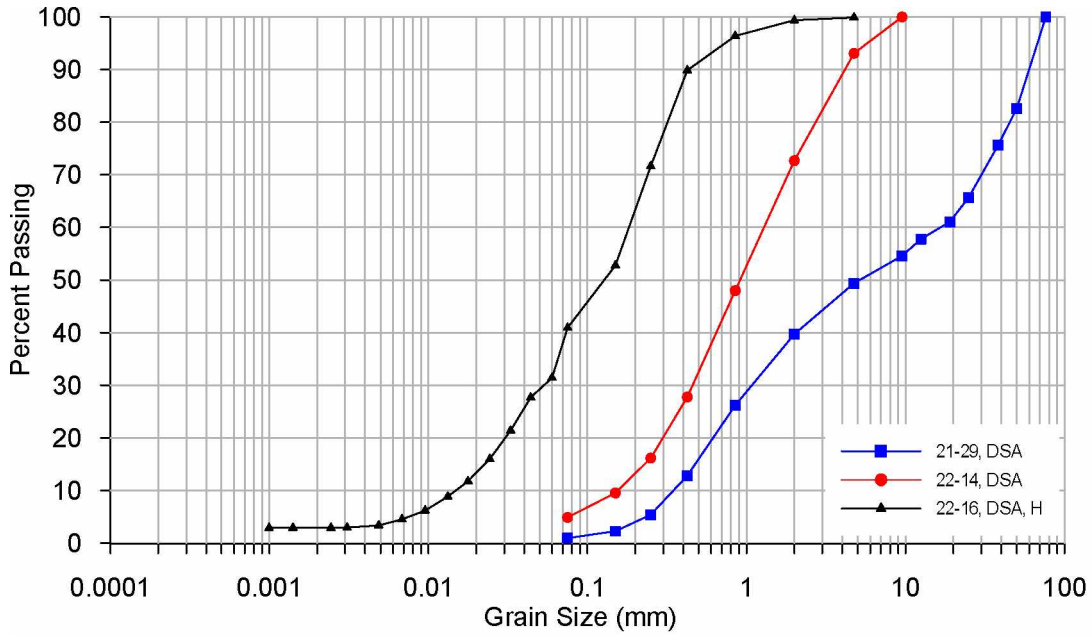

Figure 66. Grain-size distributions for samples 21-29, 22-14, and 22-16.

Figure 67. Photographs of the FEMA DOT#36 area (in June 2021): (a) the channel and head scarp area; (b) annotated view of stratigraphy visible within the right flank.

Site ID#: 26 **Date Visited:** 6/18/2021
FEMA DOT#: 37 **Field Crew:** VN, MD
Field Name: Lutak Road
GPS Coordinates: UTM Z8 470990 6573068 (fig. 68)

Samples Taken: No samples were taken at this location.

Landslide Classification: *Debris slide*

Site Description: This landslide had a minimal impact on the road and required little clearing (fig. 69; ADOT&PF, 2020).

Soil Stratigraphy: Not described; source area not investigated

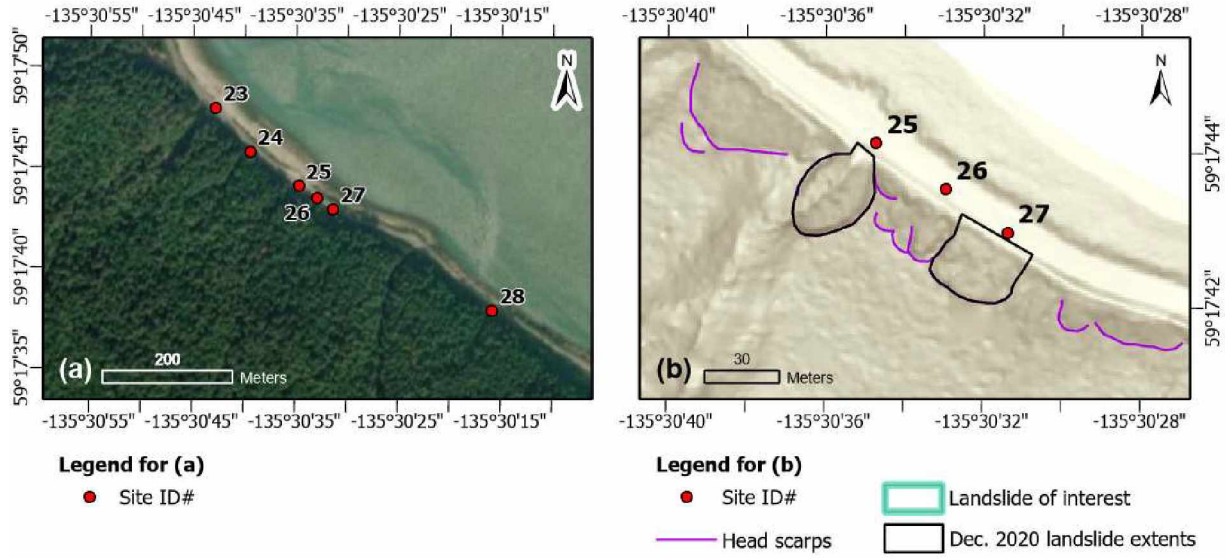

*Figure 68. Maps showing location of FEMA DOT#37 (site 26): (a) 50-cm resolution RGB imagery (basemap from ADNR, 2020); (b) slope map derived from 2020 lidar (Daanen and others, 2021). **NOTE:** the legend is standard for all maps; not all items may be present in (b).*

Figure 69. View of the failure at FEMA DOT#37 from Lutak Road (photograph courtesy of ADOT&PF).

Site ID#: 27 **Date Visited:** 6/18/2021
FEMA DOT#: 38 **Field Crew:** VN, MD
Field Name: Lutak Road
GPS Coordinates: UTM Z8 471026 6573051 (fig. 70)

Samples Taken: No samples were taken at this location.

Landslide Classification and Dimensions: *Debris slide*; length 29 m, width 32 m, L/W 0.9, aerial extent 879.5 m^2

Site Description: ADOT&PF (2020) reported this landslide as minor, depositing less than 100 cubic yards (76 cubic meters), most of which was retained in the ditch (fig. 71).

Soil Stratigraphy: Not described; source area not investigated

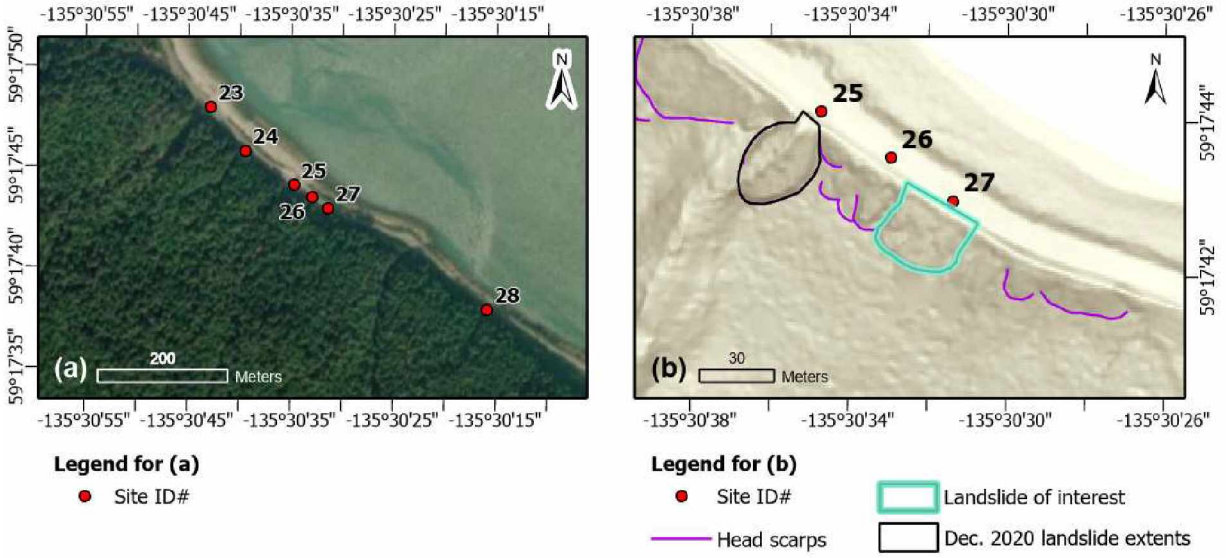

Figure 70. Maps showing location of FEMA DOT#38 (site 27): (a) 50-cm resolution RGB imagery (basemap from ADNR, 2020); (b) slope map derived from 2020 lidar (Daanen and others, 2021). ***NOTE:*** *the legend is standard for all maps; not all items may be present in (b).*

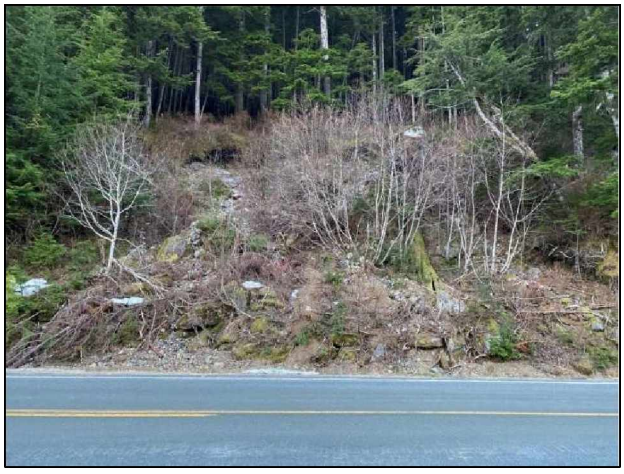

Figure 71. View of the landslide area at FEMA DOT#38 from Lutak Road in December 2020 (photograph courtesy of ADOT&PF).

Site ID#: 28 **Date Visited:** 6/18/2021
FEMA DOT#: 39 **Field Crew:** VN, MD
Field Name: Lutak Road
GPS Coordinates: UTM Z8 471271 6572894 (fig. 72)

Samples Taken: No samples were taken at this location.

Landslide Classification: *Debris flow*

Site Description: ADOT&PF (2020) reported that this was a minor landslide, with less than five cubic yards (four cubic meters) of material requiring removal (fig. 73).

Soil Stratigraphy: We observed thin soil coverage over exposed bedrock.

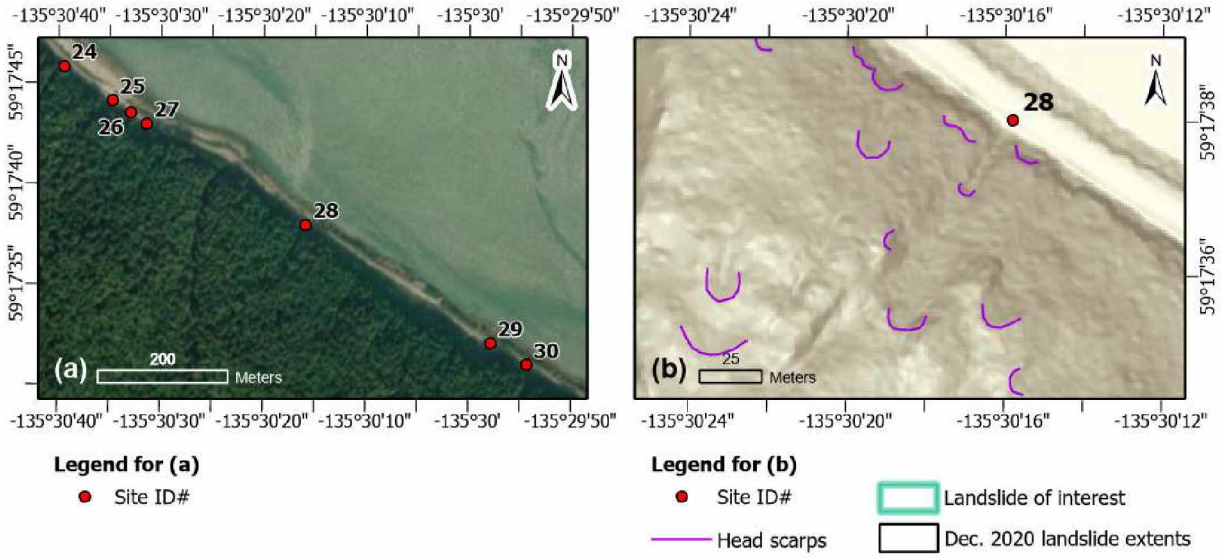

*Figure 72. Maps showing location of FEMA DOT#39 (site 28): (a) 50-cm resolution RGB imagery (basemap from ADNR, 2020); (b) slope map derived from 2020 lidar (Daanen and others, 2021). **NOTE:** the legend is standard for all maps; not all items may be present in (b).*

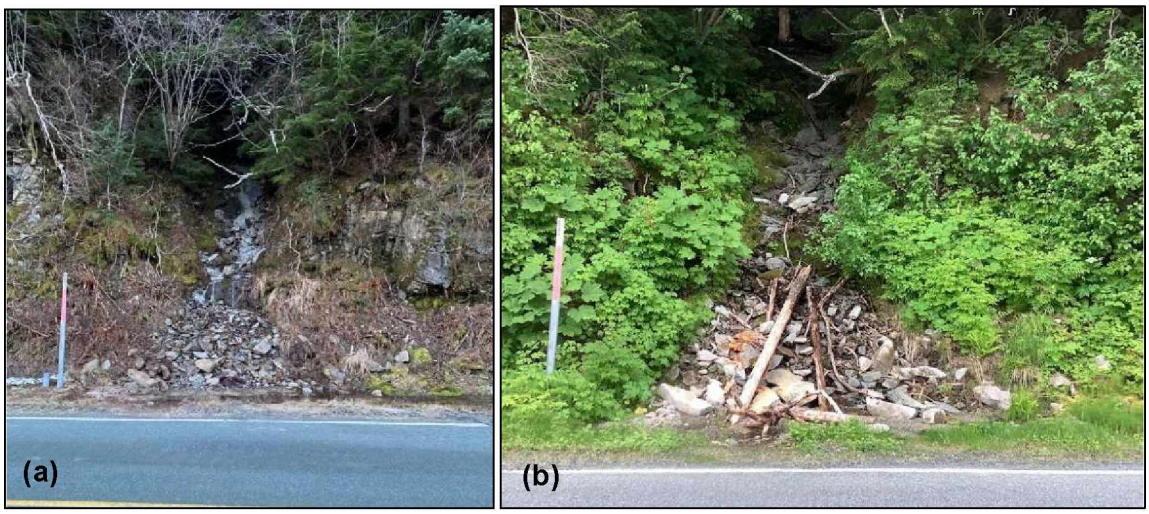

Figure 73. The FEMA DOT#39 channel in: (a) December 2020 (photograph courtesy of ADOT&PF); and (b) June 2021.

Site ID#: 29 **Date Visited:** 6/18/2021
FEMA DOT#: 40 **Field Crew:** VN, MD
Field Name: Lutak Road
Coordinates: UTM Z8 471550 6572715 (fig. 74)

Samples Taken: No samples were taken at this location.

Landslide Classification and Dimensions: *Debris slide*; length 82 m, width 54 m, L/W 1.5, aerial extent 457.8 m^2

Site Description: ADOT&PF (2020) described this site as a combined slope failure and debris flow (fig. 75); crews removed several hundred cubic yards/meters of material, which blocked both lanes of Lutak Road.

Soil Stratigraphy: We observed ~2-m thick colluvium with cobbles and boulders overlying exposed bedrock along the left flank (fig. 75).

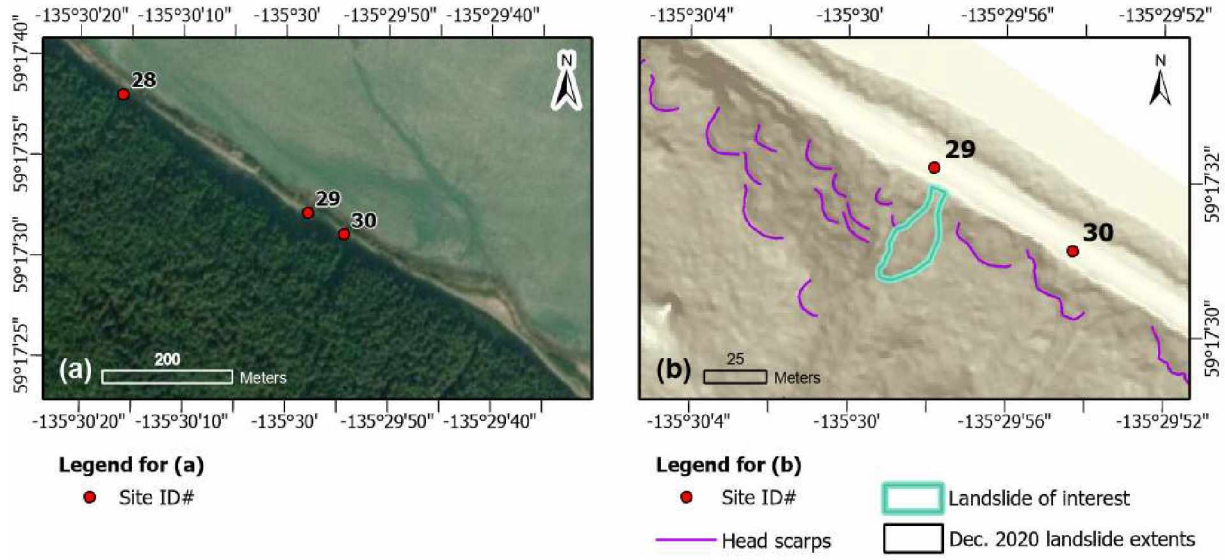

*Figure 74. Maps showing location of FEMA DOT#40 (site 29): (a) 50-cm resolution RGB imagery (basemap from ADNR, 2020); (b) slope map derived from 2020 lidar (Daanen and others, 2021). **NOTE:** the legend is standard for all maps; not all items may be present in (b).*

Figure 75. Views of the landslide at FEMA DOT#40 (June 2021): (a) annotated view of the left flank with exposed bedrock location; (b) right flank as visible from Lutak Road.

Site ID#: 30 **Date Visited:** 6/18/2021
FEMA DOT#: 41 **Field Crew:** VN, MD
Field Name: Lutak Road
GPS Coordinates: UTM Z8 471606 6572671 (fig. 76)

Samples Taken: No samples were taken at this location.

Landslide Classification: *Rock fall*

Site Description: ADOT&PF (2020) indicated approximately 50 cubic yards (38 cubic meters) of rock fall at this location, which was mostly contained within the uphill ditch. We observed that soil along the head scarp and flanks was being held in place by tree roots (fig. 77). ADOT&PF (2020) noted there was a "hazard tree" 50 ft (15 m) uphill from the road that was undercut by the failure.

Soil Stratigraphy: (head scarp area viewed from the road)

0 – 10 cm	Org mat (varies, up to 1-m thick)
>10 cm	Bn Sa with cobbles and boulders (colluvium), containing 2–3-m wide boulders (granitic)

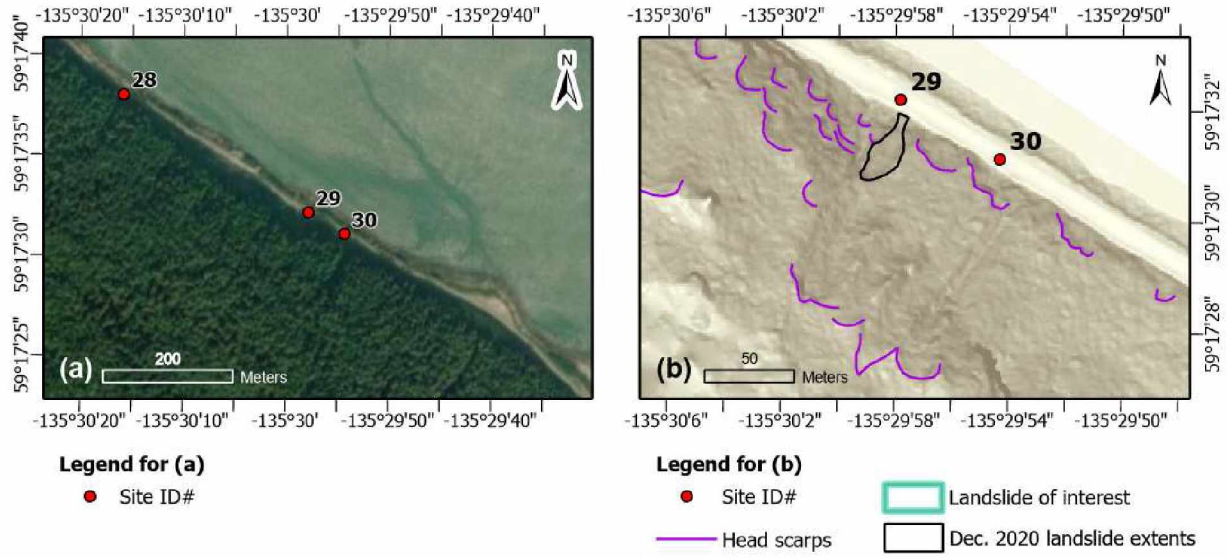

Figure 76. Maps showing location of FEMA DOT#41 (site 30): (a) 50-cm resolution RGB imagery (basemap from ADNR, 2020); (b) slope map derived from 2020 lidar (Daanen and others, 2021). ***NOTE:*** *the legend is standard for all maps; not all items may be present in (b).*

Figure 77. Views of the affected area at FEMA DOT#41: (a) slope in December 2020 (photograph courtesy of ADOT&PF); (b) head scarp area (June 2021).

Site ID#: 31 **Date Visited:** 6/18, 6/23/2021, 7/22/2022
FEMA DOT#: 42 **Field Crew:** VN, MD, MG, KB
Field Name: Stratigraphy Slide, Lutak Road
GPS Coordinates: UTM Z8 472268 6572107 (fig. 78)

Samples Taken: Samples were collected from the base of the slope *(UTM Z8 472268 6572107):*

21-05 (tin) ***MC 12.4%, Org 0.6%***
21-06 (bag) ***silty clayey sand (SC-SM)*** (fig. 79)

Vane shear testing – conducted near head scarp (UTM Z8 472253 6572072):

No. tests conducted:	10
Average shear strength:	4.9 kPa
Standard deviation:	± 1.2 kPa

Landslide Classification and Dimensions: *Debris slide*; length 103 m, width 184 m, L/W 0.6, aerial extent 4437.1 m^2

Site Description: This is a location of ongoing maintenance issues for ADOT&PF (Eckhoff, pers. comm., June 2021). In December 2020, debris from this location completely covered Lutak Road (fig. 80; ADOT&PF, 2020).

Soil Stratigraphy: (Eastern portion of landslide extent)

0 – 20 cm	Org mat
20 cm – 6 m	Bn-Rd Si Sa w/ Gr and 2-3-m dia. boulders (colluvium); cobble layer at base; sharp contact with underlying soil
6 m - ?	Gy Si Cl Sa w/ Gr, sub-horizontal stratification (elevated marine deposits) [21-05, 21-06]; contact with Bx (diorite) at base of slope is covered and uncertain; Bx exposed in lower third of slope

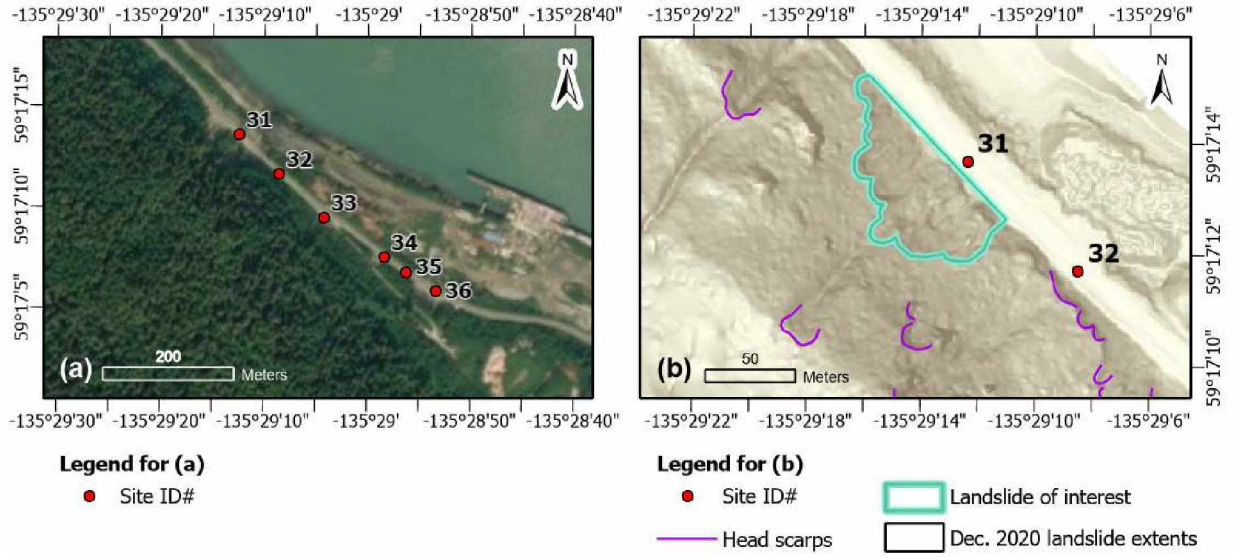

Figure 78. Maps showing location of FEMA DOT#42 (site 31): (a) 50-cm resolution RGB imagery (basemap from ADNR, 2020); (b) slope map derived from 2020 lidar (Daanen and others, 2021). ***NOTE:*** *the legend is standard for all maps; not all items may be present in (b).*

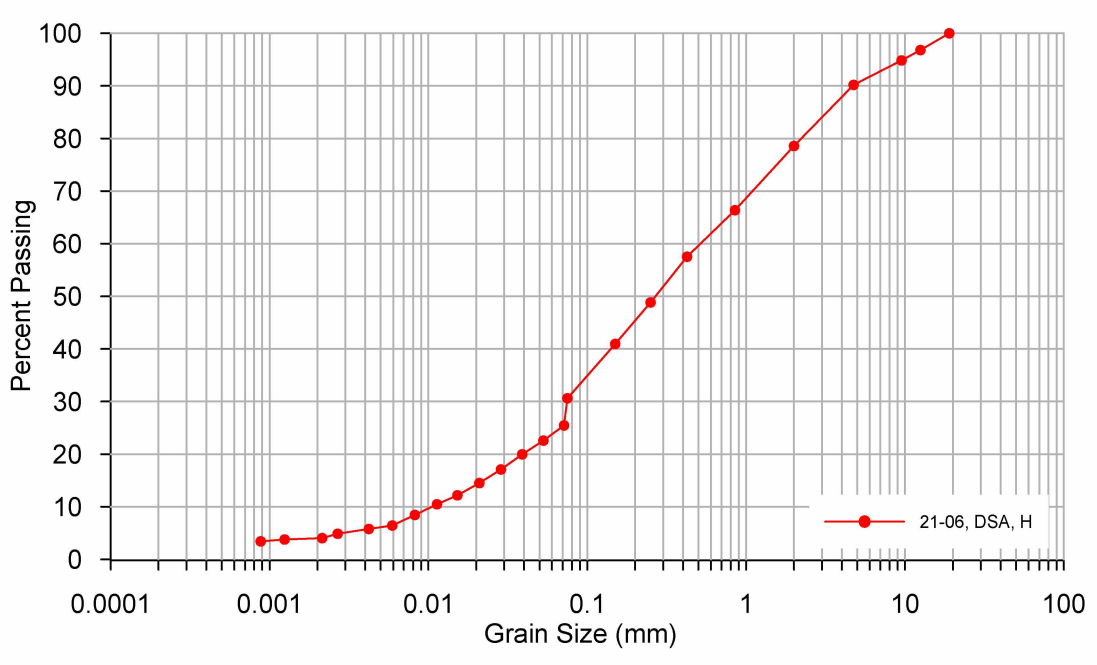

Figure 79. Grain-size distribution for sample 21-06.

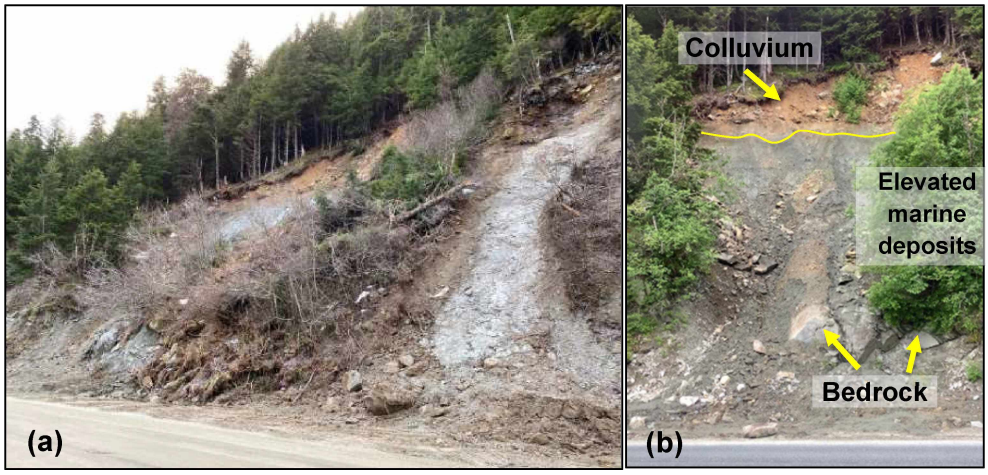

Figure 80. Views of the affected area at FEMA DOT#42: (a) extent of failure in December 2020 (photograph courtesy of ADOT&PF); (b) annotated view of debris slide area with exposed bedrock, in June 2021.

Site ID#: 32
FEMA DOT#: 43
Field Name: Lutak Road
GPS Coordinates: UTM Z8 472333 6572078 (fig. 81)

Date Visited: 6/18, 6/23/2021
Field Crew: VN, MD, MG

Samples Taken: No samples were taken at this location.

Landslide Classification: Debris slide–debris flow

Site Description: ADOT&PF (2020) noted that the slope failure occurred above the rock face. We suspect this landslide originated in an existing drainage upslope (fig. 82). Bedrock in the area is diorite.

Soil Stratigraphy: Not described; source area not investigated

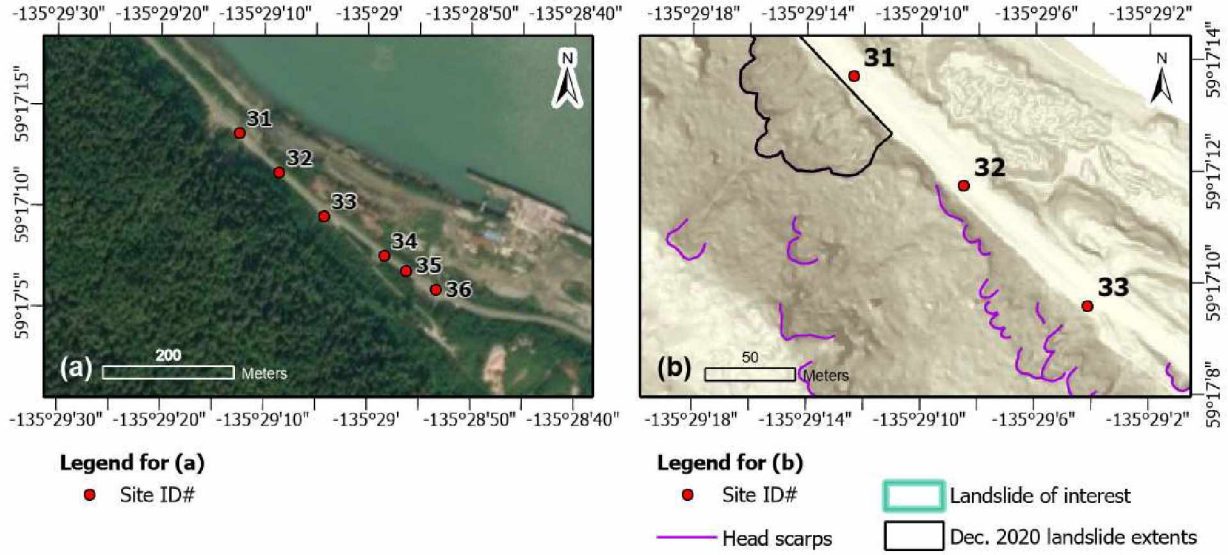

*Figure 81. Maps showing location of FEMA DOT#43 (site 32): (a) 50-cm resolution RGB imagery (basemap from ADNR, 2020); (b) slope map derived from 2020 lidar (Daanen and others, 2021). **NOTE:** the legend is standard for all maps; not all items may be present in (b).*

Figure 82. View of the landslide area at FEMA DOT#43 from Lutak Road in December 2020 (courtesy ADOT&PF).

Site ID#: 33 **Date Visited:** 6/18/2021
FEMA DOT#: 44 **Field Crew:** VN, MD
Field Name: Lutak Road
GPS Coordinates: UTM Z8 472404 6572010 (fig. 83)

Samples Taken: No samples were taken at this location.

Landslide Classification: Debris slide–debris flow

Site Description: ADOT&PF (2020) described this area as having six main debris sources ranging from 20 to 70 ft (6 to 21 m) up the slope with widths range from 20 to 50 ft (6 to 15 m), with the largest to the south (fig. 84). Several hundred cubic yards/meters of material were cleared from the area. We observed granitic cobbles at this site in June 2021; however, most of the landslide area was obscured by vegetation.

Soil Stratigraphy: Not described; source area not investigated

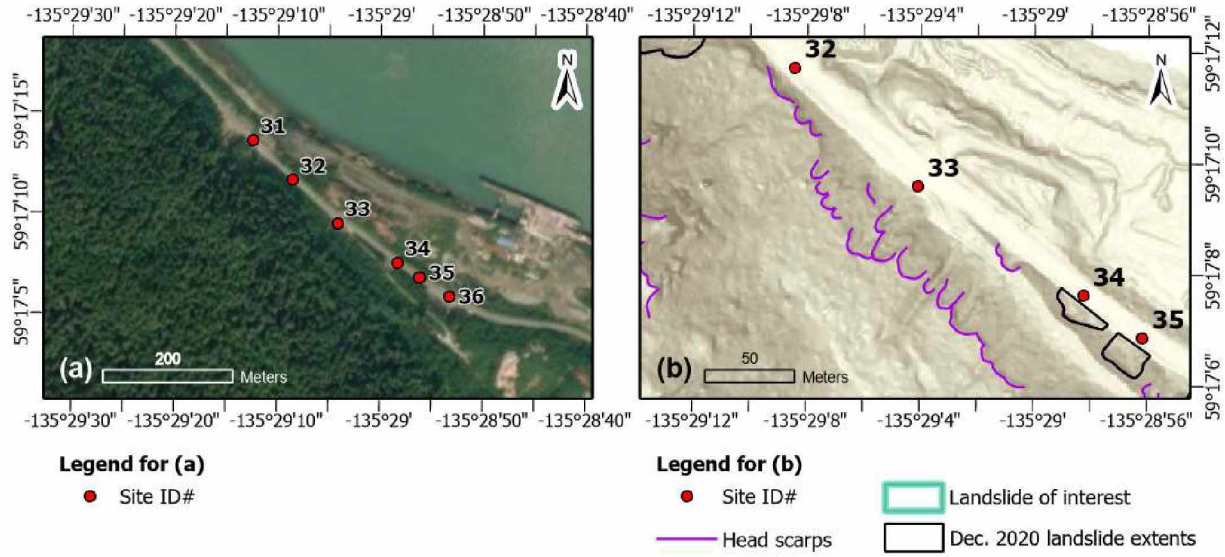

*Figure 83. Maps showing location of FEMA DOT#44 (site 33): (a) 50-cm resolution RGB imagery (basemap from ADNR, 2020); (b) slope map derived from 2020 lidar (Daanen and others, 2021). **NOTE:** the legend is standard for all maps; not all items may be present in (b).*

Figure 84. Collection of photographs of the FEMA DOT#44 landslide area in December 2020, showing evidence of both debris slides and debris flows (photographs courtesy of ADOT&PF).

Site ID#: 34 **Date Visited:** 6/18/2021
FEMA DOT#: 45 **Field Crew:** VN, MD
Field Name: Lutak Road
GPS Coordinates: UTM Z8 472490 6571942 (fig. 85)

Samples Taken: No samples were taken at this location.

Landslide Classification and Dimensions: *Debris slide*; length 11 m, width 32 m, L/W 0.3, aerial extent 260.9 m^2

Site Description: ADOT&PF (2020) described this area as a slope failure within coarse material (fig. 86).

Soil Stratigraphy: We observed ~7 m of soil consisting of silt, sand, and gravel with cobbles and boulders, outwash and ice-contact deposits or drift deposits (Lemke and Yehle, 1972). The average slope angle at this site was ~40°.

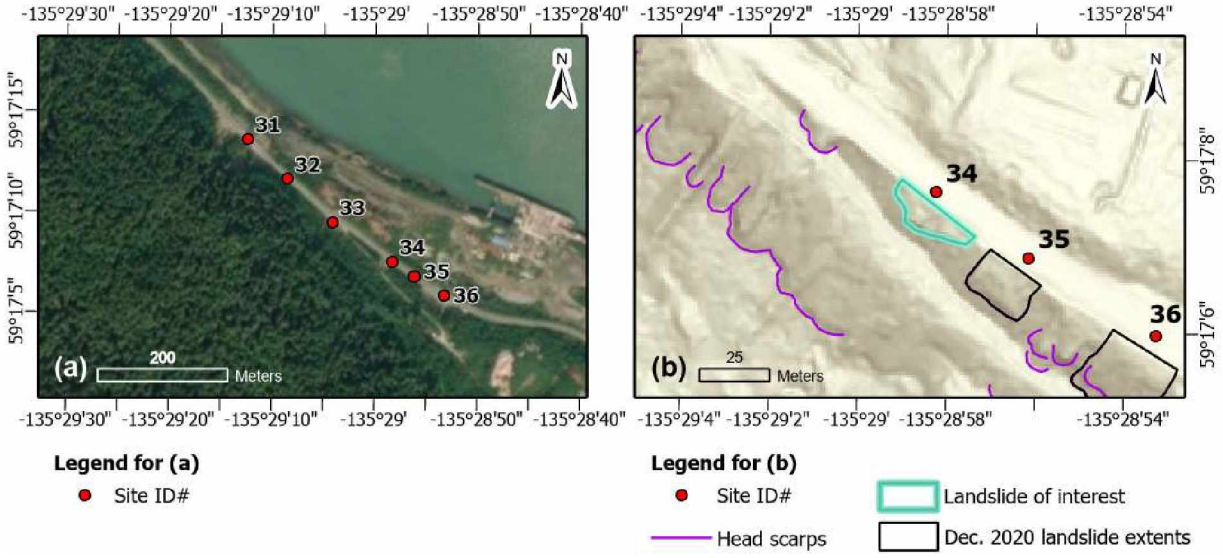

*Figure 85. Maps showing location of FEMA DOT#45 (site 34): (a) 50-cm resolution RGB imagery (basemap from ADNR, 2020); (b) slope map derived from 2020 lidar (Daanen and others, 2021). **NOTE:** the legend is standard for all maps; not all items may be present in (b).*

Figure 86. View of the failure at FEMA DOT#45 from Lutak Road in December 2020 (photograph courtesy of ADOT&PF).

Site ID#: 35 **Date Visited:** 6/18/2021
FEMA DOT#: 46 **Field Crew:** VN, MD
Field Name: Lutak Road
GPS Coordinates: UTM Z8 472523 6571920 (fig. 87)

Samples Taken: No samples were taken at this location.

Landslide Classification and Dimensions: *Debris slide*; length 16 m, width 23 m, L/W 0.7, aerial extent 358.7 m^2

Site Description: ADOT&PF (2020) cleared approximately 100 cubic yards (~76 cubic meters) from Lutak Road at this site; soil clasts were raveling from the slope as crews were clearing (fig. 88).

Soil Stratigraphy: We observed ~11 m of soil consisting of silt, sand, and gravel with cobbles and boulders. This site is similar to site 34 (outwash and ice-contact deposits or drift deposits), but with an average slope angle of ~50°.

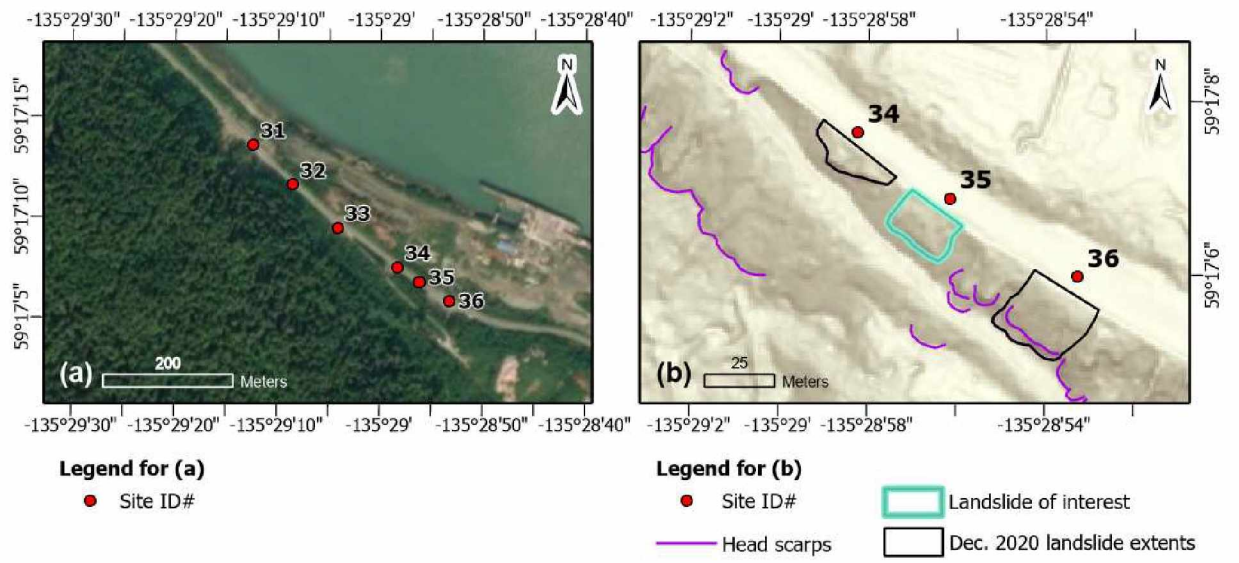

Figure 87. Maps showing location of FEMA DOT#46 (site 35): (a) 50-cm resolution RGB imagery (basemap from ADNR, 2020); (b) slope map derived from 2020 lidar (Daanen and others, 2021). ***NOTE:*** *the legend is standard for all maps; not all items may be present in (b).*

Figure 88. View of the failure at FEMA DOT#46 from Lutak Road in December 2020 (photograph courtesy of ADOT&PF).

Site ID#: 36 **Date Visited:** 6/18/2021
FEMA DOT#: 47 **Field Crew:** VN, MD
Field Name: Lutak Road
GPS Coordinates: UTM Z8 472571 6571895 (fig. 89)

Samples Taken: No samples were taken at this location.

Landslide Classification and Dimensions: *Debris slide*; length 65 m, width 120 m, L/W 0.5, aerial extent 680.7 m^2

Site Description: ADOT&PF (2020) noted that the affected area for this location was significant, and that material was still raveling from the surface after three days of no precipitation following the storm event. Several hundred cubic yards of material were deposited in the ditch and road (ADOT&PF, 2020). The landslide occurred in coarse-grained soil (fig. 90).

Soil Stratigraphy: The soil consists of silt, sand, and gravel with cobbles and boulders (outwash and ice-contact deposits or drift deposits), approximately 20-m thick.

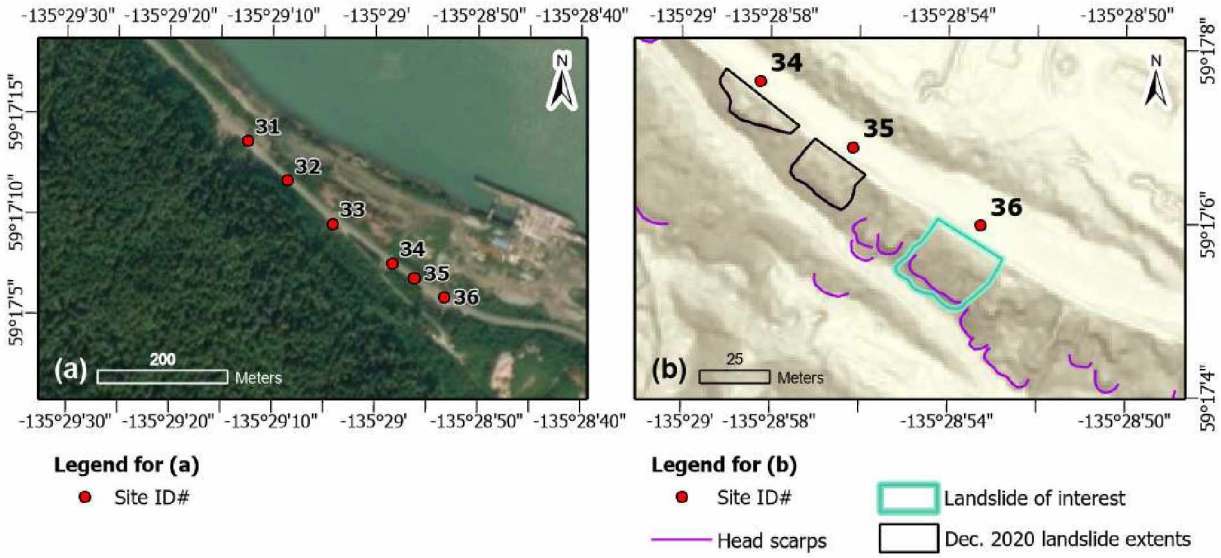

Figure 89. Maps showing location of FEMA DOT#47 (site 36): (a) 50-cm resolution RGB imagery (basemap from ADNR, 2020); (b) slope map derived from 2020 lidar (Daanen and others, 2021). ***NOTE:*** *the legend is standard for all maps; not all items may be present in (b).*

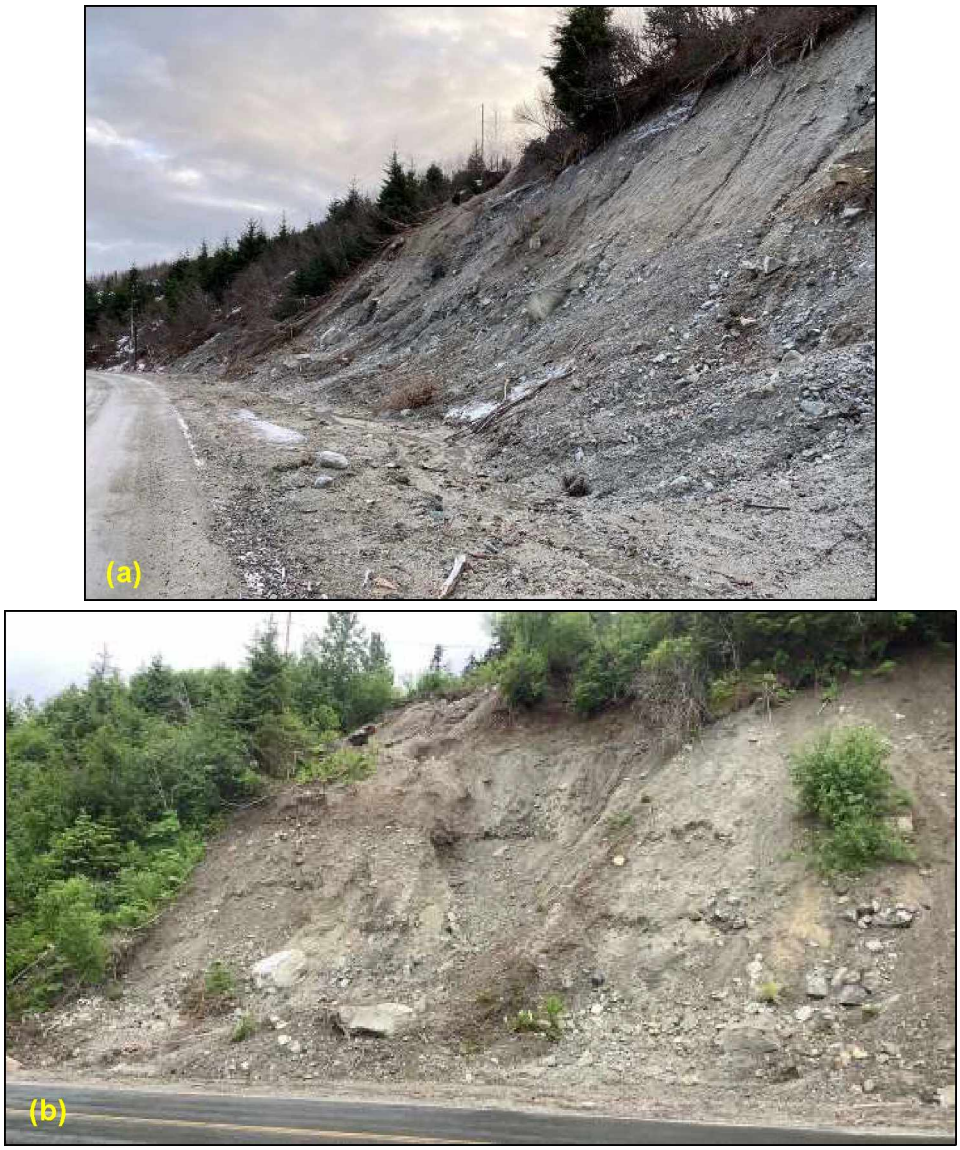

Figure 90. Views of the FEMA DOT#47 slide area in: (a) December 2020, following clean-up efforts (photograph courtesy of ADOT&PF); and (b) June 2021.

Site ID#: 37 **Date Visited:** 6/18/2021
FEMA DOT#: 48 **Field Crew:** VN, MD
Field Name: Lutak Road
GPS Coordinates: UTM Z8 472835 6571803 (fig. 91)

Samples Taken: No samples were taken at this location.

Landslide Classification: *Debris flow*

Site Description: At this site, we observed a channel containing granitic cobbles and boulders with minimal fine-grained soil (fig. 92). ADOT&PF (2020) noted that the area had a large debris source, as personnel removed several hundred cubic yards/meters of material.

Soil Stratigraphy: Not described; source area not investigated

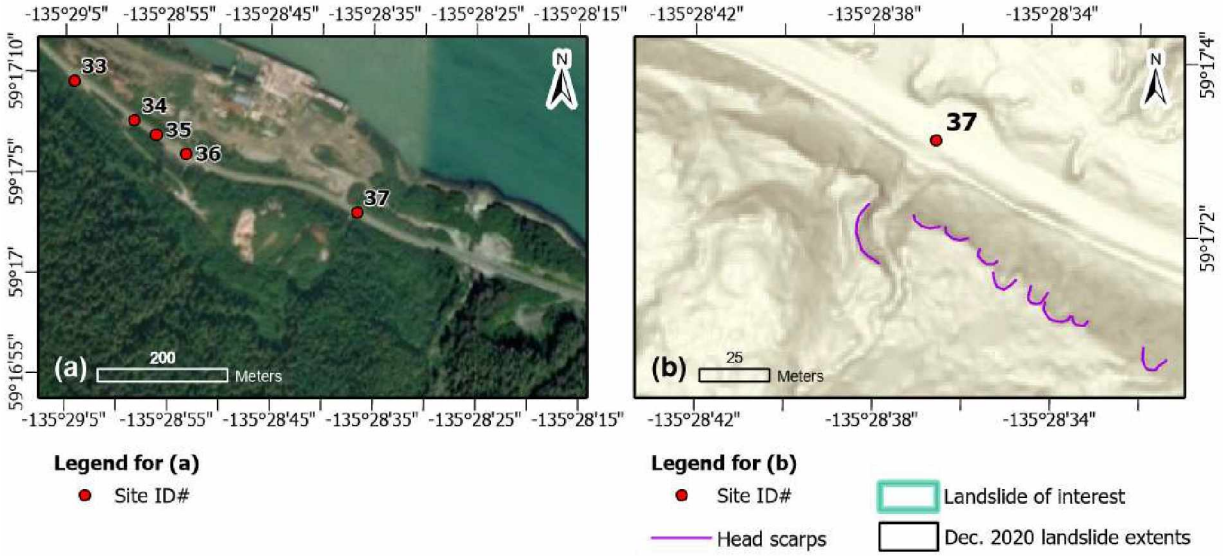

*Figure 91. Maps showing location of FEMA DOT#48 (site 37): (a) 50-cm resolution RGB imagery (basemap from ADNR, 2020); (b) slope map derived from 2020 lidar (Daanen and others, 2021). **NOTE:** the legend is standard for all maps; not all items may be present in (b).*

Figure 92. View of the FEMA DOT#48 channel from Lutak Road (facing south) in December 2020 (photograph courtesy of ADOT&PF).

Site ID#: 38 **Date Visited:** 6/18, 6/25/2021, 7/19/2022
FEMA DOT#: 49 **Field Crew:** VN, MD
Field Name: Haines Ferry Terminal
GPS Coordinates: UTM Z8 473536 6571497 (fig. 93)
Samples Taken: Samples collected from one of the head scarps above Lutak Road (elev. ~50 m).

Along right flank; *UTM Z8 473436 6571430*:
22-05 (bag) ***silty sand with gravel (SM)*** (fig. 94)
22-06 (tin) ***MC 13.2%***
Center of head scarp; *UTM Z8 473425 6571432*:
22-07 (bag) ***well-graded sand with silt and gravel (SW-SM)*** (fig. 94)
22-08 (tin) ***MC 8.0%***

Samples collected in a muskeg area on the slope above the Ferry Terminal (elev. ~150 m).
UTM Z8 473225 6571144:
22-12 (bag) ***silty sand with gravel (SM)*** (fig. 94)
22-13 (tin) ***MC 36.0%, highly organic***

Landslide Classification: *Debris flow*

Site Description: ADOT&PF (2020) reported that the affected area spanned over 500 ft (~150 m or the length of the parking area for the Ferry Terminal), with a height of between 75 and 100 ft (23 to 30 m). Small debris flows formed within multiple debris chutes along the slope face, and debris reached as far as lane number three in the Ferry Terminal parking area (fig. 95; ADOT&PF, 2020). Bedrock (metabasalt) with steeply dipping foliation (near vertical) is exposed in a ~40 m-high roadcut. The bedrock is overlain by colluvial deposits.

Soil Stratigraphy: (Near sampling location at head scarp)

0 – 20 cm	Bn Org mat
20 – 60 cm	Bn Org Si Sa w/ Gr, w/ cobbles and boulders (colluvium)
60 cm – 3.5 m	Bn – Bk Sa w/ Si and Gr, stratified, w/ evidence of consistent water seepage (fig. 95c)

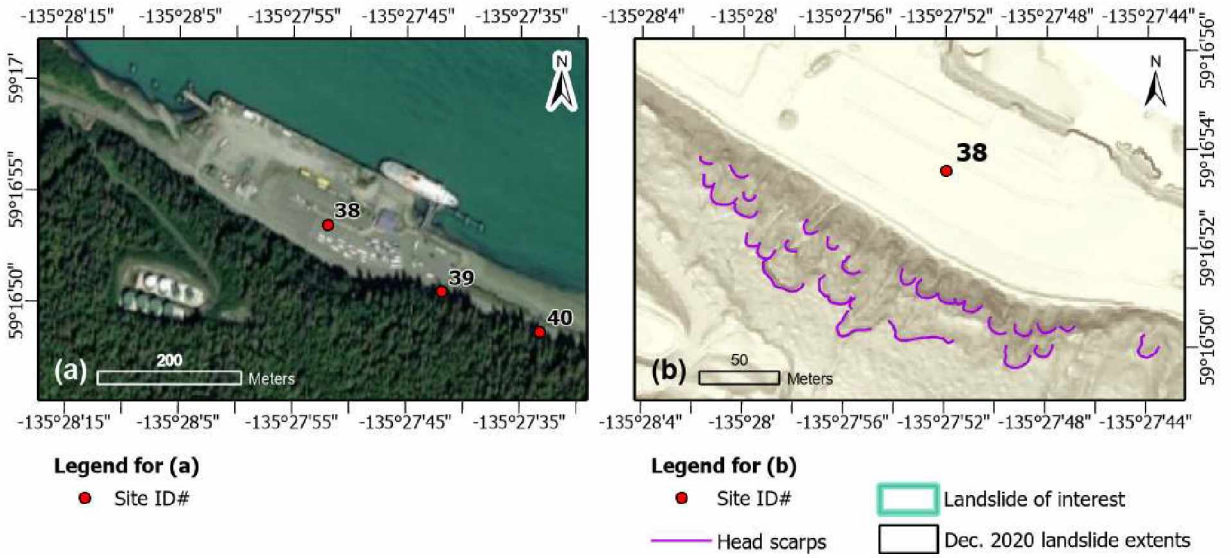

Figure 93. Maps showing location of FEMA DOT#49 (site 38): (a) 50-cm resolution RGB imagery (basemap from ADNR, 2020); (b) slope map derived from 2020 lidar (Daanen and others, 2021). ***NOTE:*** *the legend is standard for all maps; not all items may be present in (b).*

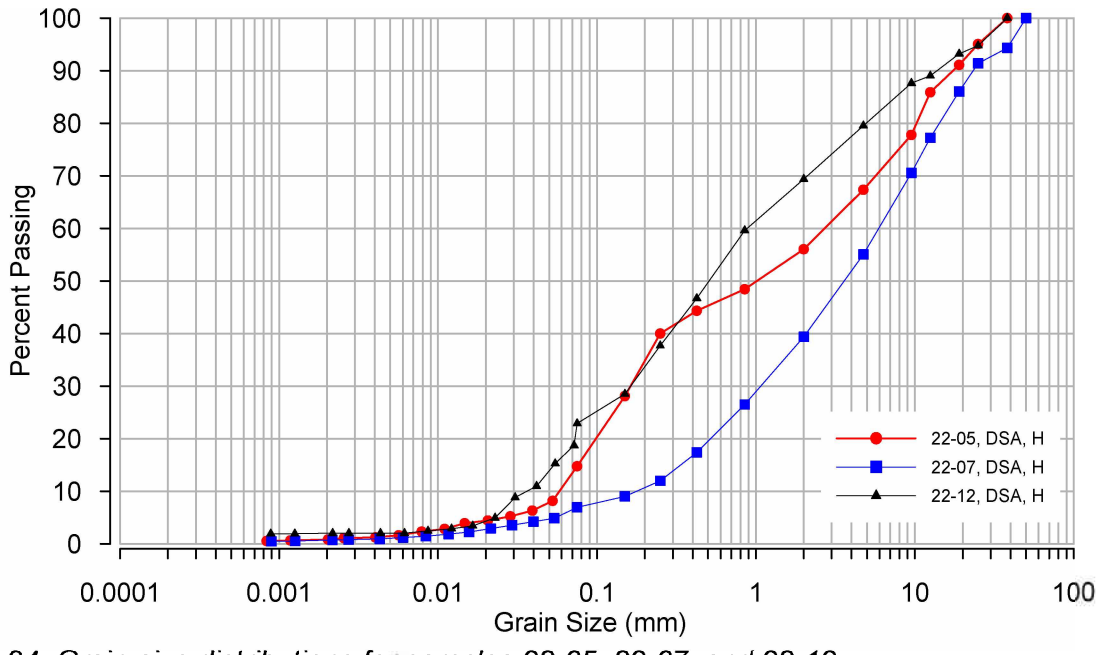

Figure 94. Grain-size distributions for samples 22-05, 22-07, and 22-12.

Figure 95. Photographs of the slope adjacent to the ferry terminal (FEMA DOT#49): (a) the entire extent of the slope across Lutak Road from the ferry terminal, post cleanup (December 2020; photograph courtesy of ADOT&PF); (b) an individual debris flow in December 2020 (photograph courtesy of ADOT&PF); (c) view in June 2022 of soil at sample location 22-07 and 22-08, demonstrating ongoing water seepage (note the algae growth in the left side of the image).

Site ID#: 39 **Date Visited:** 6/25/2021, 7/19/2022
FEMA DOT#: 67 **Field Crew:** VN, MD
Field Name: Lutak Road
GPS Coordinates: UTM Z8 473689 6571406 (fig. 96)

Samples Taken: Samples taken from right bank of drainage uphill of Lutak Road (elev. ~ 91 m); *UTM Z8 473615 6571175*:
22-10 (bag) ***poorly-graded gravel with silt and sand (GP-GM)*** (fig. 97)
22-11 (tin) ***MC 23.7%***

Landslide Classification: *Debris flow*

Site Description: A minor debris flow produced a small deposit (about 5 cubic yards/~ 4 cubic meters of material) that was contained within the ditch (fig. 98; ADOT&PF, 2020). The remnants that we observed in the ditch consisted of angular cobbles of diorite and metabasalt.

Soil Stratigraphy: (Right bank of the channel, elev. ~91 m)

0 – 10 cm	Org mat
10 cm – 11 cm	Gy Sa
11 cm – 111 cm	Or Sa w/ Gr, iron-stained
111 cm – 121 cm	Gy PG Gr w/ Si, Sa (elevated shore deposits) [22-10, 22-11]

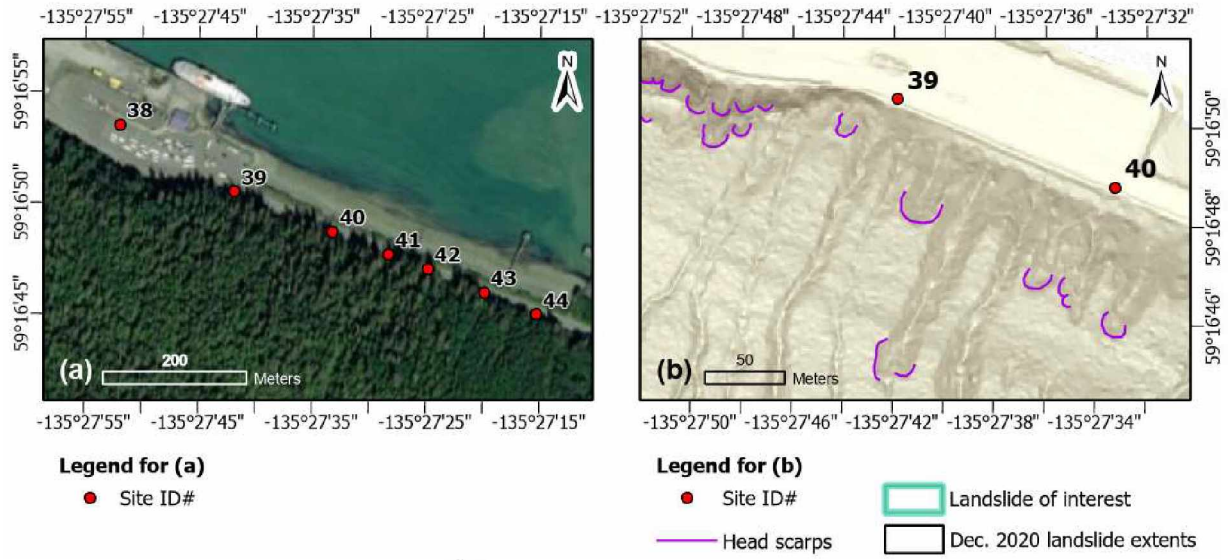

*Figure 96. Maps showing location of FEMA DOT#67 (site 39): (a) 50-cm resolution RGB imagery (basemap from ADNR, 2020); (b) slope map derived from 2020 lidar (Daanen and others, 2021). **NOTE:** the legend is standard for all maps; not all items may be present in (b).*

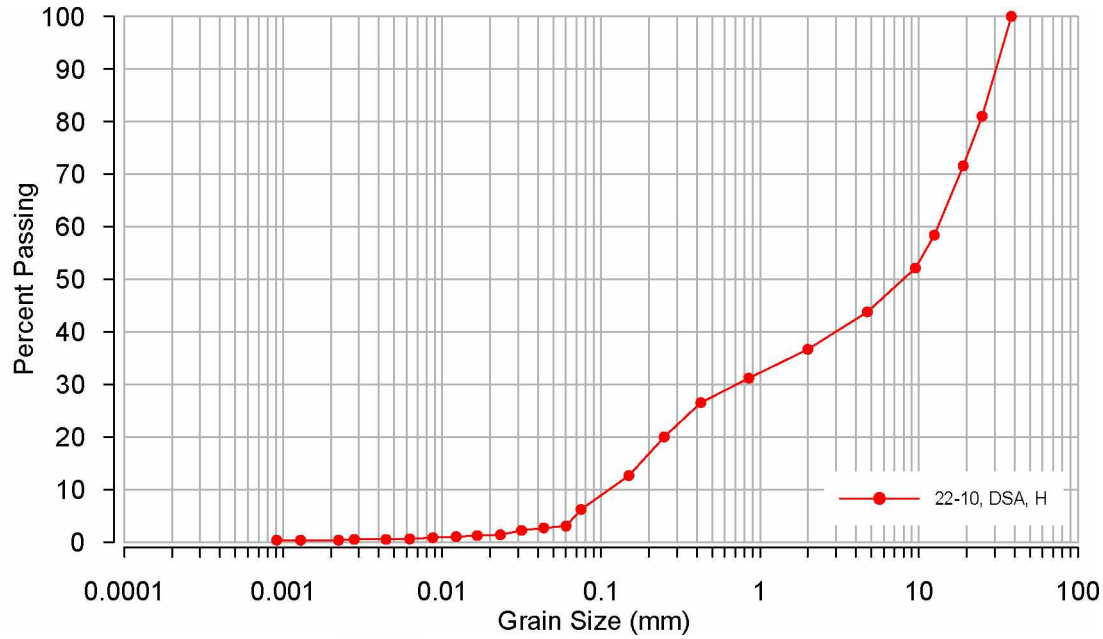

Figure 97. Grain-size distribution for sample 22-10.

Figure 98. Debris contained within the ditch at FEMA DOT#67 in December 2020 (photograph courtesy of ADOT&PF).

Site ID#: 40 **Date Visited:** 6/25/2021
FEMA DOT#: 68 **Field Crew:** VN, MD
Field Name: Lutak Road
GPS Coordinates: UTM Z8 473831 6571348 (fig. 99)

Samples Taken: No samples were taken at this location.

Landslide Classification: *Debris flow*

Site Description: ADOT&PF (2020) reported this was a small debris flow area, with approximately 5 cubic yards/~4 cubic meters of material contained within the ditch (fig. 100). We observed both rounded gravel (diorite) and angular metabasalt, as well as woody debris. No water was observed in the channel.

Soil Stratigraphy: Not described; source area not investigated

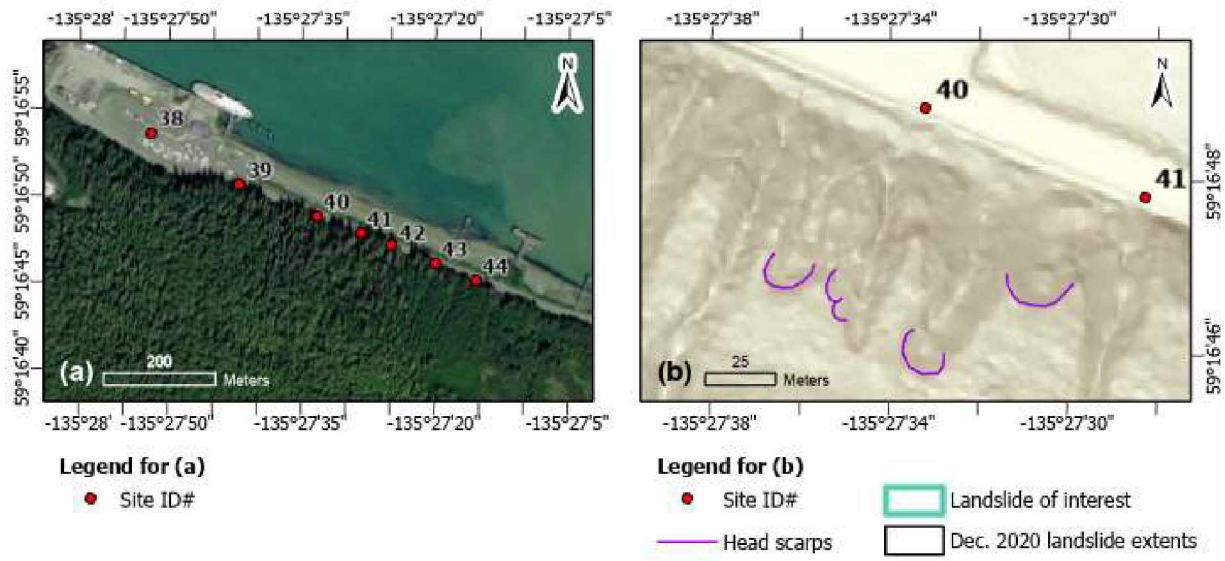

*Figure 99. Maps showing location of FEMA DOT#68 (site 40): (a) 50-cm resolution RGB imagery (basemap from ADNR, 2020); (b) slope map derived from 2020 lidar (Daanen and others, 2021). **NOTE:** the legend is standard for all maps; not all items may be present in (b).*

Figure 100. Debris contained within the ditch at FEMA DOT#68 in December 2020 (photograph courtesy of ADOT&PF).

Site ID#: 41 **Date Visited:** 6/25/2021
FEMA DOT#: 69 **Field Crew:** VN, MD
Field Name: Lutak Road
GPS Coordinates: UTM Z8 473904 6571314 (fig. 101)

Samples Taken: No samples were taken at this location.

Landslide Classification: *Debris flow*

Site Description: ADOT&PF (2020) reported this was a small debris flow area, with approximately 5 cubic yards/~4 cubic meters of material contained within the ditch (fig. 102). This channel appeared to be well-developed with flowing water, and contained boulders and cobbles of diorite.

Soil Stratigraphy: Not described; source area not investigated

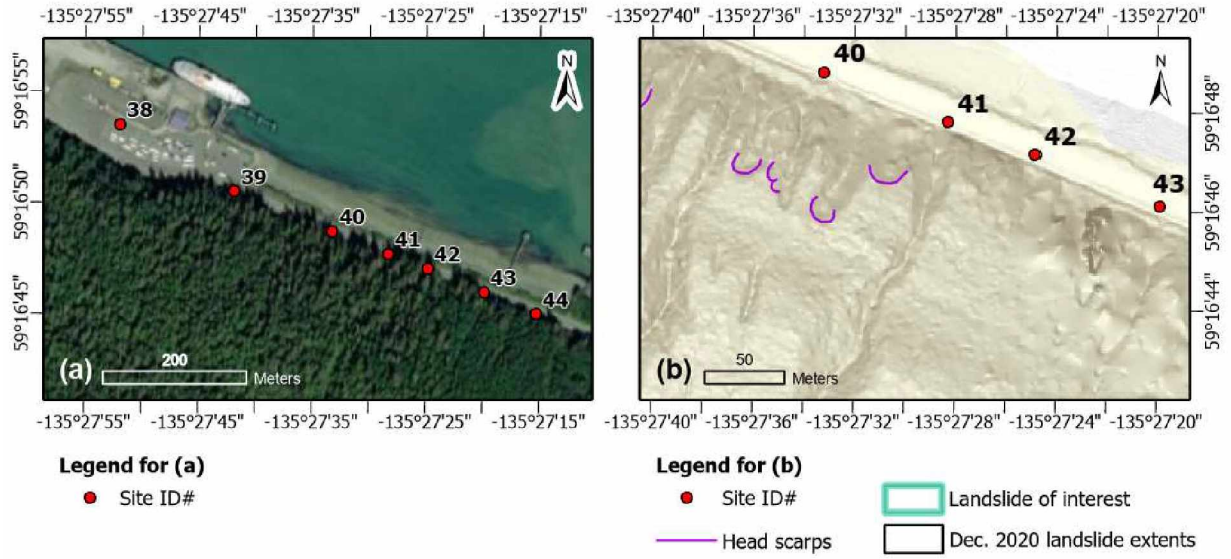

Figure 101. Maps showing location of FEMA DOT#69 (site 41): (a) 50-cm resolution RGB imagery (basemap from ADNR, 2020); (b) slope map derived from 2020 lidar (Daanen and others, 2021). ***NOTE:*** *the legend is standard for all maps; not all items may be present in (b).*

Figure 102. Debris contained within the ditch at FEMA DOT#69 in December 2020 (photograph courtesy of ADOT&PF).

Site ID#: 42 **Date Visited:** 6/25/2021
FEMA DOT#: 55 **Field Crew:** VN, MD
Field Name: Lutak Road
GPS Coordinates: UTM Z8 473966 6571298 (fig. 103)

Samples Taken: No samples were taken at this location.

Landslide Classification: *Debris slide*

Site Description: ADOT&PF (2020) reported the head scarp for this landslide was approximately 100 ft/~ 30 m uphill from the edge of pavement; we observed the soil stratigraphy at that location (fig. 104). Reports indicate the impact from this landslide was localized (0–20 ft/~6 m of the roadway was impacted), requiring minimal clearing (ADOT&PF, 2020).

Soil Stratigraphy: (head scarp area)

0 – 20 cm	Org mat
20 cm – 3 m	Bn Si Sa w/ Gr to Sa Gr; stratified with rounded clasts (elevated beach deposit)
>3 m	Bx (diorite)

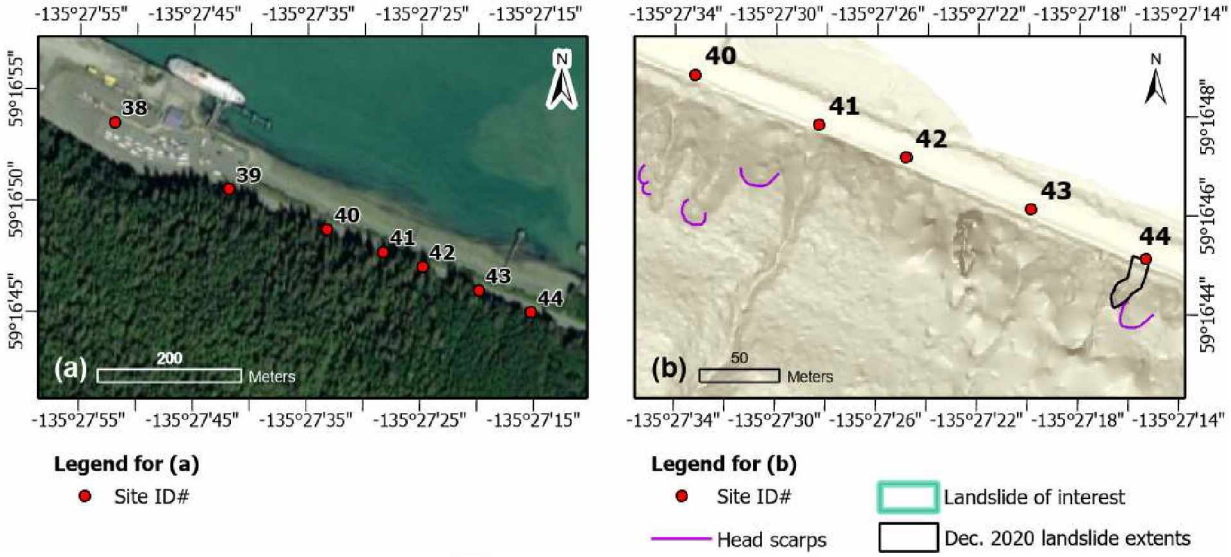

Figure 103. Maps showing location of FEMA DOT#55 (site 42): (a) 50-cm resolution RGB imagery (basemap from ADNR, 2020); (b) slope map derived from 2020 lidar (Daanen and others, 2021). ***NOTE:*** *the legend is standard for all maps; not all items may be present in (b).*

Figure 104. Photographs from the FEMA DOT#55 area: (a) view of the landslide area from Lutak Road in December 2020 (photograph courtesy of ADOT&PF); and (b) annotated image of stratigraphy at the head scarp (June 2021).

Site ID#: 43 **Date Visited:** 6/25/2021
FEMA DOT#: 70 **Field Crew:** VN, MD
Field Name: Lutak Road
GPS Coordinates: UTM Z8 474038 6571263 (fig. 105)

Samples Taken: No samples were taken at this location.

Landslide Classification: *Debris flow*

Site Description: ADOT&PF (2020) reported this was a small debris flow area, with about 5 cubic yards/~ 4 cubic meters of material contained within the ditch (fig. 106). We observed a small, pre-existing channel containing rounded cobbles and boulders and minimal flowing water.

Soil Stratigraphy: Not described; source area not investigated

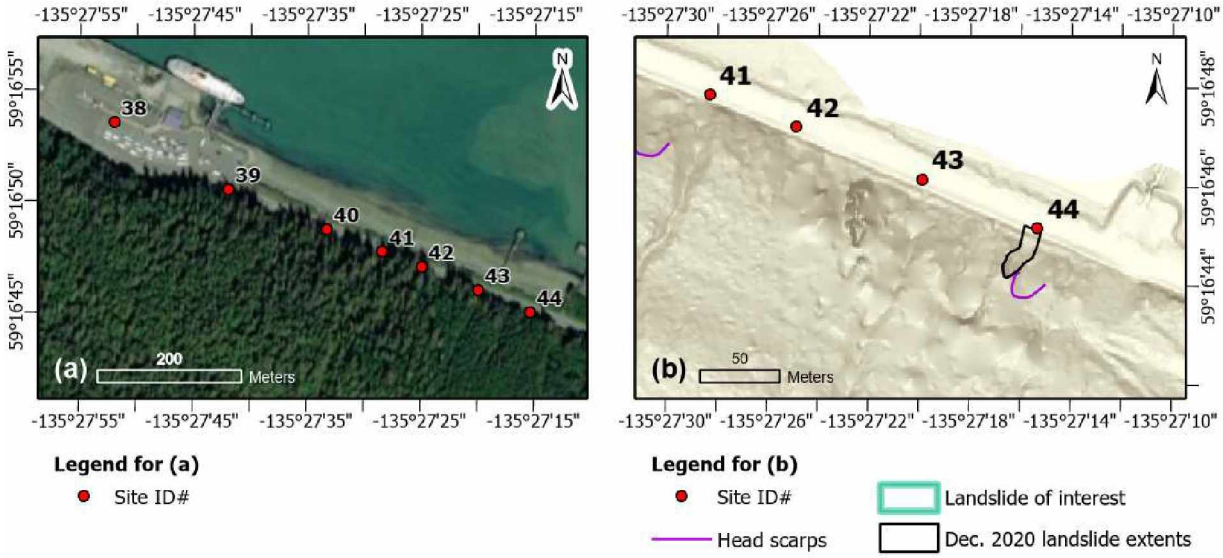

*Figure 105. Maps showing location of FEMA DOT#70 (site 43): (a) 50-cm resolution RGB imagery (basemap from ADNR, 2020); (b) slope map derived from 2020 lidar (Daanen and others, 2021). **NOTE:** the legend is standard for all maps; not all items may be present in (b).*

Figure 106. View of deposited material remaining in the ditch at FEMA DOT#70 after road clearing in December 2020 (photograph courtesy of ADOT&PF).

Site ID#: 44 **Date Visited:** 6/25/2021,7/22/2022
FEMA DOT#: 56 **Field Crew:** VN, MD, KB
Field Name: Varve site, Lutak Road
GPS Coordinates: UTM Z8 474112 6571229 (fig. 107)

Samples Taken: Samples collected from the center of the landslide extent (*UTM Z8 474104 6571216*):

21-36 (tin) ***MC 6.5%***
21-37 (bag) ***well-graded gravel with sand (GW)*** (fig. 108)

Samples taken from exposed varve deposit near the head scarp (*UTM Z8 474104 6571203)*:

22-28 A (tin) ***MC 31.2%*** (sandy silt)
22-28 B (tin) ***MC 23.9%*** (sand)
22-28 C (bag) ***sandy silt (ML)*** (fig. 108)

Vane shear testing conducted within varve deposit (UTM Z8 474106 6571203):

No. tests conducted: 10
Average shear strength: 16.6 kPa
Standard deviation: ± 4.6 kPa

Landslide Classification and Dimensions: *Debris slide*; length 35 m, width 12 m, L/W 2.9, aerial extent 347.4 m^2

Site Description: ADOT&PF (2020) reported this was a localized slide, with 20–25 cubic yards (15–19 cubic meters) of material removed. We observed varved deposits exposed in the landslide body (fig. 109), consisting of distinct alternating sandy (5-mm–1-cm thick) and silty (~3-cm thick) layers, suggesting they are elevated fine-grained marine deposits (Lemke and Yehle, 1972).

Soil Stratigraphy: (at head scarp)

0 – 20 cm	Organic mat (varies, up to 40-cm thick)
20 cm – 4 m	Gy Sa Gr to Gr Sa; well-graded, stratified (elevated beach deposits)
4.0 – 4.5 m	Sa Si
4.5 – 4.7 m	Sa Gr
4.7 – 4.9 m	Sa Si
4.9 – 5.0 m	Sa Gr
>5.0 m	Sa Si

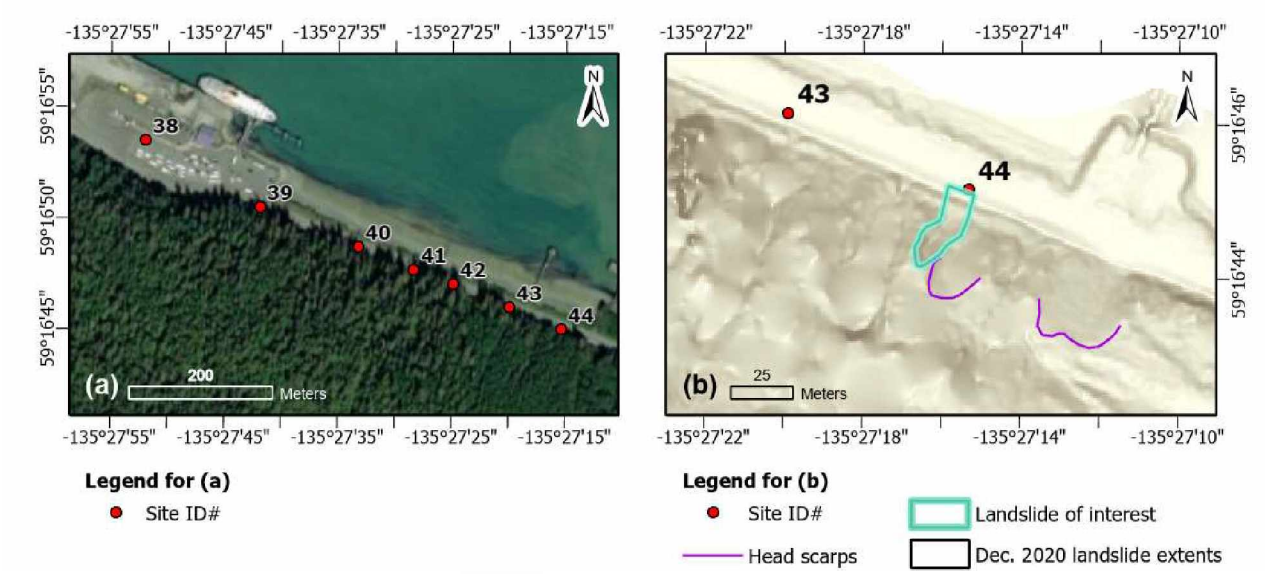

Figure 107. Maps showing location of FEMA DOT#56 (site 44): (a) 50-cm resolution RGB imagery (basemap from ADNR, 2020); (b) slope map derived from 2020 lidar (Daanen and others, 2021). ***NOTE:*** *the legend is standard for all maps; not all items may be present in (b).*

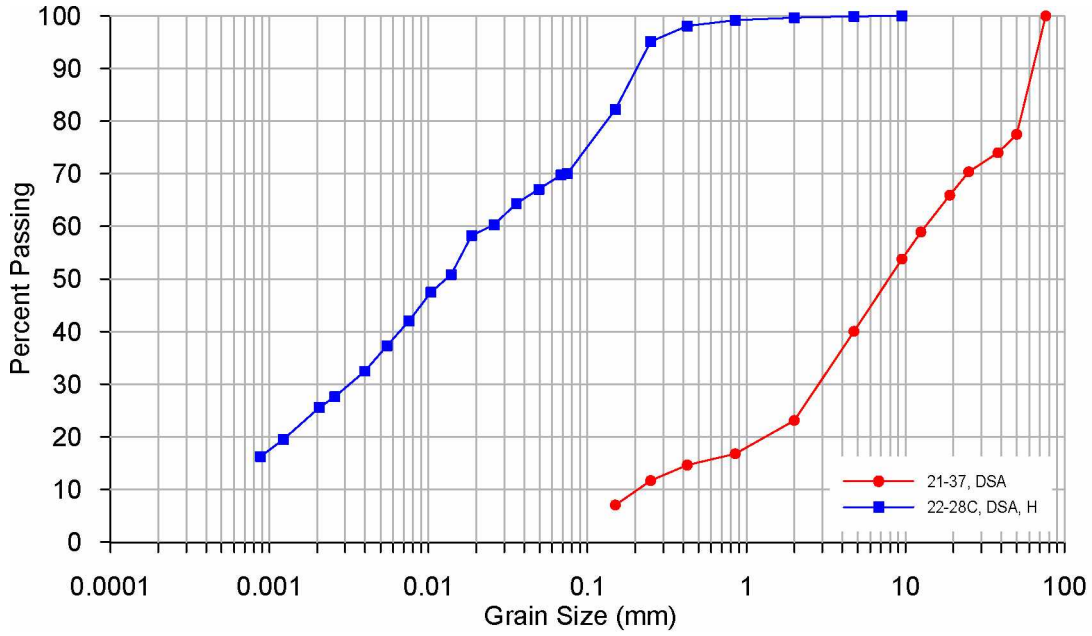

Figure 108. Grain-size distributions for samples 21-37 and 22-28C.

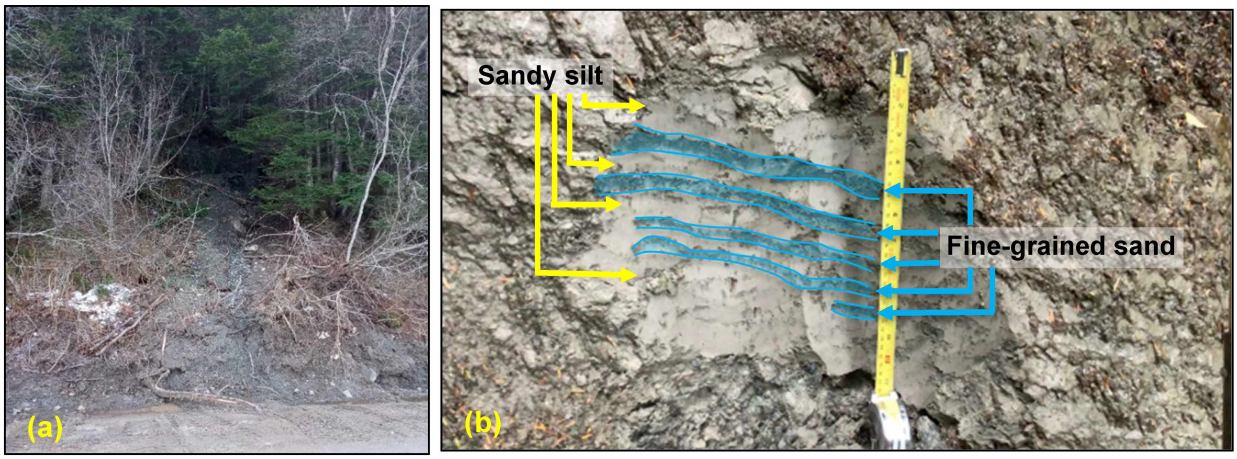

Figure 109. Photographs from FEMA DOT#56: (a) view of the landslide from Lutak Road post-cleaning in December 2020 (photograph courtesy of ADOT&PF); (b) annotated photograph of cleaned exposure of varve deposit (June 2021).

Site ID#: 45 **Date Visited:** 6/25/2021
FEMA DOT#: 66 **Field Crew:** VN, MD
Field Name: Lutak Road
GPS Coordinates: UTM Z8 474627 6569929 (fig. 110)

Samples Taken: No samples were taken at this location.

Landslide Classification: *Debris flow*

Site Description: ADOT&PF (2020) reported that, after plugging the culvert, debris overtopped the roadway at this location (fig. 111). This is a well-established creek filled with rounded cobbles. Evidence of the 2020 debris flow was still present at the site in June 2021. Our investigation of this site was brief due to time constraints; a more thorough investigation is recommended.

Soil Stratigraphy: Not described; source area not investigated

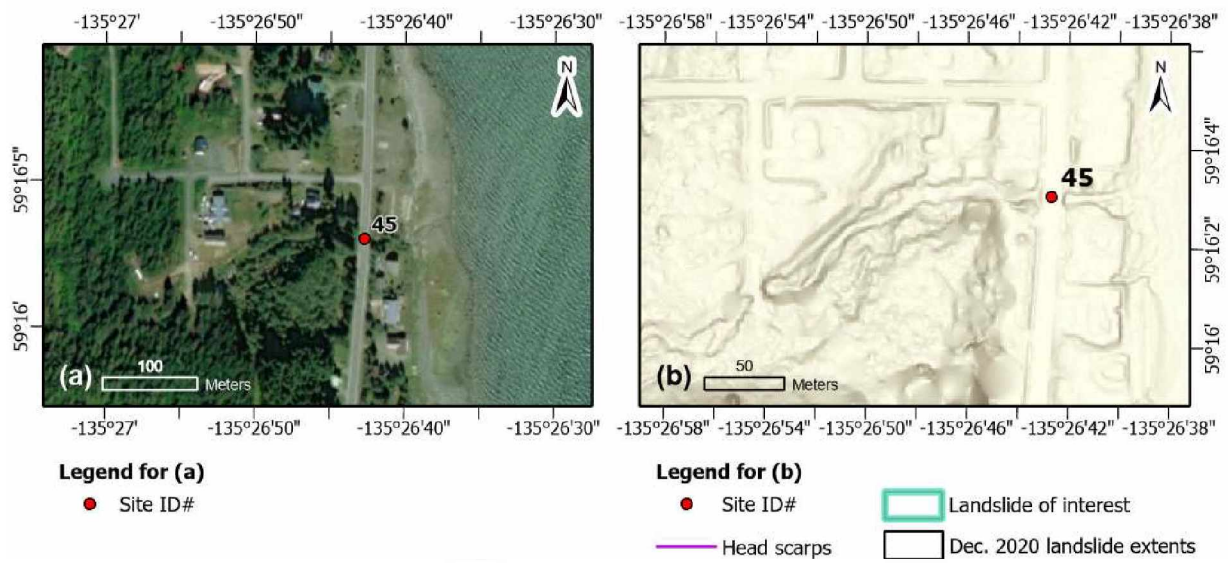

*Figure 110. Maps showing location of FEMA DOT#66 (site 45): (a) 50-cm resolution RGB imagery (basemap from ADNR, 2020); (b) slope map derived from 2020 lidar (Daanen and others, 2021). **NOTE:** the legend is standard for all maps; not all items may be present in (b).*

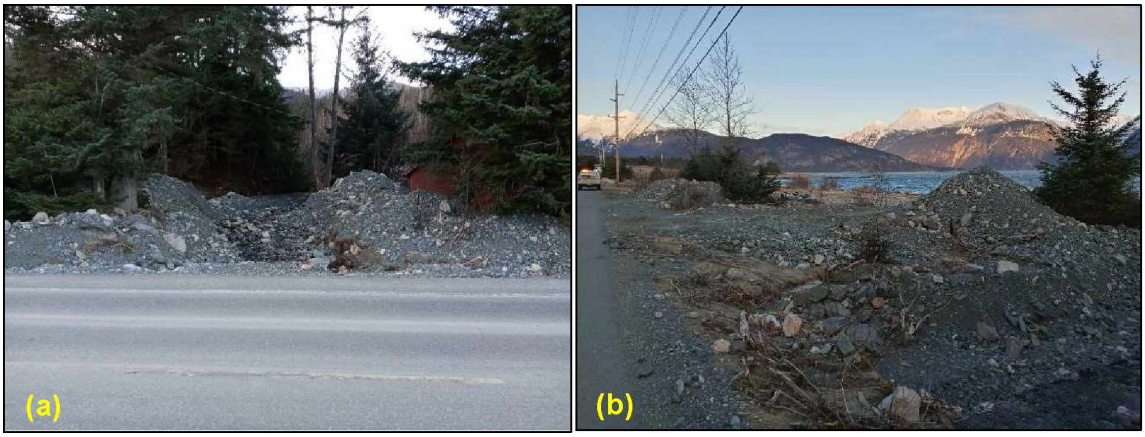

Figure 111. Photographs of FEMA DOT#66 in December 2020: (a) view of the channel from Lutak Road; (b) debris pushed off the road to the east (photographs courtesy of ADOT&PF).

Site ID#: 46 **Date Visited:** 6/25/2021
FEMA DOT#: 65 **Field Crew:** VN, MD
Field Name: Lutak Road
GPS Coordinates: UTM Z8 474605 6569508 (fig. 112)

Samples Taken: No samples were taken at this location.

Landslide Classification: *Debris flow*

Site Description: The small channel at this site produced ~30 cubic yards (23 cubic meters) of angular debris, which was contained within the ditch (fig. 113; ADOT&PF, 2020). Our investigation of this site was brief due to time constraints; a more thorough investigation is recommended.

Soil Stratigraphy: Not described; source area not investigated

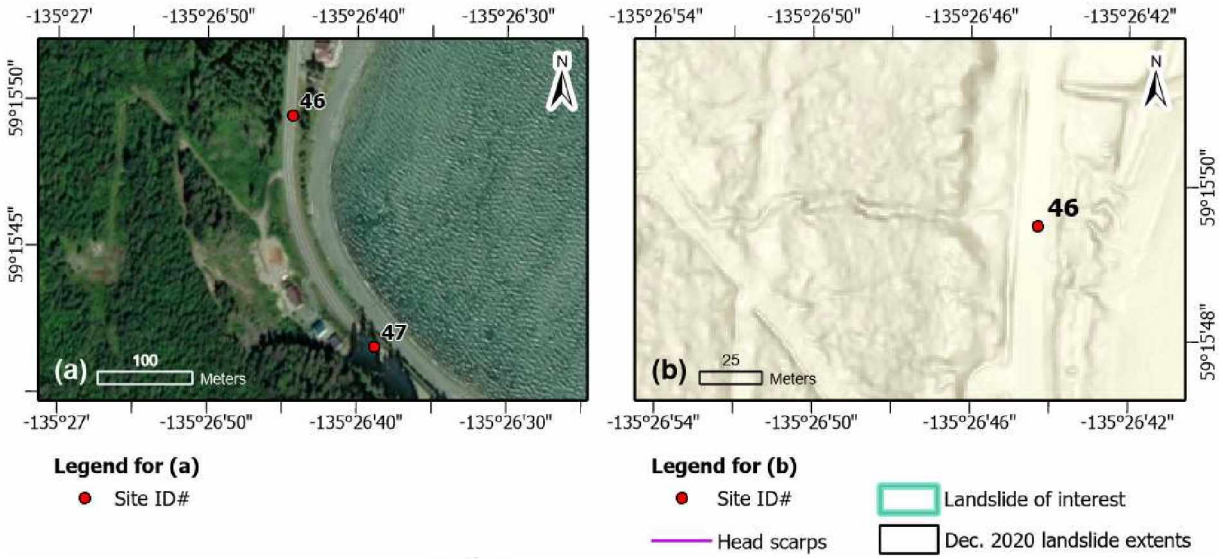

Figure 112. Maps showing location of FEMA DOT#65 (site 46): (a) 50-cm resolution RGB imagery (basemap from ADNR, 2020); (b) slope map derived from 2020 lidar (Daanen and others, 2021). ***NOTE:*** *the legend is standard for all maps; not all items may be present in (b).*

Figure 113. Views of FEMA DOT#65 in December 2020, illustrating (a) debris that was pushed off the road and (b) debris that was caught in the ditch (photographs courtesy of ADOT&PF).

Site ID#: 47 **Date Visited:** 6/25/2021
FEMA DOT#: N/A **Field Crew:** VN, MD
Field Name: Woodshed site, Lutak Road
GPS Coordinates: UTM Z8 474677 6569262 (fig. 114)

Samples Taken: Samples collected from mid-slope of the landslide body.
UTM Z8 474613 6569265:
21-34 (tin) ***MC 16.1%***
21-35 (bag) ***well-graded gravel with sand (GW)*** (fig. 115)

Landslide Classification: *Debris slide*

Site Description: This landslide impacted a small structure on the property, moving it several feet toward Lutak Road. At the time of sample collection, the soil contained enough water to liquefy and flow (fig. 116).

Soil Stratigraphy: Bn org mat (~20-cm thick), overlying Gy Sa Gr with sub-rounded cobbles and boulders interpreted as elevated shore and delta deposits (Lemke and Yehle, 1972)

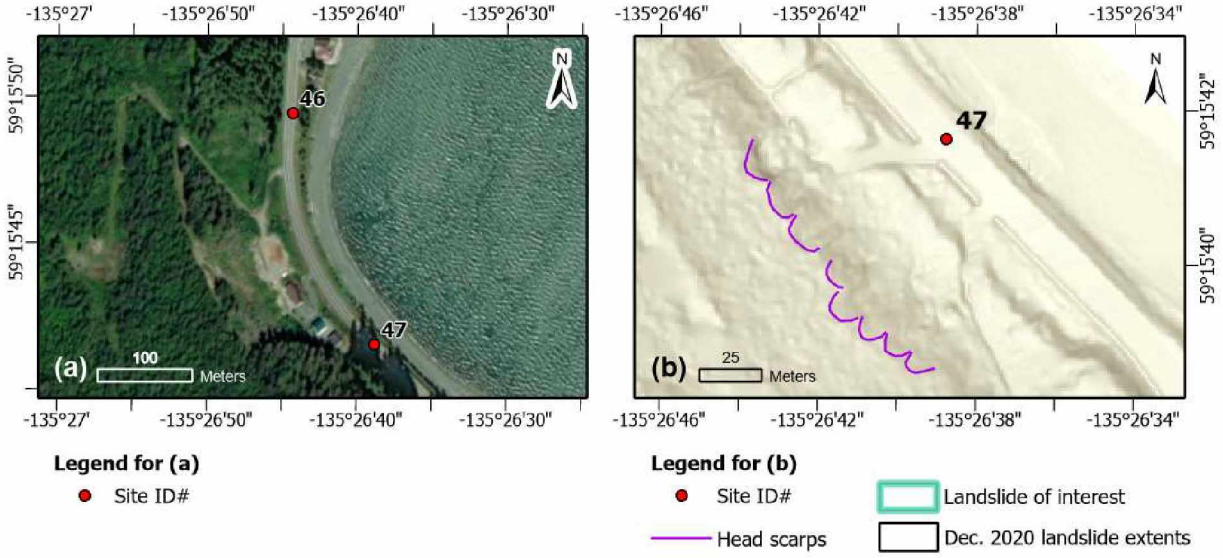

Figure 114. Maps showing location of the Woodshed site (site 47): (a) 50-cm resolution RGB imagery (basemap from ADNR, 2020); (b) slope map derived from 2020 lidar (Daanen and others, 2021). ***NOTE:*** *the legend is standard for all maps; not all items may be present in (b).*

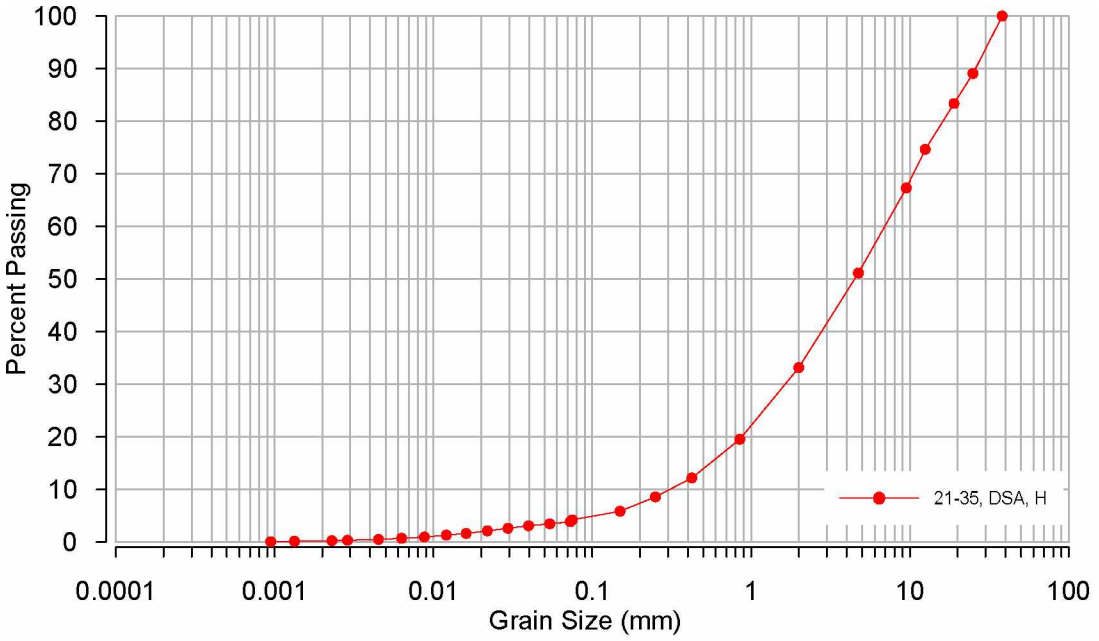

Figure 115. Grain-size distribution for sample 21-35.

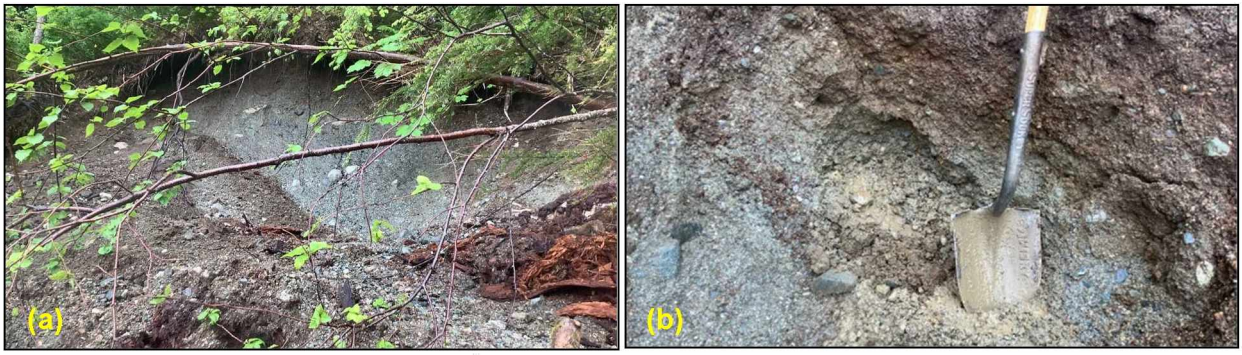

Figure 116. Photographs from the Woodshed site landslide along Lutak Road in June 2021: (a) head scarp area as seen from the property; (b) sample location, which was saturated and flowed when disturbed (shovel for scale).

Site ID#: 48 **Date Visited:** 6/25/2021
FEMA DOT#: 64 **Field Crew:** VN, MD
Field Name: Johnson Creek, Lutak Road
GPS Coordinates: UTM Z8 474782 6569139 (fig. 117)

Samples Taken: No samples taken at this location.

Landslide Classification: *Debris flow*

Site Description: Johnson Creek is well-established, containing cobles and boulders with bedrock exposed in the channel bottom. The culvert sustained heavy damage during debris removal after the December 2020 debris flow; no information on debris volume is available (fig. 118; ADOT&PF, 2020). Our investigation of this site was brief due to time constraints; a more thorough investigation is recommended.

Soil Stratigraphy: Not described; source area not investigated

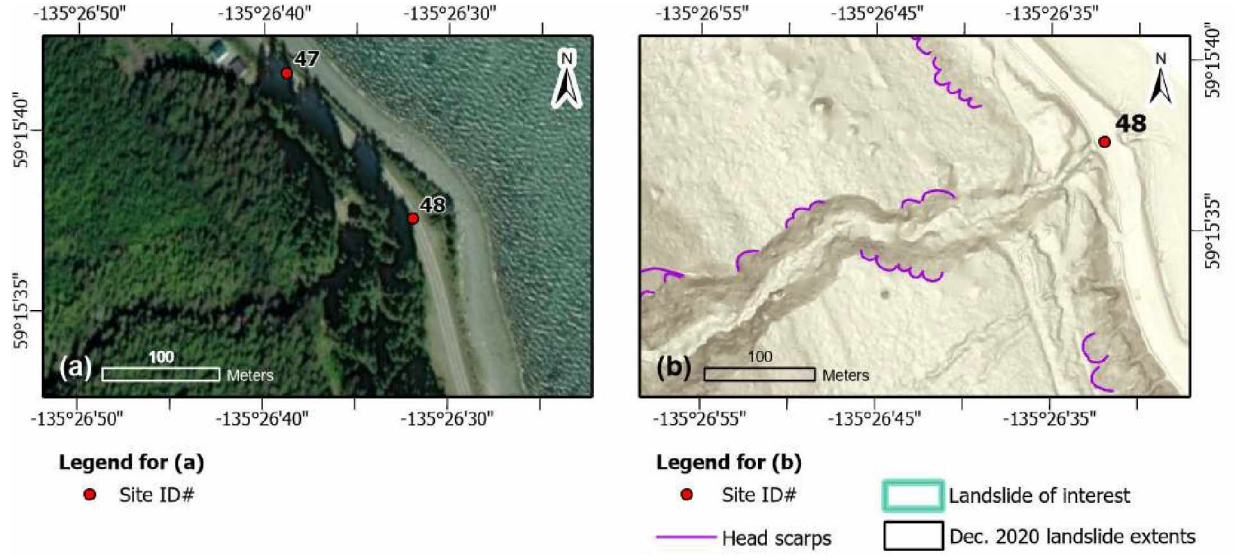

*Figure 117. Maps showing location of FEMA DOT#64 (site 48): (a) 50-cm resolution RGB imagery (basemap from ADNR, 2020); (b) slope map derived from 2020 lidar (Daanen and others, 2021). **NOTE:** the legend is standard for all maps; not all items may be present in (b).*

Figure 118. Photographs of the Johnson Creek location in December 2020: (a) the channel from Lutak Road; and (b) culvert filled by debris (photographs courtesy of ADOT&PF).

Site ID#: 49 **Date Visited:** 6/25/2021
FEMA DOT#: 57 **Field Crew:** VN, MD
Field Name: Lutak Road
Coordinates: UTM Z8 474866 6568897 (fig. 119)

Samples Taken: No samples were taken at this location.

Landslide Classification and Dimensions: *Debris slide*; length 33 m, width 24 m, L/W 1.4, aerial extent 564.8 m^2

Site Description: According to ADOT&PF (2020), approximately 50 cubic yards (~38 cubic meters) of material failed at this location in December 2020 (fig. 120). Our investigation of this site was brief due to time constraints; a more thorough investigation is recommended.

Soil Stratigraphy: (head scarp area; estimated from road level)

0 – 50 cm	Org mat
50 cm – 2 m	Gy Sa Gr to Gr Sa (colluvium)
> 2 m	Bx

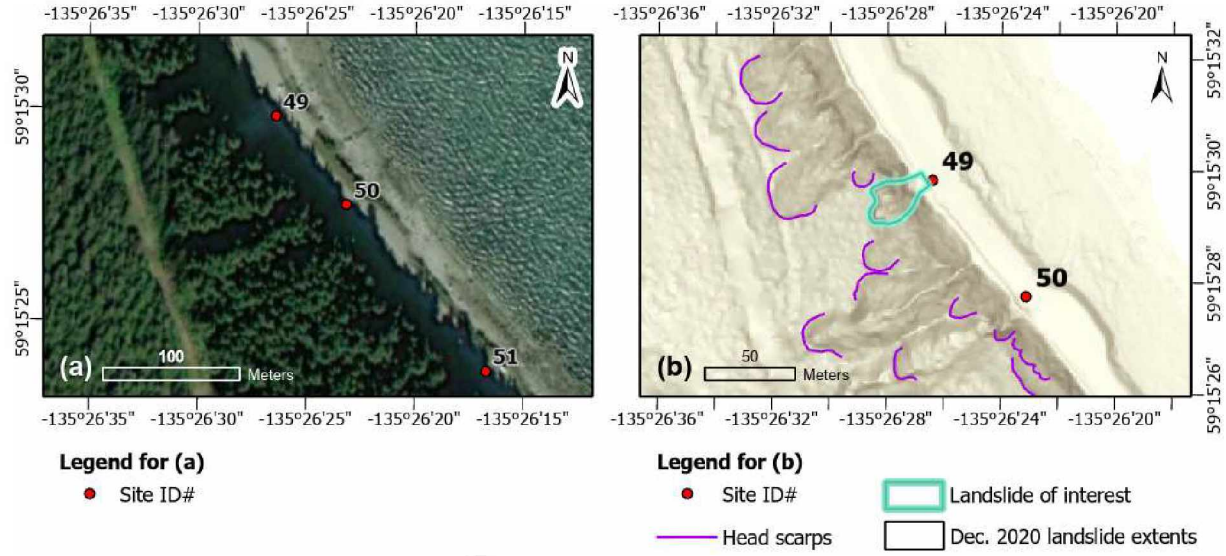

Figure 119. Maps showing location of FEMA DOT#57 (site 49): (a) 50-cm resolution RGB imagery (basemap from ADNR, 2020); (b) slope map derived from 2020 lidar (Daanen and others, 2021). ***NOTE****: the legend is standard for all maps; not all items may be present in (b).*

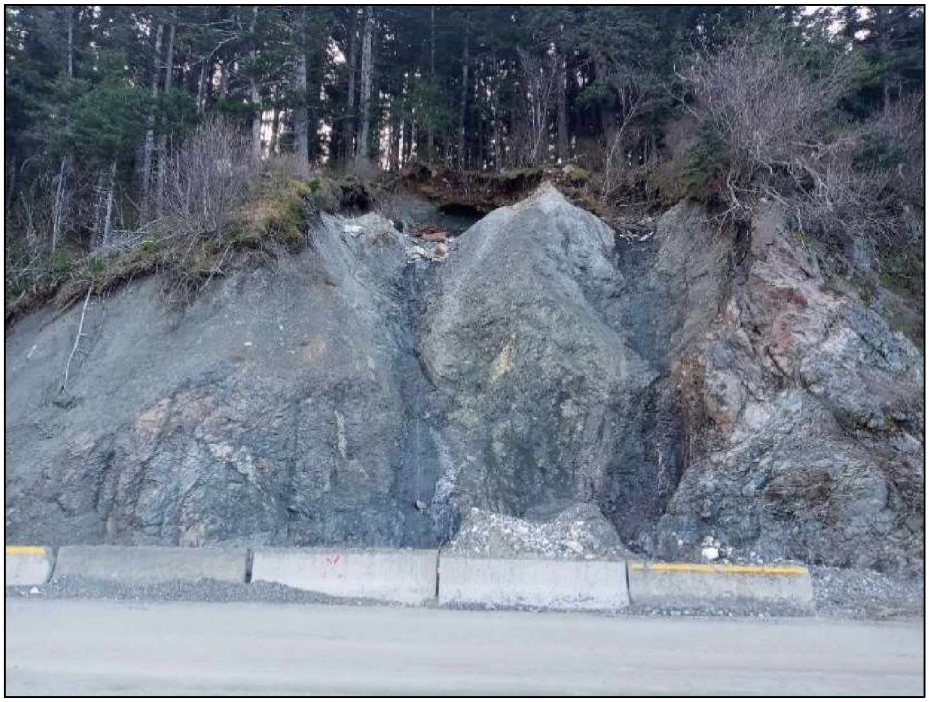

Figure 120. View of slope at DOT#57 from Lutak Road in December 2020 (photograph courtesy of ADOT&PF).

Site ID#: 50 **Date Visited:** 6/25/2021
FEMA DOT#: 63 **Field Crew:** VN, MD
Field Name: Lutak Road
GPS Coordinates: UTM Z8 474921 6568836 (fig. 121)

Samples Taken: No samples were taken at this location.

Landslide Classification: *Debris flow*

Site Description: This is a well-established channel flowing over exposed bedrock (fig. 122). According to ADOT&PF (2020), this site produced less than 5 cubic yards/~4 cubic meters of material that was contained within the ditch. Our investigation of this site was brief due to time constraints; a more thorough investigation is recommended.

Soil Stratigraphy: Not described; source area not investigated

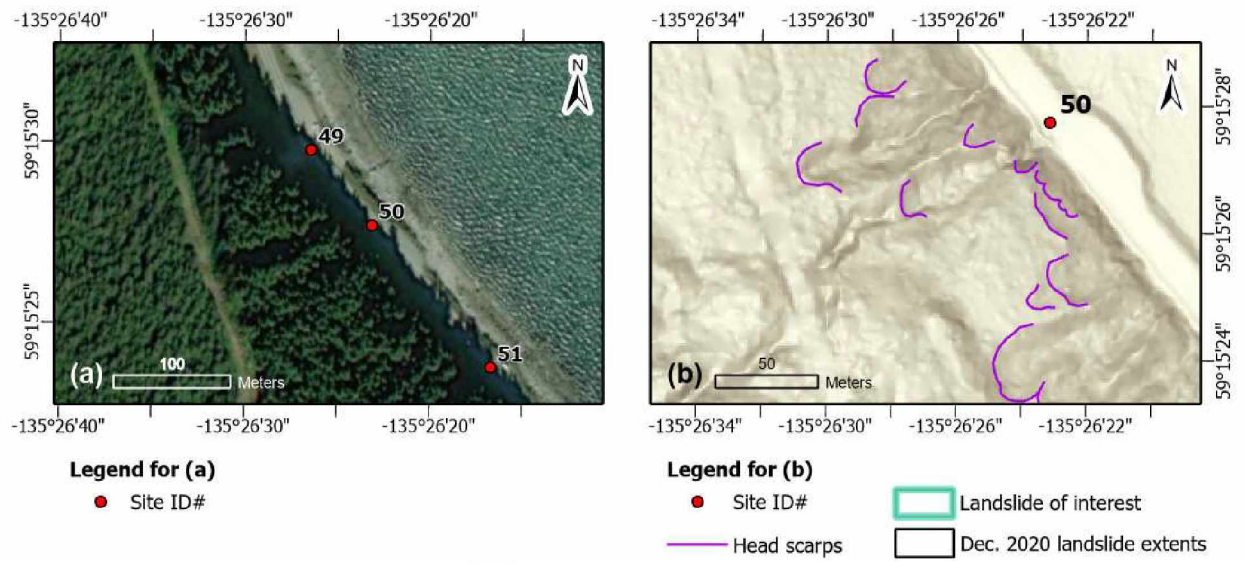

Figure 121. Maps showing location of FEMA DOT#63 (site 50): (a) 50-cm resolution RGB imagery (basemap from ADNR, 2020); (b) slope map derived from 2020 lidar (Daanen and others, 2021). ***NOTE:*** *the legend is standard for all maps; not all items may be present in (b).*

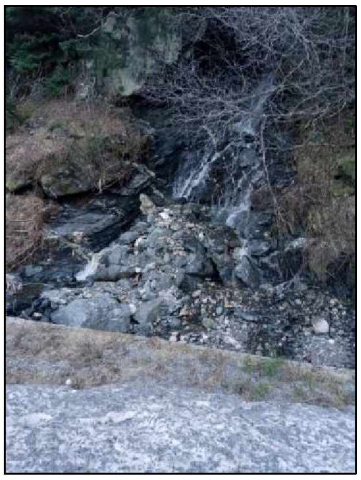

Figure 122. View of debris in the channel at FEMA DOT#63 in December 2020 (photograph courtesy of ADOT&PF).

Site ID#: 51 **Date Visited:** 6/25/2021
FEMA DOT#: 58 **Field Crew:** VN, MD
Field Name: Lutak Road
GPS Coordinates: UTM Z8 475017 6568717 (fig. 123)

Samples Taken: No samples were taken at this location.

Landslide Classification: *Rock fall*

Site Description: According to ADOT&PF (2020), less than 5 cubic yards/~4 cubic meters of rockfall debris fell at this site, and was contained within the ditch (fig. 124). Our investigation of this site was brief due to time constraints; a more thorough investigation is recommended.

Soil Stratigraphy: Not described; source area not investigated

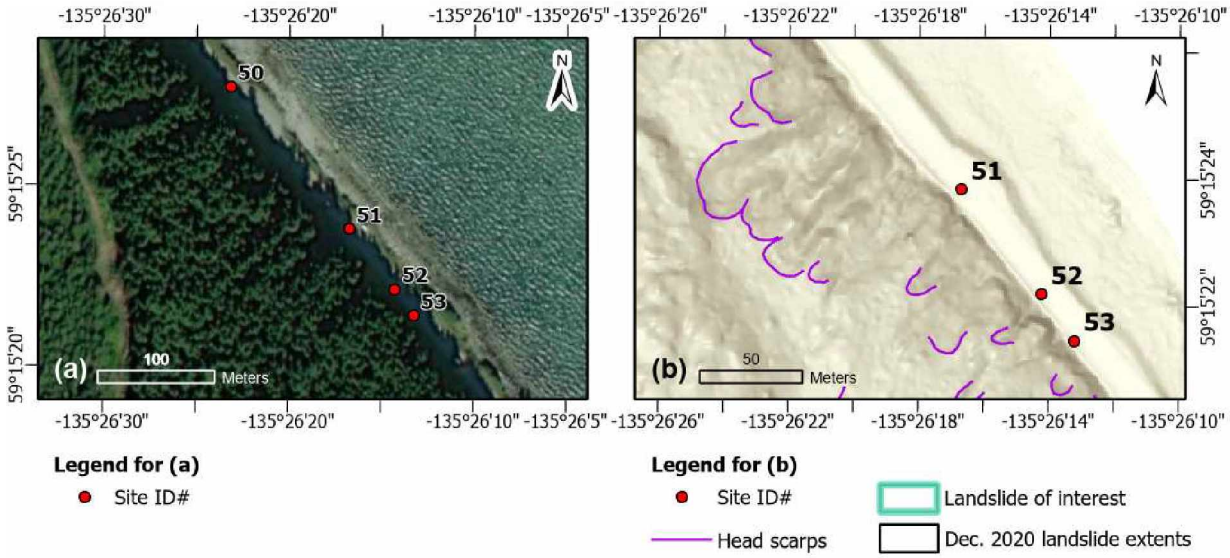

*Figure 123. Maps showing location of FEMA DOT#58 (site 51): (a) 50-cm resolution RGB imagery (basemap from ADNR, 2020); (b) slope map derived from 2020 lidar (Daanen and others, 2021). **NOTE:** the legend is standard for all maps; not all items may be present in (b).*

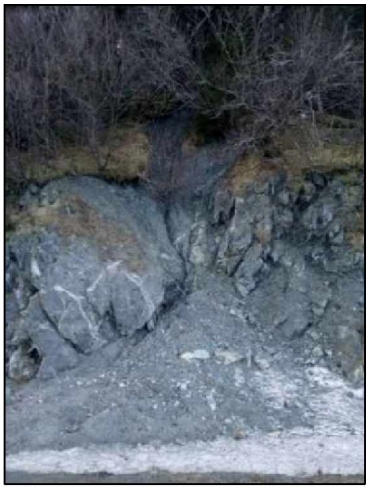

Figure 124. View of debris in the ditch at FEMA DOT#58 in December 2020 (photograph courtesy of ADOT&PF).

Site ID#: 52 **Date Visited:** 6/25/2021
FEMA DOT#: 61 **Field Crew:** VN, MD
Field Name: Lutak Road
GPS Coordinates: UTM Z8 475053 6568658 (fig. 125)

Samples Taken: No samples were taken at this location.

Landslide Classification: *Debris fall*

Site Description: According to ADOT&PF (2020), less than 5 cubic yards/~4 cubic meters of debris accumulated in December 2020, which was contained within the ditch (fig. 126). No water was flowing in the channel at the time of our field visit, which was brief due to time constraints; a more thorough investigation is recommended.

Soil Stratigraphy: Not described; source area not investigated

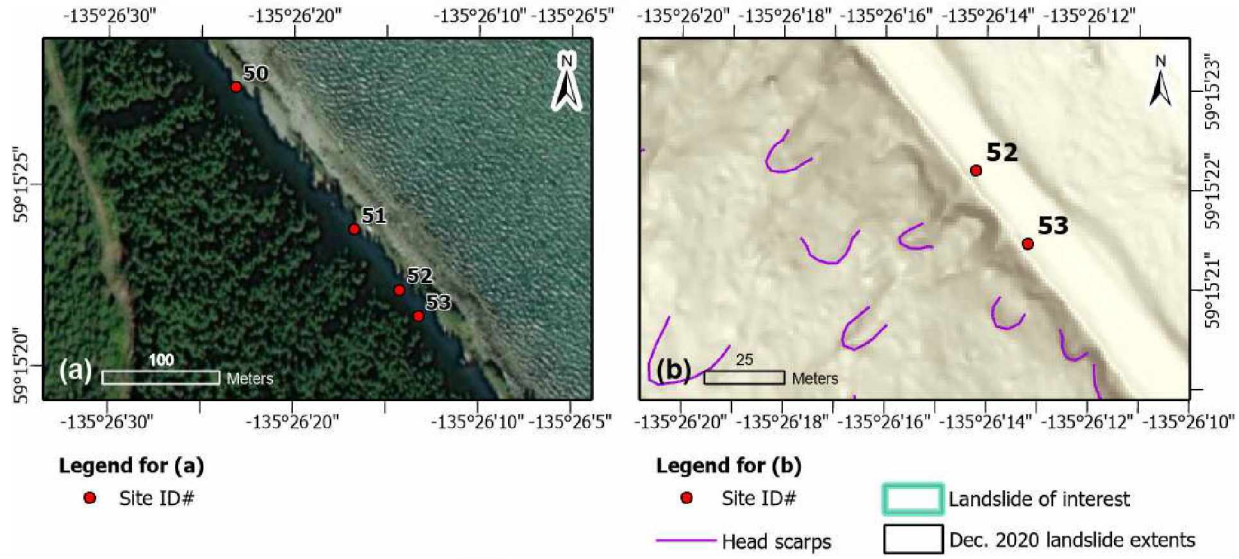

Figure 125. Maps showing location of FEMA DOT#61 (site 52): (a) 50-cm resolution RGB imagery (basemap from ADNR, 2020); (b) slope map derived from 2020 lidar (Daanen and others, 2021). ***NOTE:*** *the legend is standard for all maps; not all items may be present in (b).*

Figure 126. View of debris in the channel and ditch at FEMA DOT#61 in December 2020 (photograph courtesy of ADOT&PF).

Site ID#: 53 **Date Visited:** 6/25/2021
FEMA DOT#: 62 **Field Crew:** VN, MD
Field Name: Lutak Road
GPS Coordinates: UTM Z8 475072 6568642 (fig. 127)

Samples Taken: No samples were taken at this location.

Landslide Classification: *Debris flow*

Site Description: ADOT&PF (2020) indicated that approximately 5 cubic yards/~4 cubic meters of debris were deposited within the ditch at this site in December 2020 (fig. 128). At the time of our field visit, a trickle of water was flowing in the channel (which runs over exposed bedrock); some cobbles were present in the ditch. Our investigation of this site was brief due to time constraints; a more thorough investigation is recommended.

Soil Stratigraphy: Not described; source area not investigated

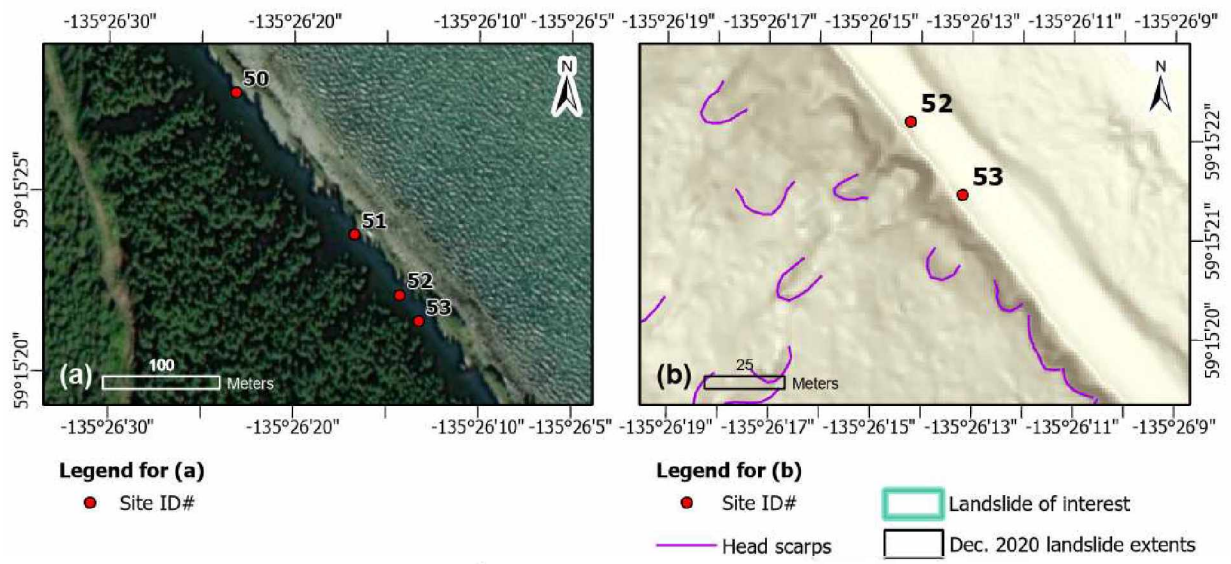

Figure 127. Maps showing location of FEMA DOT#62 (site 53): (a) 50-cm resolution RGB imagery (basemap from ADNR, 2020); (b) slope map derived from 2020 lidar (Daanen and others, 2021). ***NOTE:*** *the legend is standard for all maps; not all items may be present in (b).*

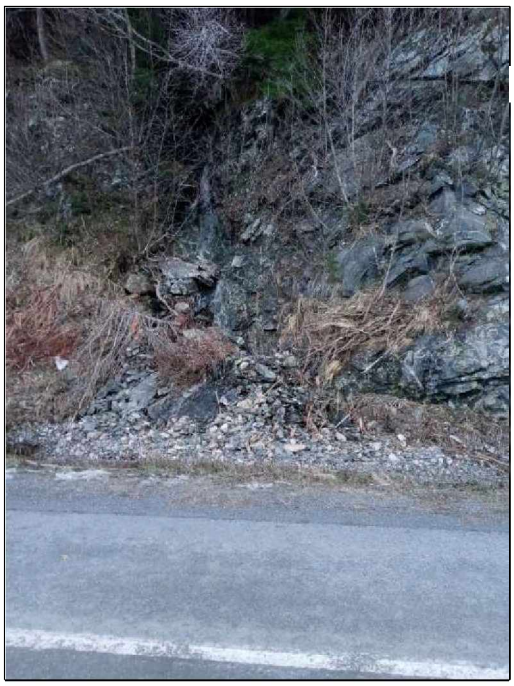

Figure 128. View of debris in the ditch at FEMA DOT#62 in December 2020 (photograph courtesy of ADOT&PF).

Site ID#: 54 **Date Visited:** 6/25/2021
FEMA DOT#: 59 **Field Crew:** VN, MD
Field Name: Lutak Road
GPS Coordinates: UTM Z8 475502 6568019 (fig. 129)

Samples Taken: No samples were taken at this location.

Landslide Classification: *Rock fall*

Site Description: This site produced approximately 5 cubic yards/~4 cubic meters of rockfall debris that the ditch contained (fig. 130; ADOT&PF, 2020). Our investigation of this site was brief due to time constraints; a more thorough investigation is recommended.

Soil Stratigraphy: We estimated approximately 1 m of gray to brown silty sand (colluvium) overlying bedrock. Large boulders are present on the slope surface above the roadcut.

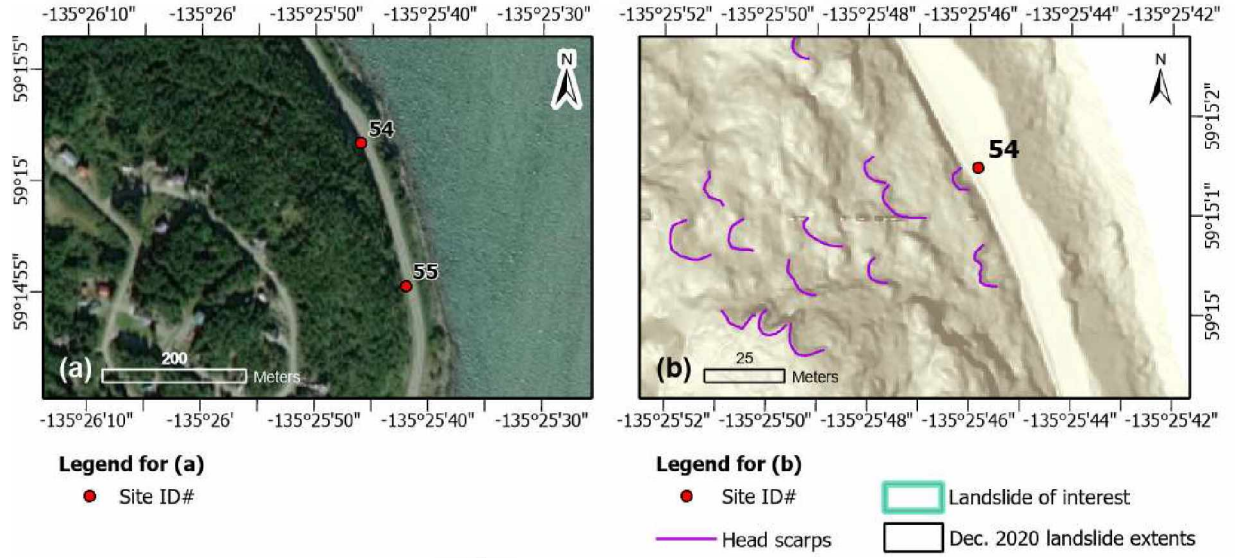

Figure 129. Maps showing location of FEMA DOT#59 (site 54): (a) 50-cm resolution RGB imagery (basemap from ADNR, 2020); (b) slope map derived from 2020 lidar (Daanen and others, 2021). ***NOTE:*** *the legend is standard for all maps; not all items may be present in (b).*

Figure 130. View of the FEMA DOT#59 slope with debris at its base in December 2020 (photograph courtesy of ADOT&PF).

Site ID#: 55 **Date Visited:** 6/25/2021
FEMA DOT#: 60 **Field Crew:** VN, MD
Field Name: Lutak Road
GPS Coordinates: UTM Z8 475573 6567833 (fig. 131)

Samples Taken: No samples were taken at this location.

Landslide Classification: *Rock fall*

Site Description: This site produced approximately 5 cubic yards/~4 cubic meters of rockfall debris that was contained within the ditch (fig. 132; ADOT&PF, 2020). Our investigation of this site was brief due to time constraints; a more thorough investigation is recommended.

Soil Stratigraphy: Not described; source area not investigated

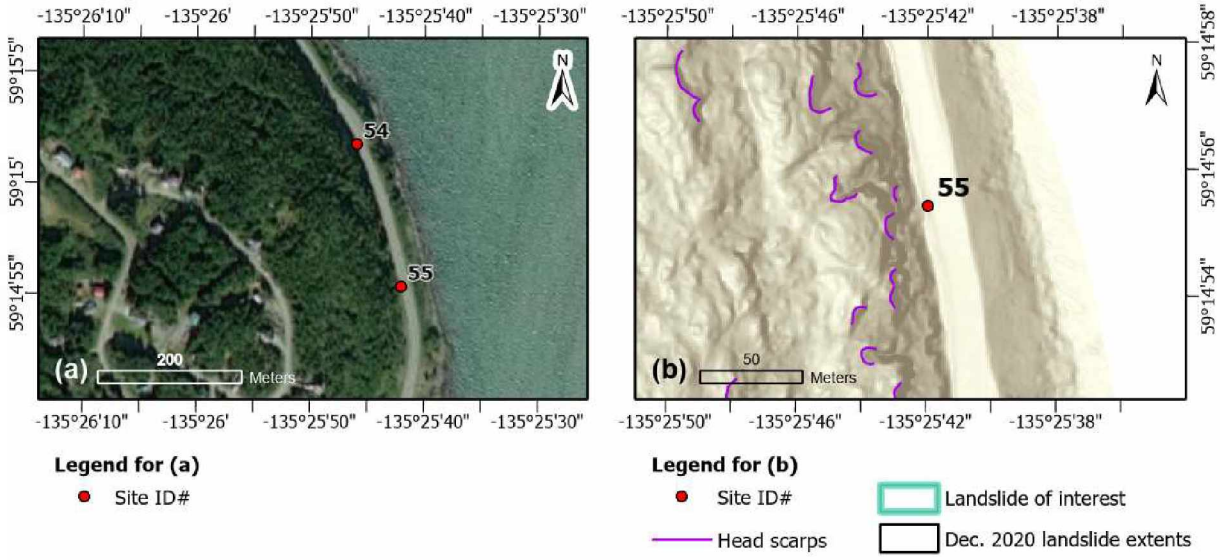

Figure 131. Maps showing location of FEMA DOT#60 (site 55): (a) 50-cm resolution RGB imagery (basemap from ADNR, 2020); (b) slope map derived from 2020 lidar (Daanen and others, 2021). ***NOTE:*** *the legend is standard for all maps; not all items may be present in (b).*

Figure 132. View of debris at the base of the slope at FEMA DOT#60 from Lutak Road in December 2020 (photograph courtesy of ADOT&PF).

Site ID#: 56 **Date Visited:** 6/25/2021, 7/16/2022
FEMA DOT#: N/A **Field Crew:** VN, MD, MG, AL
Field Name: Cunningham Creek
GPS Coordinates: UTM Z8 472569 6567470 (fig. 133)

Samples Taken: No samples were taken at this location.

Landslide Classification: Debris flow – debris flood

Site Description: This site is a well-established channel containing large boulders (>2-m diameter) and evidence of previous debris flow events visible in the exposed channel bank stratigraphy. The channel has steep banks with a wide (~9 m) relatively flat bottom, which is unlike other V-shaped channels in the area. We investigated the channel up to an elevation of ~ 209 m, noting bedrock exposure along the channel bottom at several locations (fig. 134a), as well as the head scarp of a debris slide that contributed material to the 2020 debris flow and deposited trees into the channel bottom (fig. 134b).

Soil Stratigraphy:

Observed in the right bank (~elev. 80 m), *UTM Z8 472569 6567470* (fig. 135a)*:*

0 – 2 m	Gy Sa w/ Gr, cobbles, and boulders (interpreted alluvial fan deposit)
> 2 m	Bedrock

Observed in right bank (~elev. 93 m), *UTM Z8 472608 6567507* (fig. 135b)*:*

0 – 0.2 m	Org mat
0.2 – 0.5 m	Gy Si Sa Gr over buried root layer (interpreted previous debris flow)
0.5 – 1.5 m	Gy Si Sa Gr over buried root layer (interpreted previous debris flow)
1.5 – 2 m	Bn-Or Sa with Gr, iron-cemented
> 2 m	Gy Sa with Gr

Additional notes: This creek is unnamed but is known colloquially as Cunningham Creek. The creek was reported to be out of its banks by approximately 35 ft/~10 m laterally during the December 2020 storm event, and completely washed out Piedad Road. The property owner nearest the creek worked more than 60 hours, through several debris flow pulses (likely caused by log jams forming and releasing upstream), to clear debris and build up the bank to return flow back to its channel.

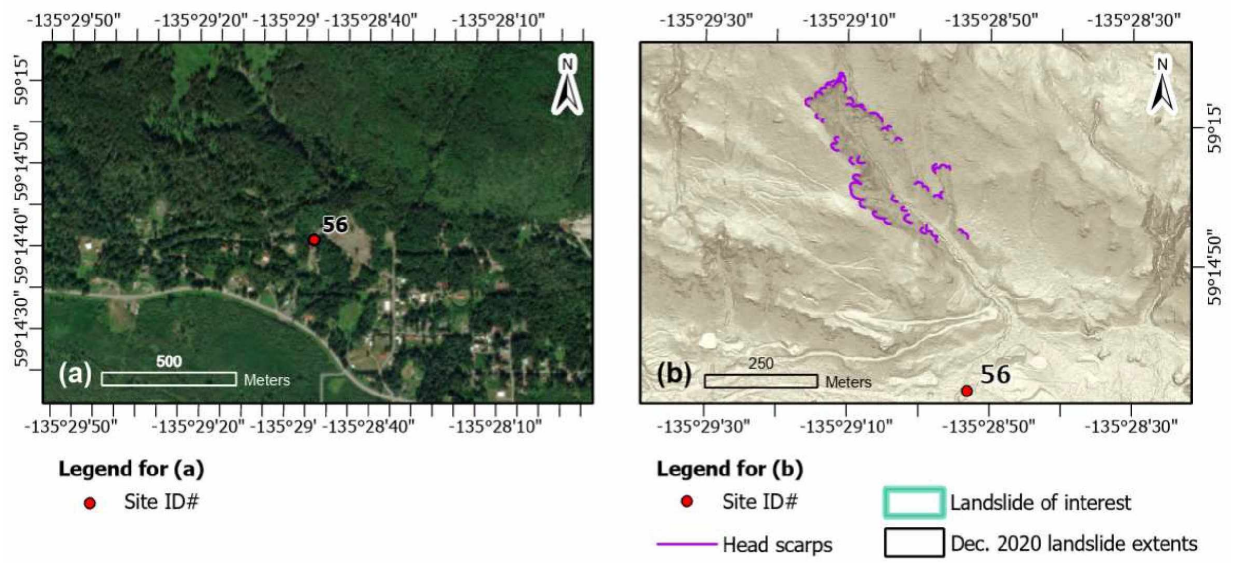

Figure 133. Maps showing location of the Cunningham Creek site (site 56): (a) 50-cm resolution RGB imagery (basemap from ADNR, 2020); (b) slope map derived from 2020 lidar (Daanen and others, 2021). ***NOTE:*** *the legend is standard for all maps; not all items may be present in (b).*

Figure 134. Photographs of upper Cunningham Creek, taken in July 2022: (a) exposed bedrock in the channel at ~126 m elev.; (b) the head scarp of one of the sources of debris for the December 2020 event (~210 m elev.).

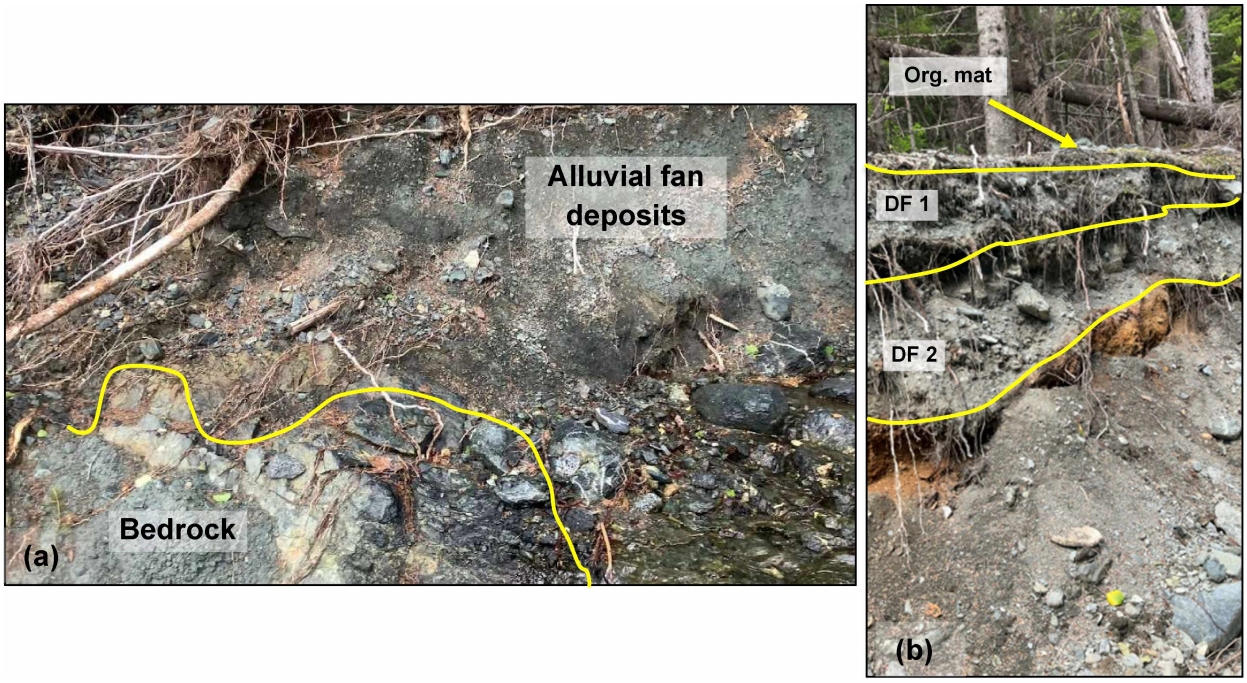

Figure 135. Annotated photographs of the stratigraphy within lower Cunningham Creek: (a) bedrock exposure within the channel, overlain by sand and gravel (June 2021); (b) two potential past debris flow (DF 1 and DF 2) burying organic mats (July 2022).

Site ID#: 57 **Date Visited:** 6/17/2021
FEMA DOT#: N/A **Field Crew:** VN, MD
Field Name: Beach Road Minor slide
GPS Coordinates: UTM Z8 476236 6564663 (fig. 136)

Samples Taken: Samples were collected from the slide body just below the head scarp.
UTM Z8 476236 6564663:
21-01 (small bag) ***poorly-graded sand with silt and gravel (SP-SM)*** (fig. 137)
21-02 (tin) ***MC 25.0%, Org 5.0%***

Landslide Classification and Dimensions: *Debris slide*; length 79 m, width 9 m, L/W 8.7, aerial extent 775.9 m^2

Site Description: This is a small debris slide accessible to the southeast from the end of Mt. Riley Road. We investigated the head scarp area, where the landslide occurred in colluvium and scoured down to the bedrock surface (fig. 138). A fiber optic cable runs up the slope to the east of the slide.

Soil Stratigraphy: (left flank near head scarp)
0 – 10 cm Org mat with roots
20 – 30 cm Bn PG Sa w/ Si and Gr [21-01, 21-02] (colluvium)
>30 cm Bx (ultramafic); Bk sandy veneer at surface

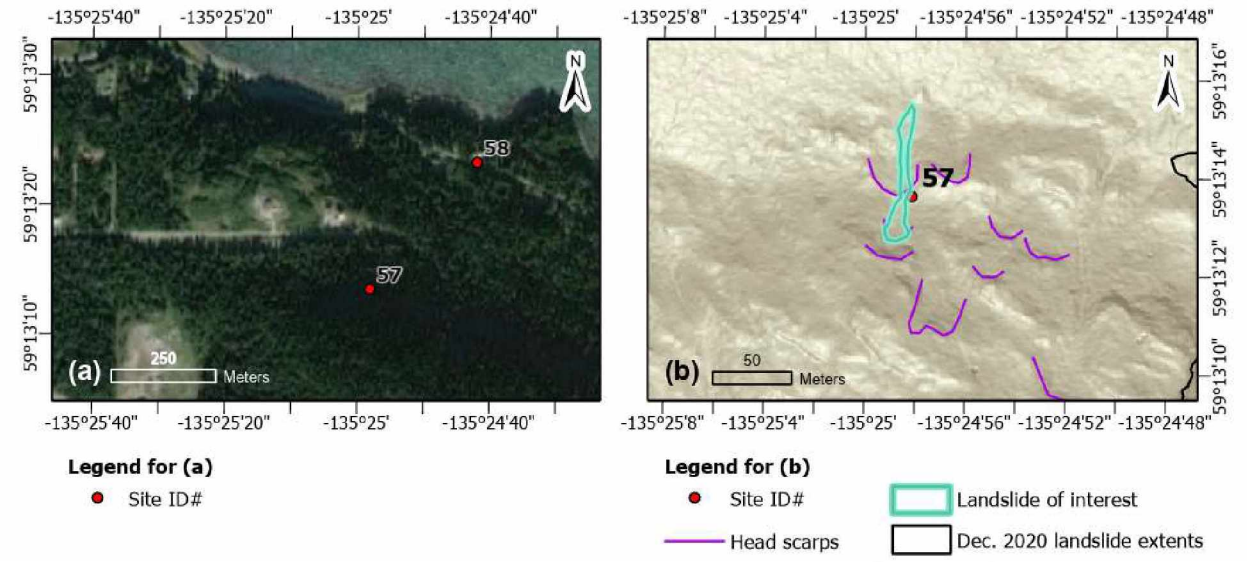

Figure 136. Maps showing location of the Beach Road Minor slide (site 57): (a) 50-cm resolution RGB imagery (basemap from ADNR, 2020); (b) slope map derived from 2020 lidar (Daanen and others, 2021). ***NOTE:*** *the legend is standard for all maps; not all items may be present in (b).*

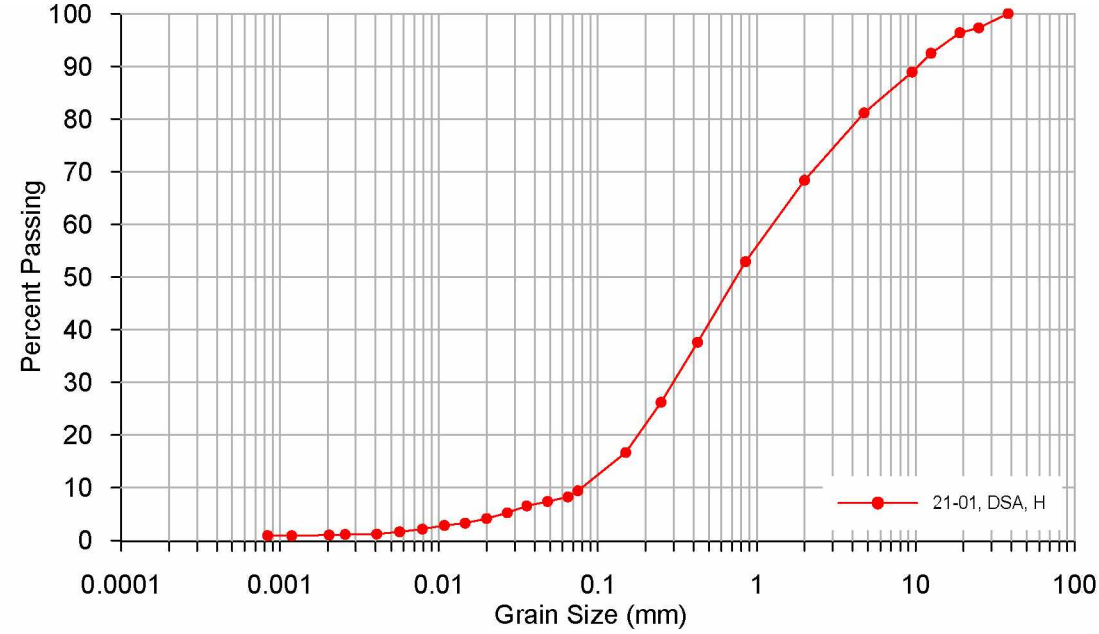

Figure 137. Grain-size distribution for sample 21-01.

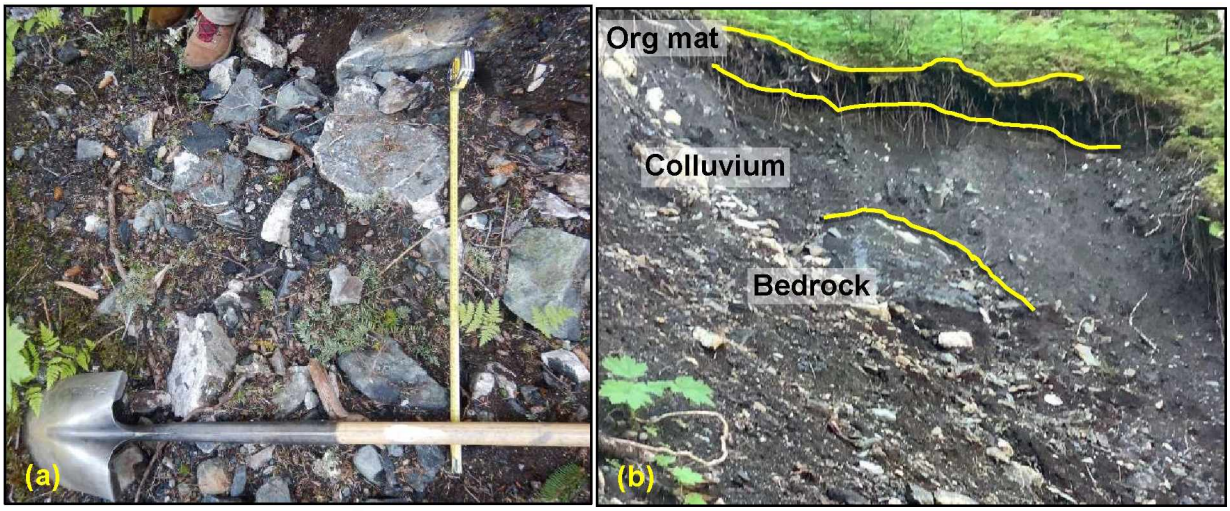

Figure 138. Photographs of the Beach Road Minor Slide (June 2021): (a) typical soil in the slide body; (b) view of left flank near the head scarp with annotated stratigraphy.

Site ID#: 58 **Date Visited:** 6/19-22/2021, 7/15-21/2023
FEMA DOT#: N/A **Field Crew:** VN, MD, JW, MG, RD
Field Name: Beach Road Landslide
GPS Coordinates: UTM Z8 476493 6564982 (fig. 139)

Samples Taken: See fig. 140 for grain-size distributions.

Samples collected from above the head scarp *(UTM Z8 476504 6564421*):

21-19 (bag) ***silty sand with gravel (SM)***
21-20 (tin) ***MC 15.0%, Org 2.7%***
21-21 (bag) ***silty sand with gravel (SM)***

Samples collected from test pits in the slide body, near Beach Road:

UTM Z8 476465 6564956:

21-24 (bag) ***poorly-graded sand with silt and gravel (SP-SM)***
21-25 (tin) ***MC 14.2%, Org 2.5%***

UTM Z8 476520 6564920:

21-26 (bag) ***well-graded sand with gravel (SW)***
21-27 (tin) ***MC 9.0%, Org 1.9%***

Point Load Testing (rock samples):

Biotite magnetite clinopyroxenite

No. tests conducted:	12
Point load strength index:	0.46 MPa
Standard deviation:	± 0.51 MPa

Diorite

No. tests conducted:	4
Point load strength index:	0.96 MPa
Standard deviation:	± 0.69 MPa

Landslide Classification and Dimensions: *Debris avalanche – debris flow*; length 687 m, width 170 m, L/W 4.0, aerial extent 107,183.1 m^2

Site Description: The Beach Road Landslide (BRLS) was the largest of the December 2020 mass movements, having an approximate volume of 187,100 m^3. It destroyed or severely damaged four residences, and killed two occupants of one of the residences (Darrow and others, 2022). Analysis of lidar data and field investigations revealed evidence (e.g., head scarps, displaced rock masses) of other large paleolandslides along North Riley Ridge, where the BRLS originated (Darrow and others, 2022). The bedrock is biotite magnetite clinopyroxenite with intrusions of diorite (fig. 141).

Soil Stratigraphy: (above head scarp, *UTM Z8 476504 6564421*)

0 – 10cm	Org mat
10 – 64 cm	Bn Sa Si w/ Gr [21-19, 21-20] (colluvium), ultramafic clasts up to 10 cm in diameter
64 – 98 cm	Gy Si Sa w/ Gr [21-21] (glacial deposits)
> 98 cm	Bx (Biotite magnetite clinopyroxenite)

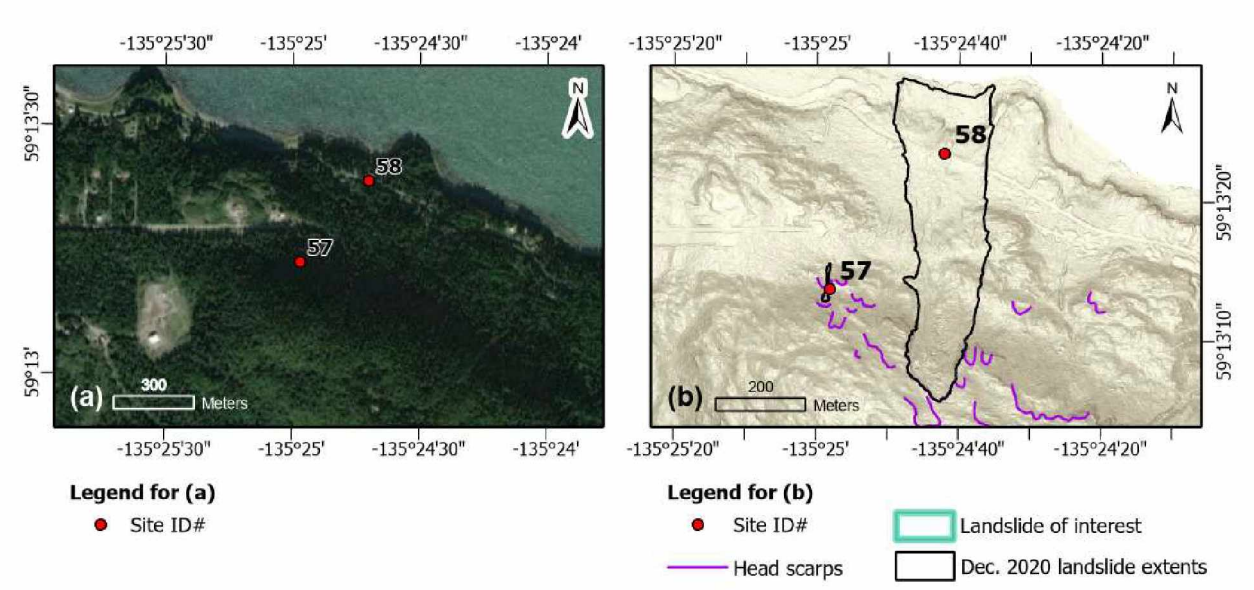

Figure 139. Maps showing location of the Beach Road Landslide (site 58): (a) 50-cm resolution RGB imagery (basemap from ADNR, 2020); (b) slope map derived from 2020 lidar (Daanen and others, 2021). ***NOTE:*** *the legend is standard for all maps; not all items may be present in (b).*

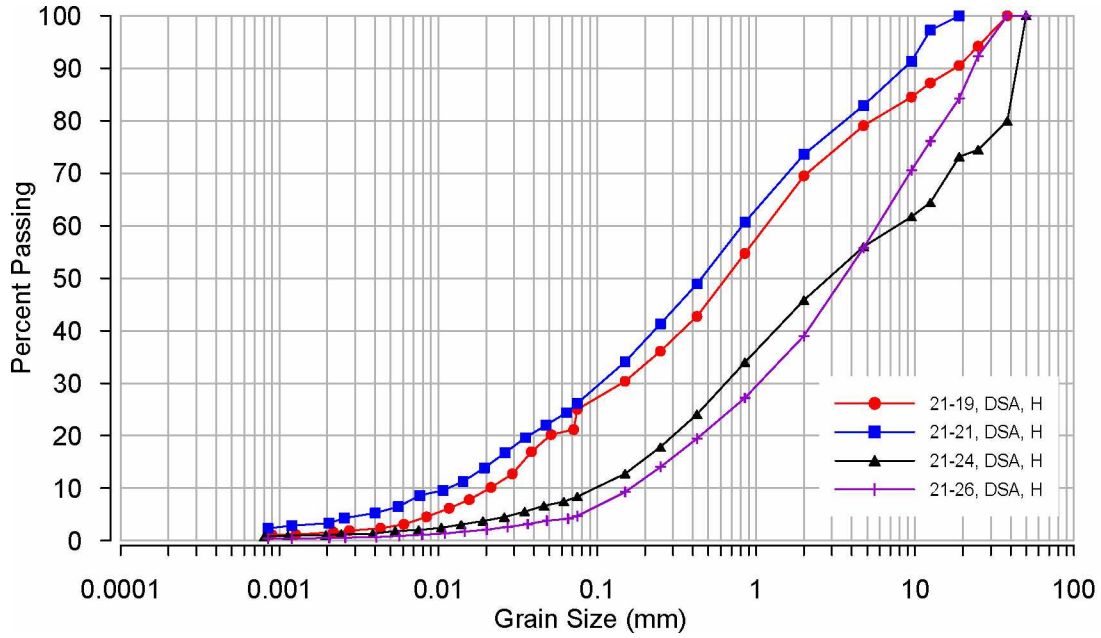

Figure 140. Grain-size distributions for samples 21-19, 21-21, 21-24, and 21-26.

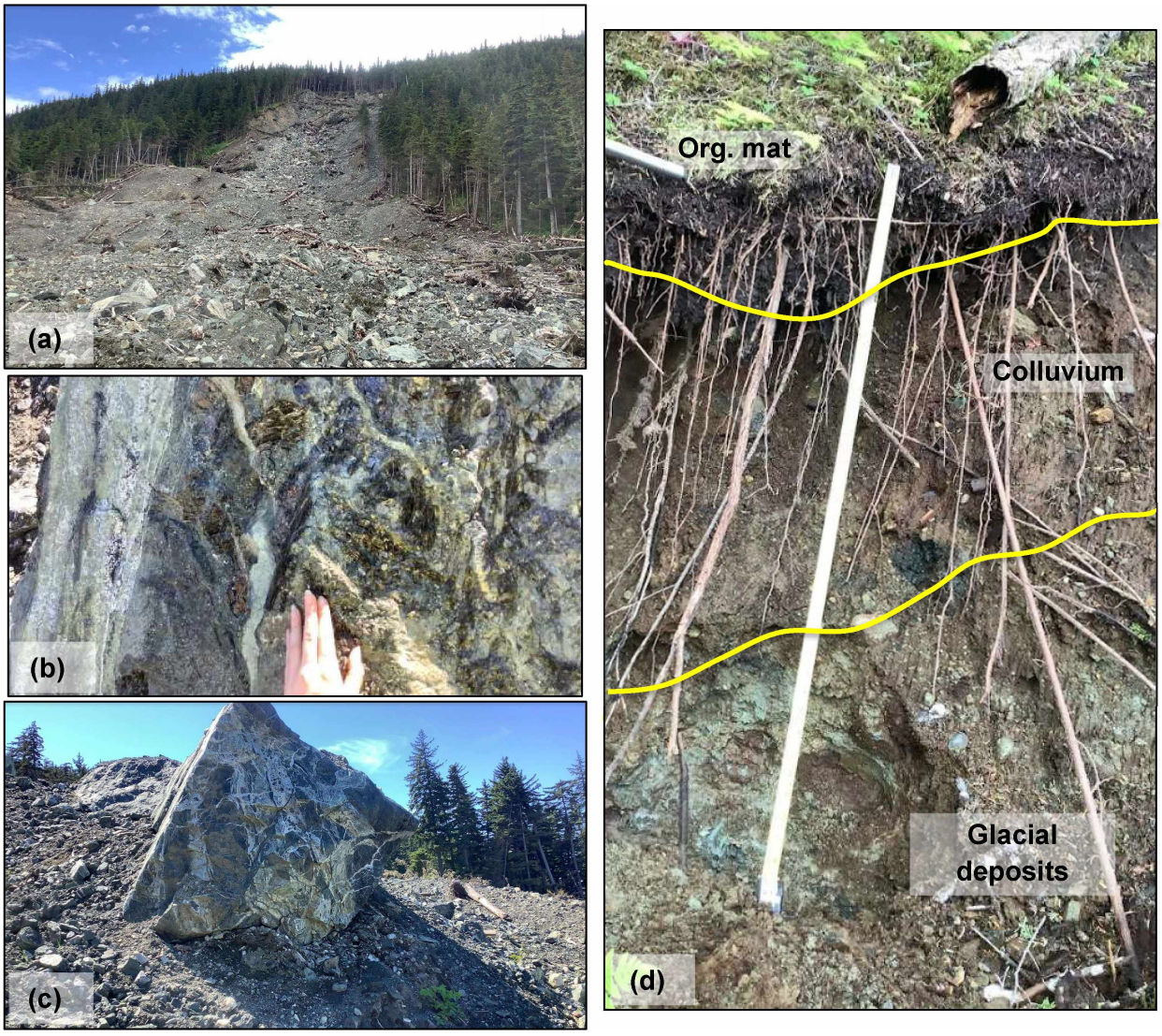

Figure 141. Photographs from the Beach Road Landslide (BRLS): (a) looking up to the head scarp from the road (~ 200 m elevation difference; July 2022); (b) a close-up view of a biotite magnetite clinopyroxenite boulder with diorite veins and large (8 cm) biotite crystals (June 2021); (c) the entire ~5 m dia. boulder seen in (b) (June 2021); (d) annotated photograph of soil stratigraphy above the BRLS head scarp (June 2021).

CHAPTER 5: ANALYSIS

Our research question is: What factors contributed to the widespread landslides in the Haines area in December 2020? This is an important question, as the answer will help to explain why certain slopes failed and others did not. The factors that we studied in the field, from laboratory testing, and through my desktop analysis, were: 1) mass movement type; 2) soil type and depositional environment; 3) slope angle; 4) potential anthropogenic impacts; and 5) previous history of landslides. It must be stressed that the landslides described in this catalog, although significant in number, do not include all of the areas within the Haines Borough affected by the December 2020 weather event. We hope that by finding shared factors among the sites we studied, it will be possible to draw overall conclusions and identify areas of higher risk for landslides in the event of another AR or other historic rainfall event.

OVERALL SUMMARY OF MASS WASTING EVENTS

The 58 sites presented in the catalog (Chapter 4) fall into eight landslide types (table 2, fig. 142), following the classification of Hungr and others (2001; 2014). The most common mass wasting events that occurred as a result of the December 2020 storm were debris flows, followed by debris slides; both of these types are widespread in mountainous regions.

Debris flows are rapid surging flows of saturated debris usually confined within a steep channel (Highland and Bobrowsky, 2008); these were commonly observed along Lutak Road within existing drainage channels from the Takshanuk Mountains. The channelization of these flows localizes their effects, but also concentrates them. Periodic damming and release of material can contribute to a debris flow's strength (Hungr and others, 2014); this was observed at site 56 along Piedad Road. As the soil in these flows begins to fail and move downslope, the bed of the

Table 2. *Summary of landslide types, classified based on Hungr and others (2001; 2014).*

Landslide Classification	No. of Sites
Debris flow	26
Debris slide	19
Rock fall	4
Sand flowslide	4
Debris fall	2
Debris slide–debris flow	2
Debris flow–debris flood	1
Debris avalanche–debris flow	1

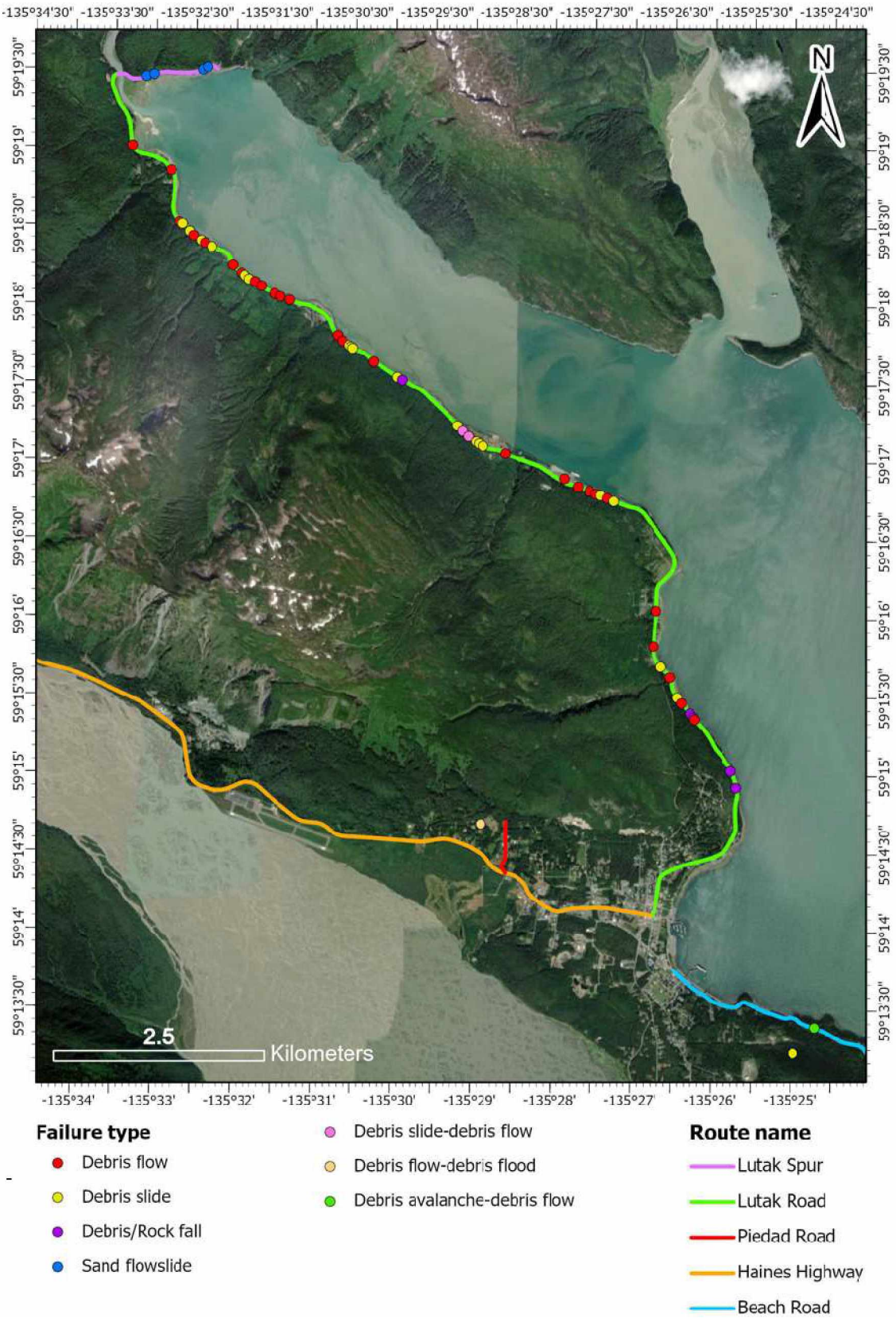

Figure 142. Location map of investigated landslides, colored based on classification according to Hungr and others (2001; 2014) (basemap from ADNR, 2020).

channel experiences what could be considered impact loading, which can result in the liquefaction of coarse-grained materials that become part of the surge (Sassa, 1985). This surge can also include material from banks that fail, organic debris, and even existing water in the channel (Hungr and others, 2014). Most of the material within a debris flow is debris that is picked up along the way and coalesced into the surge, rather than the initial failed material (Hungr and others, 2014). Sand flowslides are a type of debris flow that involve excess pore water pressure as a failure mechanism (Hungr and others, 2014).

Debris flows were the most common type of landslide that occurred during the December 2020 AR. Most of the significant debris flows that occurred along Lutak Road originated within well-established drainage channels that have source areas up to 200 m in elevation in the Takshanuk Mountains. These observations correlate with the fact that debris flows are widespread phenomena in mountainous terrain, and usually occur within previously-established paths, such as gullies and drainage channels (Hungr and others, 2014). A handful of smaller debris flows generated only enough material to fill the ditch beside Lutak Road (ADOT&PF, 2020). Several established creeks, such as Shakuseyi Creek (site 6) and Johnson Creek (site 48), also generated debris flows in 2020. All of these drainage channels and creeks demonstrate evidence of past activity in the form of visible scarps in the lidar. Average channel gradients are between 16° and 28°, as measured from profiles drawn in ArcGIS Pro; Hungr and others (2014) reported that channels steeper than 10–20° are optimal for debris flow occurrence. We did not investigate the debris flows in-depth for several reasons: nearly all of the catchments were difficult to access by foot; there were no remaining deposits at the time of our field visits due to clean-up efforts; and most of the channels are so scarred by previous landslides that it is impossible to tell using only the lidar which scarps were the debris sources.

Debris slides are defined as masses of granular material on shallow, planar surfaces that have failed parallel to the ground surface (Hungr and others, 2014). The granular material is typically colluvium or weathered soil overlaying a strong substrate (which could be a more solid soil layer or bedrock) (Hungr and others, 2014). Colluvium over bedrock is a common soil profile within the mountainous regions of the world (Hungr and others, 2014). These veneers of soil are notoriously unstable, and their stability is often reliant on outside influences such as vegetation (Hungr and others, 2014). Debris slides can be triggered by extreme rainfall, and there are often spatial correlations between rainfall intensity and landslide density (Hungr and others, 2014). Debris slides also often initiate other failures such as debris flows and debris avalanches. We observed both rock falls and debris falls within the study area. Falls involve the detachment of

rock fragments or blocks of soil from larger bodies; while the impact of a fall is usually limited, falls are common triggers for avalanche-type landslide events (Hungr and others, 2014).

While some landslide types can fall into one classification, it is also possible—and usually more often the case—that a landslide is a combination of two types, with one type being the initiating event that leads to the second type (Hungr and others, 2014). There were debris slide–debris flows at sites 32 and 33 along Lutak Road. As an example, site 32 has a compound classification because the debris flow occurred within an existing drainage channel, but the channel also experienced widening as a result of debris sliding. A debris flow–debris flood occurred at site 56 along Piedad Road. This event was a series of debris flow surges, with periodic damming and releasing within the banks of Cunningham Creek. It later transitioned into a debris flood, which is a rapid flow of water containing some debris that is usually pulled from the banks or bed of a channel (Hungr and others, 2014). The BRLS is a debris avalanche–debris flow. Debris avalanches occur on steep slopes and are typically associated with failures in colluvium (Hungr and others, 2014; Highland and Bobrowsky, 2008). In the case of the BRLS, an initial debris avalanche caused a successive failure downslope, generating a debris flow through impact loading of an area known for having poor drainage (Palmieri, pers. comm., 2021). Hungr and others (2014) note that clusters of debris avalanches and debris flows during rainstorms are responsible for some of the most catastrophic landslide-related disasters on record.

Our overall assessment of factors that we initially hypothesized may have contributed to these 58 landslides, in addition to the high intensity rainfall, are as follows: 1) the soil type and depositional environments of the sediments that failed did not appear to have a significant effect on the types and extents of most of the failures observed; 2) the average slope angles of the failures were at or exceeded typical values for angles of internal friction for these soils; 3) there are potential anthropogenic factors that contributed to slope instability; and 4) there is extensive evidence of previous landslides visible in the lidar. Each of these observations will be discussed in more detail within this chapter.

Table 3 summarizes the soil and geomorphic characteristics of the sampled landslides. The typical angles of internal friction of the types of soils sampled were taken from Bowles (1984) and are an average of the ranges provided for loose and dense material. The slope angles of these landslides were measured by generating elevation profiles along the centerline of the

Table 3. Summary of soil and geomorphic characteristics of sampled sites; L/W stands for length-to-width; '---' indicates not measured.

Site ID	Landslide classification	L/W ratio	Soil classification	Typical frictional angle[1]	Slope angle	Permeability[2]	Depositional environment
1	Sand flowslide	2.0	PG Sa w/ Gr, PG Sa	35°	37°	Pervious	Delta (uplifted)
2	Sand flowslide	1.8	PG Sa	35°	30°	Pervious	Delta (uplifted)
3	Sand flowslide	0.5	PG Sa	35°	45°	Pervious	Delta (uplifted)
4	Sand flowslide	2.4	PG Sa	35°	26°	Pervious	Delta (uplifted)
16	Debris slide	2.9	Si Sa w/ Gr	32°	27°	Impervious	Shore (uplifted)
17	Debris slide	2.7	Si Sa w/ Gr	32°	27°	Impervious	Shore (uplifted)
25	Debris slide	0.4	PG Gr w/ Sa PG Sa Si Sa	40° 35° 32°	38°	Pervious to-semipervious Pervious Impervious	Shore (uplifted)
31	Debris slide	0.6	Si Cl Sa	35°	40°	Impervious	Marine (uplifted)
38	Debris flow	---	Si Sa w/ Gr, WG Sa w/ Si and Gr	34°	---	Pervious to-impervious	Shore (uplifted)
39	Debris flow	---	PG Gr w/ Si and Sa	32°	---	Pervious to-semipervious	Shore (uplifted)
44	Debris slide	2.9	WG Gr w/ Sa Sa Si	40° 32°	28°	Pervious Impervious	Marine (uplifted)
47	Debris slide	---	WG Gr w/ Sa	35°	---	Pervious	Shore (uplifted)
57	Debris slide	8.7	PG Sa w/ Si and Gr	35°	32°	Pervious to-impervious	Colluvium

[1] *values from Bowles (1984)*

[2] *values from Coduto (1999), and Lambe and Whitman (1969)*

landslide extent polygon (from the head scarp to the terminus) and then solving for the angle created by the profile using trigonometric functions. No values for slope angle or length-to-width (L/W) ratio are reported for landslides without mapped extents. The descriptions of soil permeability are from Coduto (1999) and Lambe and Whitman (1969). These descriptors are based on the USCS soil classification for the samples collected at each landslide.

SOIL TYPE AND DEPOSITIONAL ENVIRONMENT

One of the key factors in evaluating landslide hazards is soil type. Properties such as the angle of internal friction, grain size, and permeability all play a role in slope stability. This portion of the analysis is focused on areas that we mapped and sampled. Because we mainly focused on soils during the 2021 and 2022 field visits, and as Darrow and others (2022) provided a more detailed investigation of the role bedrock quality played in the BRLS, we do not include an analysis of bedrock strength properties here. We tested and classified 41 soil samples based on grain-size distribution and plasticity. The most common classifications were poorly-graded sand with varying amounts of silt and/or gravel content, and silty sand with varying amounts of gravel (table 3). The soils we sampled came from the following four depositional environments: elevated shore deposits, elevated marine deposits, glacial-related deposits, and colluvial deposits.

Defining the depositional environments

Shore deposits consist mostly of sand and gravel-sized soil, but also may contain pockets of finer-grained soil like silt (Thornbury, 1954). In the lidar-based slope maps, paleo-shorelines are evident in the areas adjacent to the BRLS, around the Haines Ferry Terminal, along Lutak Road, and along Lutak Spur (fig. 143). These uplifted shorelines are most commonly observed below 100 m elevation and near most of the sampled landslides (for example, see figs. 61 and 96). Marine deposits consist of fine-grained silt and clay, but also can contain seams of fine- to medium-coarse sand (Bowles, 1984). These deposits were observed mostly around the Haines Ferry Terminal, and in areas lower in elevation than the paleo-shorelines (often immediately adjacent to Lutak Road), which is stratigraphically consistent for marine-related deposits. These elevated deposits are the result of the significant GIA that has occurred in the Haines area (Larsen and others, 2005; Motyka and others, 2007). One distinct feature of marine deposits is varves, which form as a result of the seasonal deposition of silt in the summer months and clay in the winter months (Terzaghi and Peck, 1948). We observed and sampled a varved deposit,

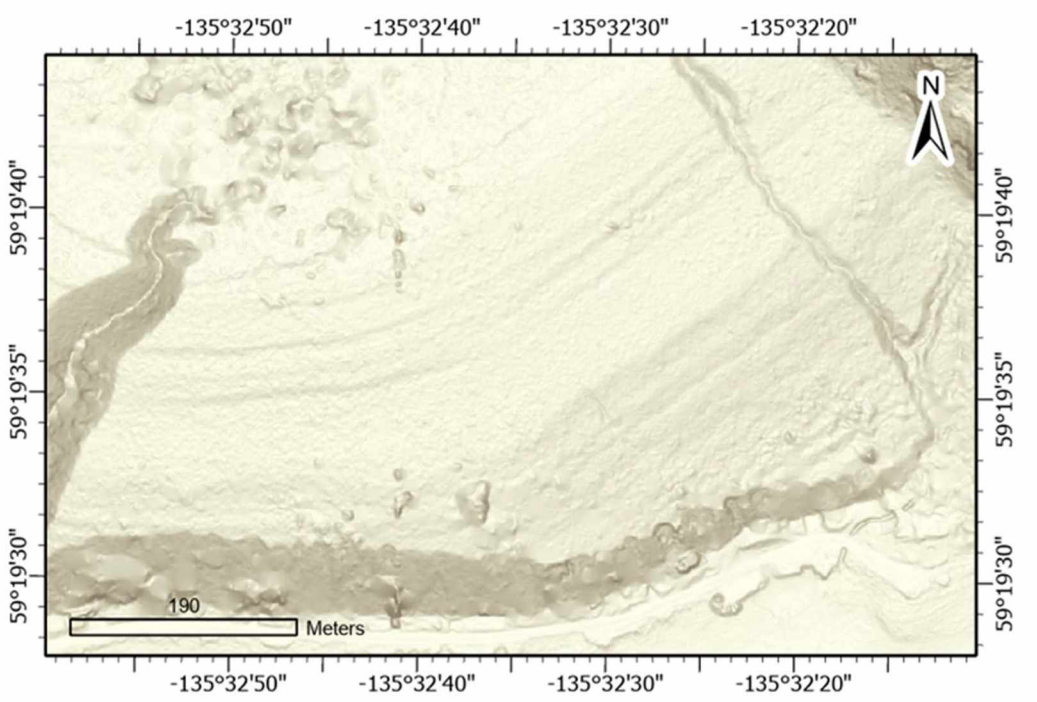

Figure 143. Paleo-shorelines visible above Lutak Spur, as seen in the slope map derived from 2020 lidar (Daanen and others, 2021)

consisting of alternating silt and sand, that was exposed by the debris slide at site 44. In the head scarp, we noted sandy gravel and gravelly sand, indicating a shore deposit directly upslope of the varved strata.

Glacial deposits are commonly erratic and irregularly deposited, lack stratification, and consist of a combination of silt, sand, gravel, cobbles, and boulders (Terzaghi and Peck, 1948). As mentioned in Chapter 2, the Haines area, including North Riley Ridge, was formerly covered by glaciers. The pocket of soil that was observed at the top of the BRLS stratigraphically below colluvium and above bedrock, was likely deposited by a glacier. Lemke and Yehle (1972) reported that the pyroxenite bedrock south of Haines that forms Mt. Riley was streamlined by glacial action, and that glacial sediments form the surface mantle on the ridge. Additionally, the soil observed was silty sand with gravel, and was found at an elevation similar to other glacial deposits mapped by Lemke and Yehle along Lutak Road (~ 260 m).

At nearly all of the sites summarized in table 3, a thin organic layer overlies a layer of colluvium ranging from 30-cm to 2-m thick. The colluvium blankets the uplifted shore and marine deposits at most locations. Colluvium is defined as superficial deposits that are transported downslope predominantly by gravity and contain less than 50% of soil that is greater than 60 mm in

diameter (Parry, 2011; Lemke and Yehle, 1972). Observed and sampled colluvium deposits in the study area were often a mix of silt and sand with some gravel; this is attributed to the mixing of soil from downslope movement. Tree roots were predominant in the colluvium layer. This is an important observation since colluvium is often reliant on outside factors for stability. Lemke and Yehle (1972) also noted that the colluvium has several potential origins, including the typical slow downslope movement caused by gravity as well as fast-moving deposits like landslides and avalanches.

Explaining length-to-width (L/W) ratios

For the landslides in table 3 with mappable extents, we determined the L/W ratio. The length was measured starting from the center of the head scarp down the centerline of the landslide extent to the center of the toe area, which was terminated at the edge of the road (or the bottom of the slope, in the case of Lutak Spur sites) due to the lack of an actual toe deposit. The width was measured at the center of the landslide, from flank to flank. For landslides with uneven shapes, we measured the width in an area that represented the average width of the overall extent.

Taylor and others (2018) summarized L/W ratios from 21 studies of landslides triggered by several different mechanisms; several of the studies focused on shallow landslides that were triggered by rainfall and reported average L/W ratios of between 1.4 and 2.5, with a minimum of 0.6 and a maximum of 4.2. The overall average L/W ratio for measured events in the Haines study area is 1.9, which is consistent with the results of Taylor and others (2018) and reinforces the observation that the landslides in the study area were shallow and likely triggered by precipitation. An outlier is the Beach Road Minor landslide, with a L/W ratio of 8.7; this is likely due to the topography on Riley Ridge constraining and directing the flow down an existing drainage path (Orris and Williams, 1984). Taylor and others (2018) also posited that L/W ratios less than 0.5 are indicative of multiple failures that have coalesced to form one larger failure; this situation matches some of the slides with L/W ratios less than 1.0 along Lutak Road.

In situ shear strength soil testing along Lutak Road

We conducted *in situ* strength testing in 2022 using a vane shear device, following the ASTM D2573 standard (ASTM 2018) at two sites along Lutak Road: site 31 (the “Stratigraphy slide”) and site 44 (the “Varve site”). At site 31, the silty clayey sand (elevated marine deposits) had an average shear strength of 4.9 ± 1.2 kPa. At site 44, the sand to silty sand (varve deposit)

produced an average shear strength of 16.6 ± 4.6 kPa. It is difficult to locate sources for standardized shear strengths of soils because so many factors can influence this value; however, both of these samples are within the "very soft soil" classification based on Davison (2000). Very soft soils, with their low permeability and low shear strength, are considered undesirable, and present problems when disturbed (Jwaida and others, 2017).

Role of soil type in slope failure

A common failure mechanism of landslides is increased pore water pressure resulting from rainfall or an increase in other shallow groundwater sources that results in a reduction of soil shear strength (NAVFAC, 1986). Sand, gravel, and non-plastic silt are considered cohesionless soils unless special conditions exist that create environments for apparent cohesion (Earle, 2015). Most cohesionless soils, specifically sand and gravel, have good drainage and are pervious to groundwater flow. Thus, in normal conditions, excess pore water pressure dissipates quickly (Coduto and others, 2016); however, sand and silt both have potential to become "quick" when pore water pressure exceeds soil strength (Bowles, 1984; Lambe and Whitman, 1969). When a soil becomes quick, the effective strength within the soil is zero, and the slope will fail. Additionally, silt in particular is an easily erodible, impermeable material that is known to contribute to erosion during rainfall events and is cited as being inherently unstable (Lambe and Whitman, 1969; Sun and others, 2021).

We did not conduct hydraulic conductivity tests on the collected samples, so our evaluation is based on the USCS soil classifications and associated permeability classifications by Coduto (1999) and Lambe and Whitman (1969). For the sampled sites (table 3), nearly the same number of landslides occurred in good and poor drainage conditions (we averaged drainage classifications for sites with multiple soil types). There was no clear pattern in whether debris slides or debris flows occurred more often in soils with good or poor drainage, suggesting that this factor may not be as important as we initially postulated for the 2020 landslides occurrences. It is worth stating that, while there appears to be no overall qualitative correlation between soil type and landslide type for most of the studied landslides, there is a correlation with the sand flow slides and their location along Lutak Spur. As will be discussed in a later section, Lutak Spur is a depositional feature that is almost purely sand, so it is logical for sand flows to occur in this area.

Why did so many landslides occur during this one storm, when high amounts of precipitation are expected annually in Southeast Alaska? While it is true that Southeast Alaska has a wet climate, the amount of precipitation between December 1 and 2, 2020, was equal to the average total precipitation for the entire month of December (NWS, 2023b). Thus, the number of failures and the lack of correlations among soil type, landslide type, and landslide occurrence are likely because there was so much precipitation and snowmelt that none of the soil types present, even the well-draining soils, could drain fast enough to prevent the significant increase in pore water pressure.

Lutak Spur: A unique formation in the study area

The landform separating Chilkoot Lake from Lutak Inlet (which Lutak Spur traverses) represents a depositional feature that is unique within the Haines area. Lemke and Yehle (1972) suggested that the landform (referred to herein as "the Spur") is an elevated delta that buried a moraine from a glacier in the Chilkoot Valley. Based on field observations of the geomorphology of the Spur, the authors do not fully support Lemke and Yehle's designation. We concur that the Spur itself is deltaic in nature, but question the presence of a buried moraine.

Deltas can have complex and atypical structures due to constantly shifting channels; however, there is often a specific set of bedding features present in delta formations, known as the bottom-set, fore-set, and topset beds (Terzaghi and Peck, 1948; Thornbury, 1954). We did not observe this entire sequence of bedding features, though it is possible that we observed only the topset beds, and the bottom-set and fore-set beds were either buried or eroded. Wherever soil was exposed, we observed only sand with some rounded gravel and cobble layers; the sand layers are typical of deltaic environments, and the gravel and larger grain sizes are attributed to a glacial source (Terzaghi and Peck, 1948; Bowles, 1984). Residents along Lutak Spur reported that they encountered only sand when digging or drilling groundwater wells; one resident intercepted sandy soil for the full depth of his well, approximately 24 m (Buck, pers. comm., 2022). There are also paleo-shorelines that are visible across the Spur, which indicate that the sand was deposited in a subaqueous environment and that the area is rising due to GIA. We also observed cross-bedding, as well as dark (fine-grained) and light (coarse-grained) sand layers in exposures created by the sand flows, most prominently at site 3. We hypothesize these to be the result of seasonal deposition, which furthers the idea that the Spur was once submerged, since seasonal deposition is characteristic of low-energy environments, like deltas or lakes (Bowles, 1984). The following is one hypothesis for the formation of the Spur. As

glaciers retreated from the area, Lutak Inlet may have been dammed by the glacier that occupied the valley that leads to Skagway, creating a proglacial lake. The glacier retreating up valley from what is now Chilkoot Lake continued to produce sediment, which was deposited as a delta into the proglacial lake. The delta rose above current sea level as the area uplifted with GIA. The steep slope currently facing Lutak Inlet is likely the result of a combination of ongoing uplift, wave action, and even previous landslides.

The presence of a buried moraine beneath the Spur is questionable since during our field investigations in 2021 and 2022 we found no deposits or landforms that resemble typical moraines (e.g., well-graded, coarser material). The possibility exists, however, that a moraine is deeply buried by the sand. To confirm its presence would require additional investigation of the subsurface, including the use of geophysical methods for broad coverage of the subsurface, with targeted boreholes to confirm observations from the geophysics.

At site 3, we observed “slope-forming” behavior of the coarse-grained sand layers and “cliff-forming” behavior of the fine-grained sand layers. Visual evaluation of the different layers revealed that the fine-grained sand was darker than the coarse-grained sand, which we attributed to a higher magnetite content in the fine-grained sand. We hypothesize that the magnetite content of the sand is a potential factor in the slopes of Lutak Spur standing at an average angle of 40°. Another factor in the ability of the sand to stand at such a steep angle is related to its moisture content. The sampled fine-grained sand had a higher moisture content (6.6%) than the coarse-grained sand (0.9%). While sand is a cohesionless soil, the presence of small amounts of water can result in a phenomenon known as apparent cohesion. Water molecules stick to one another, and also stick to other surfaces; this is why a meniscus forms when water is in a glass. Sand is also hydrophilic, or water-loving (Scalia, 2022). As sand is wetted, water covers some grains as a film; then, some pores within the matrix are filled with water; and finally water forms bridges between sand grains, helping them to stick together (Earle, 2015). This allows a sand slope to stand at angles steeper than the typical internal friction angles for sand (table 3). Too much water, however, results in the water molecules pushing the sand grains apart, reducing friction between the grains, and causing the slope to fail (Earle, 2015). We suggest that this phenomenon and the sand’s magnetite content allow the slopes along Lutak Spur to stand at an average angle that far exceeds the expected maximum angle of internal friction.

SLOPE ANALYSIS

As mentioned in Chapter 2, the area around Haines is mountainous and has been sculpted by glacial processes over tens of thousands of years, resulting in steep slopes. The following is an analysis of the effect of slope angle on landslide potential within the study area.

Slope angle at head scarps in the study area

Slope angle is one of the most recognized factors in slope stability; however, there is a lack of consensus with regards to what angles are more likely to produce landslides (Çellek, 2020). This is likely due to the interdependency of slope angle and other factors, such as soil and bedrock type and vegetation cover, influencing landslide potential. That said, steeper slope angles tend to fail more frequently due to gravity acting on the potential landslide mass. Generally, debris slides tend to occur on slopes with angles between 20°–40° (Highland and Bobrowsky, 2008). Figure 144 is a slope map generated from the 2020 lidar (Daanen and others, 2021). We converted the mapped head scarps into points and correlated their locations with values from the slope map to determine the slope of the surface on which the landslide originated. These points are color-coded based on the slope angle, with low angles in green and high angles in red. The minimum slope angle of the studied points was approximately 4.0°, and the maximum angle was approximately 74.5°.

Based on 768 scarp points, the average slope at the head scarps is approximately 39° ±13° (1 standard deviation), and the median slope angle is approximately 40° (fig. 145). The data in figure 145 have a normal distribution; this indicates that many factors (discussed in later sections) contributed to the slope failures (Charan 2020). Within drainage channels, the average slope angle for the scarps is between 40°–50°. Of the points located within 100 m of a roadway, the average slope is 40°, and for the points located within 50 m of a roadway, the average slope angle increases to 46°. Of the 768 points, 329 (43%) have slope angles of 20°–40°, which is the expected range for debris slides (Highland and Bobrowsky, 2008), and 698 of the points (91%) have a slope angle greater than 20°, which Hungr and others (2014) indicate as the necessary steepness for debris flows. This helps to explain why debris flows were the most observed landslide type within the study area.

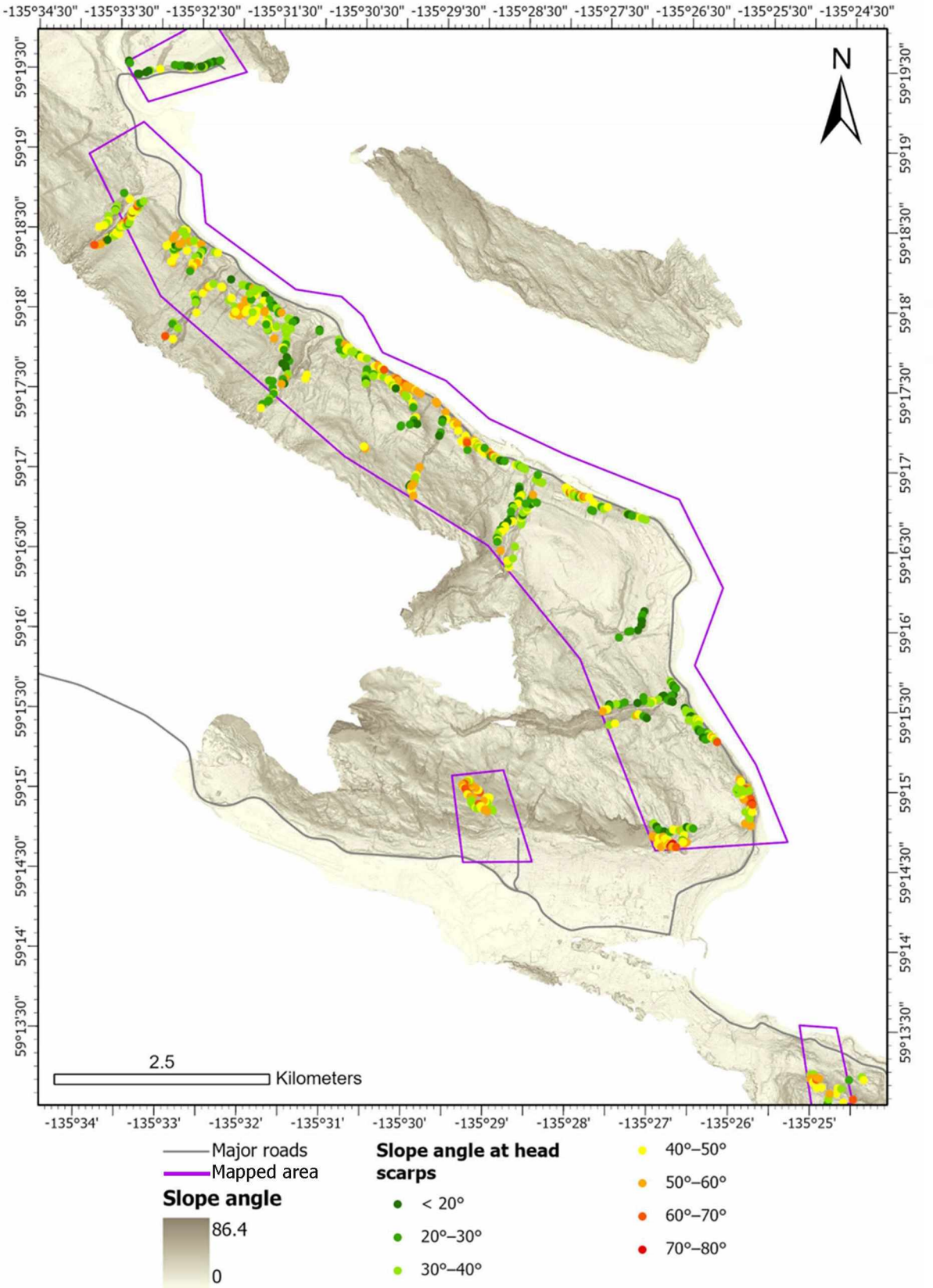

Figure 144. Slope map of the study area including slope angles of points at the head scarps of mapped landslides. Map derived from 2020 lidar (Daanen and others, 2021).

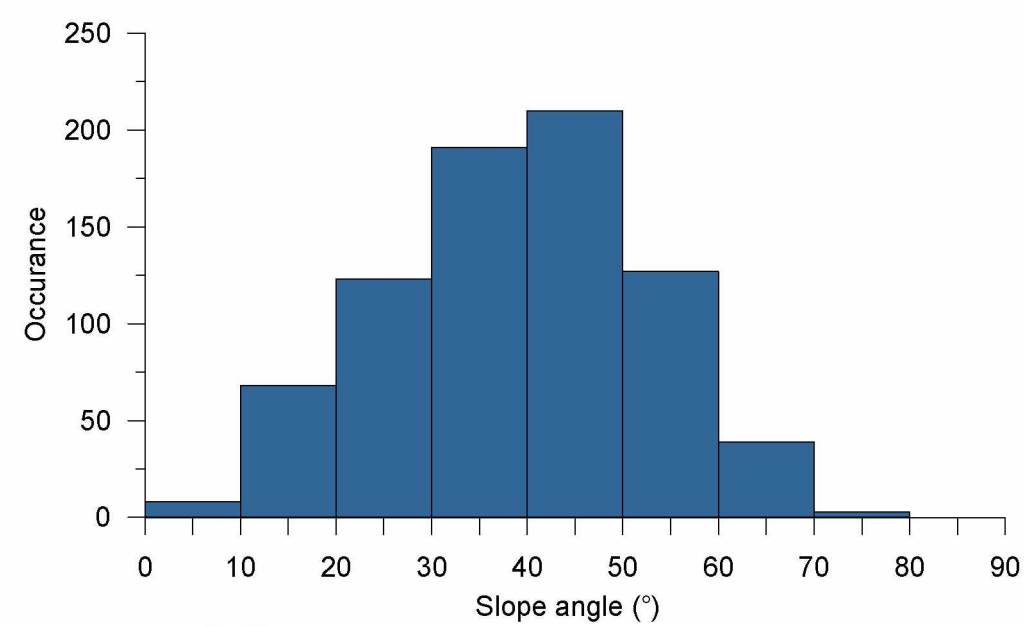

Figure 145. Histogram of slope angle at head scarp locations in the study area. Slope angle data from Daanen and others (2021)

The 768 mapped points are located within an area of interest delineated at the start of this thesis (see pink outline in fig. 144). We mapped scarps in a ~200-m wide buffer along Lutak Road and Lutak Spur, and within drainages that produced debris flows. Given this narrow linear mapping corridor, it is difficult to generalize slope relationships broadly for the area; however, observations can still be made regarding certain localized trends within the data. For example, there is an extended area of yellow and orange dots in the middle of figure 145; this area corresponds to sites 28–36. Seven of these 10 sites were debris slides, and all the landslides occurred in either colluvium or in drift deposits, both of which are a mix of silt, sand, gravel, and cobbles. As summarized in table 3 and mentioned in previous sections, a slope that is steeper than a soil's angle of internal friction is unstable. The yellow and orange dots along this section represent slopes steeper than 40°, which is greater than the highest average angle of internal friction for a soil containing gravel (Bowles, 1984). On the other hand, along Lutak Spur (i.e., the deltaic landform) the slopes are less steep, as indicated by the green dots. These slopes are either below or just above the angle of internal friction for sand. It is likely that the high-intensity rainfall played a larger role than slope angle in slope failure in this area. The red dots at the end of Lutak Road closest to downtown Haines (around sites 54 and 55) are areas of exposed bedrock (as observed in the field) that produced rock fall during the storm event. Our site investigations indicated the presence of fractured bedrock. The catchment of Cunningham Creek is also steep, with most of the dots representing slope angles greater than 40°. We posit that this is due to previous landslide activity exposing bedrock within the catchment.

Slope angles of landslides with mapped extents

Table 3 contains the average slope angles of the slide extents, based on profiles measured from the head scarp to the terminus at the road, as an estimate of pre-failure slope angles. Table 3 also contains estimated soil internal friction angles based on analysis by Bowles (1984). The angle of internal friction is typically the maximum stable slope angle for loose soil. This value is often reported for drained or dry soil conditions, and it usually decreases with increasing moisture content (Pei-yong and Chao, 2016). As noted in the discussion of Lutak Spur, it is possible for small amounts of moisture to result in an apparent strengthening of the soil, but there is a limit that varies depending on grain size and soil composition, and past this limit the soil will fail. Four of the 10 measured landslides in table 3 had overall slope angles that were either equal to or exceeded the average maximum internal friction value for the type of soil present. This suggests that failure of some of the slopes observed can be attributed to slope angle.

Given that a majority of the landslides scoured to bedrock to some extent, and that the slope angles of undisturbed slopes tend to match the measured slope angle of the slide areas, we hypothesize that the high slope angles indicate the slope angle of the underlying bedrock surface. This means that, under normal conditions, the soil is already sitting at an angle close to or at its angle of internal friction. Other factors, such as the presence of vegetation, are keeping the soil in place; anything that disturbs this delicate equilibrium (e.g., high intensity rainfall, vegetation removal, etc.) results in slope failure.

Role of vegetation in slope stability

Vegetation plays an important role in keeping soil in place on steep slopes. A study by the U.S. Forest Service reported that not only do plant roots provide mechanical reinforcement, but they also modify soil moisture distribution as well as pore water pressure (Ziemer, 1981). For most sites that we investigated, it was clear that the soil above the head scarp was held in place by the root systems of trees. When the trees are undercut by slope failure, or are knocked over by other trees or wind, the root systems are torn out of the ground, removing the stabilizing element as well as exposing the less stable underlying soils. This layer is then easily eroded, which can exacerbate the failure, as we saw at sites 9 and 25, for example.

Windthrow, also known as wind snap, is a phenomenon that occurs when applied force during a storm event overcomes the anchorage of a tree or the strength of the trunk; the tree can either

snap or be overturned, the latter of which is more common in areas where roots are limited vertically or in saturated soils (Quine and others, 2021). Fallen trees can impact other trees either directly by knocking them down, or indirectly by creating a gap in the canopy for further wind infiltration and damage, creating a domino effect that exists for the storm duration (Quine and others, 2021). At station HAXA2, wind speed is measured every 10 minutes over the course of 24 hours. Analysis of wind speed and wind gust data from this station (NOAA, 2020) for the duration of the storm event (Nov. 30 to Dec. 2) revealed that the average wind speed was 3.6 m/s (8.1 mph), with average gusts of 7.9 m/s (17.7 mph). On December 2, a maximum wind speed gust of 15 m/s (33 mph) was recorded. For comparison, the average hourly wind speed for the windy season in Haines (from October to April) is approximately 2.8 m/s (6.3 mph) (Weather Spark, 2023). While the wind speeds were just above average, we hypothesize that the significant gusts were responsible for some of the windthrow observed after the storm, as sustained wind speeds and gusts, combined with high intensity rainfall, create conditions that are optimal for windthrow to occur (Negrone-Juarez and others, 2023). With that said, there is no way to distinguish which landslides may have been initiated by windthrow or if the fallen trees were the result of the landslides.

POTENTIAL ANTHROPOGENIC INFLUENCES

In addition to the previously-mentioned naturally-occurring factors, anthropogenic factors such as vegetation removal and modification of slopes also can contribute to landslide occurrence. Along Lutak Road, sites 14 through 22 are located within a clear-cut that was logged in the 1990s (Palmieri, pers. comm., 2021). This approximately 800-m stretch had the most landslides of any section along Lutak Road with nine total: two debris slides and seven debris flows. Lidar data and site investigations indicated that the head scarps of sites 16 and 17 were on the edge of the logging roads (and even took part of the roads with them). The head scarp of site 17 contained a culvert outlet from the logging road, which may have concentrated additional water to the land below and contributed to the landslide. Many scarps are visible in the lidar directly below the logging roads, suggesting a correlation between landslides and the construction of logging roads or clear-cutting. Additionally, the source areas for the debris flows in the clear-cut appear to be wider than surrounding debris flow channels. The average width of debris channels at their origins is about 20 m, but channels at sites 18 and 19 have widths of approximately 95 m and 48 m, respectively. As previously mentioned, vegetation plays a role in the stability of a slope, and the removal of vegetation disrupts the established equilibrium and

creates conditions in which landslides are more likely to occur (Ziemer, 1981; Highland and Bobrowsky, 2008; Hungr and others, 2014).

Examples of slope modifications that cause instability are oversteepening and removing the toe of the slope. Given the mountainous environment of the study area, it is difficult to locate areas for structures that are not at the base of slopes. The section of Lutak Road that comprises sites 31 through 36 is a prime example of slope failures as a result of toe removal, likely during the construction of Lutak Road and the associated easements. The removal of the toe of a slope reduces the buttressing forces that act against gravity, resulting in slope failure (AK&K, 2016). All four of the debris slides in this section had L/W ratios below 1.0, and failed directly adjacent to the road. These failures, examples of which can be seen in figures 80, 88, and 90, were shallow, but the remaining slope faces are steeper than the angle of internal friction typical for these soils. From these observations, we hypothesize that a stabilizing factor, such as vegetation or the toe of the slope, was removed, eventually resulting in failure. Sites 34–36 were vegetated with shrubby vegetation instead of the larger spruce and hemlock trees that were observed on the other slopes.

EVIDENCE OF PREVIOUS LANDSLIDES

The lidar data contain extensive evidence of previous landslide events throughout the study area. Arcuate shapes form scalloped edges that line most cliffs and ridges, and the concave rupture surfaces of landslides are visible adjacent to new failures from the December 2020 events. It is known that landslides often occur repeatedly in the same area, and that just because a slope fails once, there is no guarantee that it will not fail again (Mirus and others, 2017; Guo and others, 2020). In this section, we focus on two areas: Cunningham Creek and Lutak Spur. Both of these locations demonstrate evidence of previous landslides.

Cunningham Creek

The catchment that feeds Cunningham Creek near Piedad Road is lined by dozens of scarps, suggesting a tumultuous history. We observed geomorphologic evidence, both in the field and in lidar data, of previous landslide events in the form of scarp scars (fig. 146). During our field investigation of this channel we observed what appeared to be two potential debris flow deposits in the channel bank. Each of the 0.5–1-m thick debris flow deposits buried an organic layer containing roots, which we interpreted as buried organic mats of paleosurfaces (fig. 135b).

One of our objectives for investigating Cunningham Creek was to determine if another significant storm event could result in more material coming down the channel and into the residential areas below. Interpretation of the lidar data indicates that the creek bed is wide (~9 m) with a relatively flat bottom. Our field observations indicate that soil and debris has filled in the creek bed to form the flat bottom, which suggests that more debris is available to be released in another 2020-magnitude storm event.

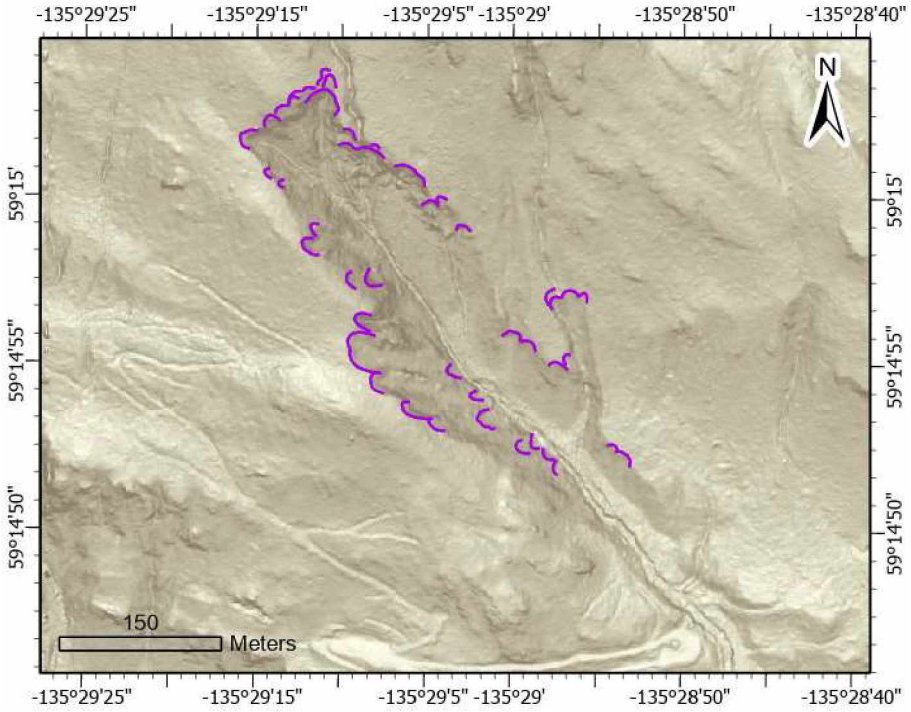

Figure 146. Scarps (purple) visible in the catchment area of Cunningham Creek, site 56. Slope map derived from 2020 lidar (Daanen and others, 2021)

Lutak Spur

Lutak Spur also demonstrates evidence of previous landslides. Arcuate shapes are visible along most of the bluff edge, at the bottom of which many residents have built structures (fig. 147). Lidar mapping indicates nested scarps, providing evidence for repeated slope failures.

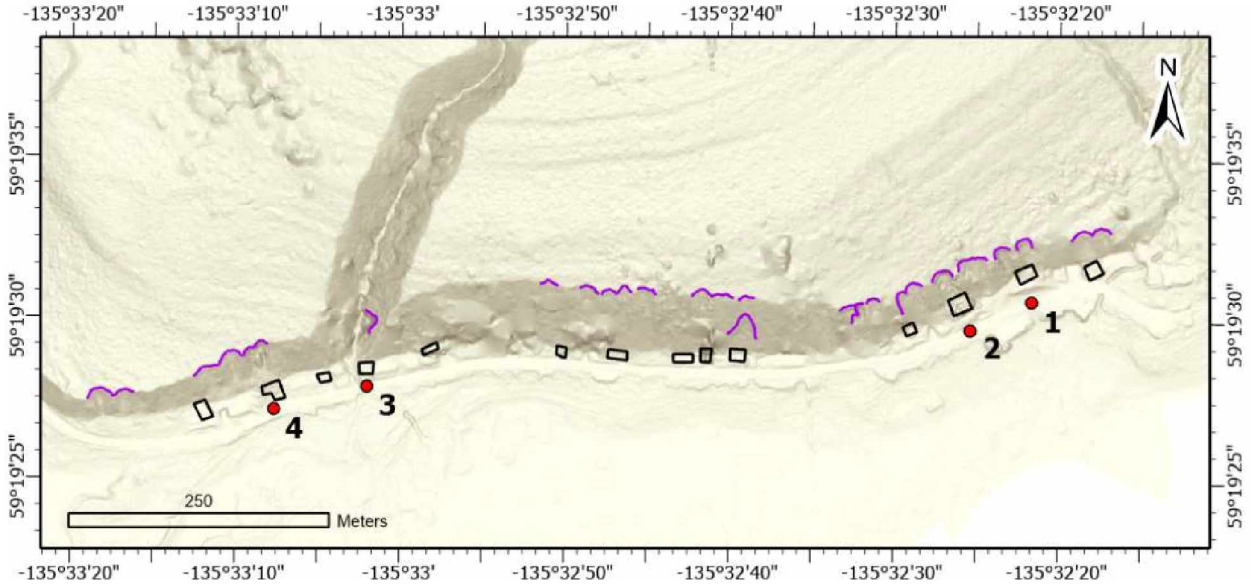

Figure 147. Scarps (purple) visible along the slopes of Lutak Spur. Figure includes locations of sites 1 through 4. Approximate locations of structures are outlined in black. Slope map derived from 2020 lidar (Daanen and others, 2021).

CHAPTER 6: CONCLUSIONS

The question we are seeking to answer with this report is: "What factors contributed to the widespread landslides near Haines, Alaska in December 2020?" To answer this question, we used existing literature that detailed the geologic history of the region, studied the severity of the December 2020 AR, collected samples and field observations during two field campaigns in 2021 and 2022, and mapped scarps and landslide extents using available lidar data. We conducted engineering index property tests on the collected samples, and compiled the results along with field observations and other relevant information provided by ADOT&PF and Haines residents into a landslide catalog with 58 entries, which correspond to affected areas. This catalog is intended for publication by the Alaska Division of Geological & Geophysical Surveys in partial fulfillment of the FEMA CTP Grant "Landslide Resiliency Project for Haines, Alaska," and the mapped scarps and landslide extents in the catalog will be included as part of a landslide inventory map of the study area and its surroundings.

Analysis of the collected data suggests that the most significant factor that contributed to the December 2020 landslides was the amount and intensity of precipitation. This precipitation exacerbated the preexisting condition of high slope angles in the surrounding areas, and resulted in excess pore pressure in soil types that usually drain well. Anthropogenic factors, such as removal of vegetation and excavating the toe of the slope, likely also played a role in the distribution of the landslides, especially along Lutak Road. My purpose in addressing these contributing factors is to raise awareness of what they are and how they are distributed in the Haines area. The 2020 landslides were not slow-moving, but rather fast, weather-triggered events. Mitigating such landslides is difficult; the best recommendations are to be aware of the potential for landslides and to understand their triggering mechanisms.

Based on the results of this research, we recommend future studies that could both provide additional insight into the December 2020 events and assist in preparation for potential future storm events. Dating the mapped landslides will determine the frequency of landsliding in the area; radiometric dating (Cosmic Ray Exposure) can be used for areas with bedrock exposures, and dendrochronology techniques can be used for timescales on the order of a few centuries (Pánek 2014). By obtaining dates for past landslides, we can determine the landslide frequency in the area. Landslide frequency could be linked with historical weather data to determine if rainfall is a common trigger for landslides. This type of information can be helpful in preparing the community in case of another high-intensity rainfall event, as it can determine potential

areas of higher risk that could be prioritized for emergency response and evacuation, both of which can help to prevent loss of life. Analysis of the weather data in the days after the storm indicates a lack of reliable data-collecting stations. With only a few stations located in the area, it is difficult to determine any localized effects of the storm due to the geomorphology of the area. For example, Lutak Road had the greatest landslide distribution of all the observed areas; the area is geomorphologically similar to the Haines Highway, which had fewer landslides despite being considered a long-term problem area by ADOT&PF. One of the few differences that could have affected the distribution of slope failures is localized higher intensity precipitation and/or wind; spatial correlations between rainfall intensity and landslide density have been observed (Hungr and others, 2014). Additionally, data from additional weather stations in areas such as Lutak Spur, Lutak Road, and Riley Ridge can be useful for real-time reporting as extreme weather events happen, and for studying their aftermaths. Future researchers also could gather strength data for both soil and bedrock from multiple failure areas to expand on the results presented here. Ideally, this would include *in situ* strength tests conducted on coarse-grained soils.

REFERENCES

Abdulkareem, S.W., 2019, The effects of water on the shear strength behavior of ground soil: Teesside University, MS Thesis.

Alan Kropp and Associates, Inc. (AK&K), 2016, Temporary slope protection method for shallow or surficial failures. https://www.akropp.com/wp-content/uploads/2013/06/Temporary-Slope-Protection-Method-original-2016-1.pdf

Alaska Department of Natural Resources (ADNR), 2020, AK RGB High Resolution Imagery (50cm) Accessed via ArcGIS Pro Basemaps tool. https://www.arcgis.com/home/item.html?id=13dd1ccf165845eea5db36465e7d565c

Alaska Department of Transportation and Public Facilities (ADOT&PF), 2020, Southcoast Region Emergency Response Database.

———2023, Alaska DOT&PF Roadway Data, Accessed via the Transportation Geographic Information Section map portal. https://dot.alaska.gov/stwddes/gis/

Alaska Division of Community and Regional Affairs (ADCRA), 2021, Open Data Portal, Alaska Department of Commerce, Community, and Economic Development. https://dcra-cdo-dcced.opendata.arcgis.com/ [accessed September 22 2022]

American Geosciences Institute (AGI), 2023, Landslides (website): American Geosciences Institute. https://www.americangeosciences.org/critical-issues/landslides

American Society for Testing and Materials (ASTM), 2014, D854-14: Standard Test Methods for Specific Gravity of Soil Solids by Water Pycnometer: ASTM International, West Conshohocken, PA.

———2017a, D2487-17e1: Standard Practice for Classification of Soils for Engineering Purposes (Unified Soil Classification System): ASTM International, West Conshohocken, PA.

———2017b, D5731-16: Standard Test Methods for Determination of the Point Load Strength Index of Rock and Applications to Rock Strength Classifications: ASTM International, West Conshohocken, PA.

———2017c, D4318-17e1: Standard Test Methods for Liquid Limit, Plastic Limit, and Plasticity Index of Soils: ASTM International, West Conshohocken, PA.

———2017d, D6913M-17: Standard Test Methods for Particle-Size Distribution (Gradation) of Soils Using Sieve Analysis: ASTM International, West Conshohocken, PA.

———2018, D2573M-18: Standard Test Method for Field Vane Shear Test in Saturated Fine-Grained Soils: ASTM International, West Conshohocken, PA.

———2019, D2216-19: Standard Test Methods for Laboratory Determination of Water (Moisture) Content of Soil and Rock by Mass: ASTM International, West Conshohocken, PA.

———2020, D2974-20e1: Standard Test Methods for Determining the Water (Moisture) Content, Ash Content, and Organic Material of Peat and Other Organic Soils: ASTM International, West Conshohocken, PA.

———2021b, D7928-21:Standard Test Method for Particle-Size Distribution (Gradation) of Fine-Grained Soils Using the Sedimentation (Hydrometer) Analysis: ASTM International, West Conshohocken, PA.

Baichtal, J.F., Lesnek, A.J., Carlson, R.J., Schmuck, N.S., Smith, J.L., Landwehr, D.J., and Briner, J.P, 2021, Late Pleistocene and early Holocene sea-level history and glacial retreat interpreted from shell-bearing marine deposits of southeastern Alaska, USA: Geosphere, v. 17, no. 6, p. 1,590-1,615. https://doi.org/10.1130/GES02359.1

Bowles, J.E., 1984. Physical and Geotechnical Properties of Soils: New York City, New York, McGraw-Hill, Inc., 578 p.

Brew, D.A., and Ford, A.B., 1994, The Coast Mountains Plutonic-Metamorphic Complex and Related Rocks between Haines, Alaska, and Fraser, British Columbia – Tectonic and Geologic Sketches and Klondike Highway Road Log: United States Geological Survey Open-file Report 97-268, 25 p. https://doi.org/10.3133/ofr94268

Brothers, D.S., Elliott, J.L., Conrad, J.E., Haeussler, P.J., and Kluesner, J.W, 2018, Strain partitioning in Southeastern Alaska: Is the Chatham Strait Fault active?: Earth and Planetary Science Letters, v. 481, p. 362-371. https://doi.org/10.1016/j.epsl.2017.10.017

Çellek, S., 2020, Effect of the slope angle and its classification on landslide (preprint): Natural Hazards and Earth System Sciences. https://doi.org/10.5194/nhess-2020-87

Charan, R., 2020, Why is the normal distribution so normal?: Towards Data Science, June 14, 2020. https://towardsdatascience.com/why-is-the-normal-distribution-so-normal-e644b0a50587

Clayton, K., 2020, 2020: Pandemic, natural disaster and upheaval: Chilkat Valley News, December 24, 2020. https://www.chilkatvalleynews.com/story/2020/12/24/news/2020-pandemic-natural-disaster-and-upheaval/14494.html

Coduto, D.P., 1999, Geotechnical Engineering: Principles and Practices (1st Ed.): Upper Saddle River, New Jersey, Prentice Hall.

Coduto, D.P., Kitch, W.A., Yeung, M.R., 2016, Foundation Design: Principles and Practices (3rd Ed.): Upper Saddle River, New Jersey, Pearson.

Cravens, C., 2021, Atmospheric River Impacts Southeast Alaska (ArcGIS storymap): National Weather Service. [accessed January 30 2023] https://storymaps.arcgis.com/stories/8d7a98b9dd514ff199f1e8c5b4d20a8b

Daanen, R.P., Herbst, A.M., Wikstrom Jones, Katreen, and Wolken, G.J., 2021, High-resolution lidar data for Haines, Southcentral Alaska, December 8–12, 2020: Alaska Division of Geological and Geophysical Surveys Raw Data File 2021-4, 8 p. https://doi.org/10.14509/30595

Darrow, M.M., Nelson, V.A., Grilliot, Michael, Wartman, Joseph, Jacobs, Aaron, Baichtal, J.F., Buxton, Cindy, 2022, Geomorphology and initiation mechanisms of the 2020 Haines, Alaska landslide: Landslides, v. 19, p. 2,177-2,188. https://doi.org/10.1007/s10346-022-01899-3

Davis, A., and Plafker, G., 1985, Comparative geochemistry and petrology of Triassic basaltic rocks from the Taku terrane on the Chilkat Peninsula and Wrangellia: Canadian Journal of Earth Science, v. 22, p. 183-194. https://doi.org/10.1139/e85-016

Davison, L., 2000, Basic mechanics of soils: University of the West of England, Bristol. http://environment.uwe.ac.uk/geocal/soilmech/basic/soilbasi.htm

Earle, S., 2015, Physical Geology: Victoria, British Columbia, BCcampus. https://opentextbc.ca/physicalgeology2ed/

Evans, S.G., and Clague, J.J, 1999, Rock avalanches on glaciers in the Coast and St. Elias Mountains, British Columbia: Proceedings of the 13th Annual Vancouver Geotechnical Society Symposium, 28 May 1999, p. 115-123.

Guo, C., Montgomery, D.R., Zhang, Y., Zhong, N., Fn, C., Wu, R., Yang, Z., Ding, Y., Jin, J., and Yanm, Y, 2020, Evidence for repeated failure of the giant Yigong landslide on the edge of the Tibetan Plateau: Scientific Reports, v. 10, no. 1, p. 14371. https://doi.org/10.1038/s41598-020-71335-w

Highland, L.M., Bobrowsky, P., 2008, The landslide handbook—A guide to understanding landslides: Reston, Virginia, U.S. Geological Survey Circular 1325, 129 p.

Hungr, O., Evans, S.G., Bovis, M.J., Hutchinson, J.N, 2001, A review of the classifications of landslides of the flow type: Environmental and Engineering Geoscience, v. 7, no. 3, p. 221-238. http://dx.doi.org/10.2113/gseegeosci.7.3.221

Hungr, O., Leroueil, S., Picarelli, L., 2014, The Varnes classification of landslide types, an update: Landslides, v. 11, p. 167-194. https://doi.org/10.1007/s10346-013-0436-y

Jackson, S.T., Rafferty, J.P, 2023, Little Ice Age: Encyclopedia Britannica, March 3, 2023. https://www.britannica.com/science/Little-Ice-Age

Jacobs, A., Holloway, E., Dixon, A., 2016, Atmospheric rivers in Alaska—Yes they do exist, and are usually ties to the biggest and most damaging rain-generated floods in Alaska (poster): Center for Western Weather and Water Extremes International Atmospheric Rivers Conference August 8-11, La Jolla, CA.

Lambe, T.W., and Whitman, R.V., 1969, Soil Mechanics, SI Version: New York, NY, John Wiley and Sons.

Larsen, C.F., Motyka, R.J., Freymuller, J.T., Echelmeyer, K.A., and Ivins, E.R, 2005, Rapid viscoelastic uplift in southeast Alaska caused by post-Little Ice Age glacial retreat: Earth

and Planetary Science Letters, v. 237, no. 3-4, p. 548-560. https://doi.org/10.1016/j.epsl.2005.06.032

Lemke, R.W., and Yehle, L.A., 1972, Reconnaissance engineering geology of the Haines area, Alaska, with emphasis on evaluation of earthquake and other geologic hazards: U.S. Geological Survey Open-File Report 72-229, 109 p., 2 sheets, scale 1:24,000.

Lesnek, A.J., Briner, J.P., Baichtal, J.F., and Lyles, A.S, 2020, New constraints on the last deglaciation of the Cordilleran Ice Sheet in coastal Southeast Alaska: Quaternary Research, v. 96, p. 140-160. https://doi.org/10.1017/qua.2020.32

Mirus, B.B., Smith, J.B., and Baum, R.L, 2017, Hydrologic impacts of landslide disturbances: Implications for remobilization and hazard persistence: Water Resources Research, v. 53, no. 10, p. 8250-8265. https://doi.org/10.1002/2017WR020842

Motyka, R.J., Larsen, C.F., Freymueller, J.T., and Echelmeyer, K.A, 2007, Post Little Ice Age rebound in the Glacier Bay Region, *in* Piatt, J.F. and Gende, S.M., eds., Proceedings of the Fourth Glacier Bay Science Symposium, October 26-28, 2004: US Geological Survey Scientific Investigations Report 2007-5047, 57-59.

Mundhenk, B.D., Barnes, E.A., and Maloney, E.D, 2016a, All-season climatology and variability of atmospheric river frequencies over the North Pacific: Journal of Climate, v. 29, no. 13, p. 4,885-4,903. https://doi.org/10.1175/JCLI-D-15-0655.1

Mundhenk, B.D., Barnes, E.A., Maloney, E.D., and Nardi, K.M, 2016b, Modulation of atmospheric rivers near Alaska and the U.S. West Coast by northeast Pacific height anomalies: Journal of Geophysical Research*:* Atmospheres, v. 121, no. 21, p. 12,751-12,765. https://doi.org/10.1002/2016JD025350

National Oceanic and Atmospheric Administration (NOAA), 2020, National Data Buoy Center station data: National Oceanic and Atmospheric Administration. https://www.ndbc.noaa.gov/station_page.php?station=haxa2. [accessed March 14 2023]

———2023a, What are atmospheric rivers?: National Oceanic and Atmospheric Administration. https://www.noaa.gov/stories/what-are-atmospheric-rivers [accessed March 22 2023]

———2023b, What are *El Niño* and *La Niña*?: National Ocean Service. https://oceanservice.noaa.gov/facts/ninonina.html. [accessed March 11 2023]

National Weather Service (NWS), 2023a, Hydrometeorological design studies center precipitation frequency data server (PFDS): National Oceanic and Atmospheric Administration. https://hdsc.nws.noaa.gov/hdsc/pfds/pfds_map_ak.html [accessed November 14 2021]

———2023b, NOWData – NOAA Online Weather Data: National Oceanic and Atmospheric Administration. https://www.weather.gov/arh/climate?wfo=ajk. [accessed November 14 2021]

Naval Facilities Engineering Command (NAVFAC), 1986, Soil Mechanics – Design Manual 7.01: Alexandria, Virginia, Naval Facilities Engineering Command

Negrone-Juarez, R., Magnabosco-Marra, D., Feng, Y., Urquiza-Muñoz, J.D., Riley, W.J., Chambers, J.Q., 2023, Windthrow characteristics and their regional associations with rainfall, soil, and surface elevation in the Amazon: Environmental Research Letters, v. 18, no. 1, 12 p. https://doi.org/10.1088/1748-9326/acaf10

Nelson, V., 2022, Mapping and Categorizing Landslides Around Haines, Alaska (abstract): 65th Annual Meeting, Association of Environmental and Engineering Geologists Las Vegas, NV, p. 86. https://www.aegweb.org/aeg-news-2

Orris, G.J., and J.W. Williams, 1984, Landslide length-width ratios as an aid in landslide identification and verification: Bulletin of the Association of Engineering Geologists, v. 21, no. 3, p. 371-375. https://doi.org/10.2113/gseegeosci.xxi.3.371

Pánek, T., 2014, Recent progress in landslide dating: A global overview: Progress in Physical Geography, v. 39, no. 2, p. 168-198. https://doi.org/10.1177/0309133314550671

Parry, S., 2011, The application of geomorphological mapping in the assessment of landslide hazard in Hong Kong, in Smith, M.J., Paron, Paolo, Griffiths, J.S., Developments in Earth Surface Processes: Elsevier, v. 15, p. 413-441. https://doi.org/10.1016/B978-0-444-53446-0.00015-X

Pei-yong, L.,and G. Chao, 2016, Shear strength of unsaturated sands: Electronic Journal of Geotechnical Engineering, v. 21, no. 10, p. 3,857-3,864.

Quine, C.P., Gardiner, B.A., and Moore, J., 2021, Wind disturbance in forests: The process of wind created gaps, tree overturning, and stem breakage, *in* , Johnson, E.A. and Miyanushi, Kiyoko, eds., Plant Distrubance Ecology, 2nd Ed: Academic Press, p. 117-184. https://doi.org/10.1016/B978-0-12-818813-2.00004-6

Ralph, M., and Jacobs, A., 2019, What is an atmospheric river (AR)? How do Alaska forecasters monitor these impactful events? (presentation): Alaska Center for Climate Assessment and Policy Virtual Alaska Weather Symposium, August 21, 2019.

Sassa, K., 1985, The mechanism of debris flows, *In*: Proceedings, 11th International Conference on Soil Mechanics and Foundation Engineering, San Francisco, v. 1, p.1173–1176

Scalia, J., 2022, Sandcastle Engineering: A geotechnical engineer explains how water, air, and sand create solid structures: Scientific American, August 23, 2022. https://www.scientificamerican.com/article/sandcastle-engineering-a-geotechnical-engineer-explains-how-water-air-and-sand-create-solid-structures/ [accessed February 15 2023]

Slaughter, S.L., Burns, W.J., Mickelson, K.A., Jacobacci, K.E., Biel, A., Contreras, T.A, 2017, Protocol for Landslide Inventory Mapping from Lidar Data in Washington State: Washington Geological Survey Bulletin 82, 27 p. http://www.dnr.wa.gov/Publications/ger_b82_landslide_inventory_mapping_protocol.zip

State of Alaska (SOA) (2020), Declaration of Disaster Emergency, Office of the Governor, Juneau, Alaska.

———continuously updated, State of Alaska Open Data Geoportal. https://gis.data.alaska.gov/ [accessed February 1 2023]

Sun, L., Zhou, J.L., Cai, Q., Liu, S., Xiao, J., 2021, Comparing surface erosion processes in four soils from the Loess Plateau under extreme rainfall events: International Soil and Water Conservation Research, v. 9, no. 4, p. 520-531. https://doi.org/10.1016/j.iswcr.2021.06.008

Taylor, F.E., Malamud, B.D., Witt, A., and Guzzetti, F., 2018, Landslide shape, ellipticity and length-to-width ratios: Earth Surface Processes and Landforms, v. 43, no. 15, p. 3164-3189. https://doi.org/10.1002/esp.4479

Terzaghi, K., and R.B Peck., 1948, Soil Mechanics in Engineering Practice: Hoboken, New Jersey, John Wiley & Sons.

Thornbury, W.D., 1954, Principles of Geomorphology: Hoboken, New Jersey, John Wiley & Sons.

United States Census Bureau, 2022, QuickFacts: Haines Borough, Alaska. https://www.census.gov/quickfacts/hainesboroughalaska [accessed February 15 2023]

Waldholz, R., and Woosley, R., 2015, Update: missing 3 presumed dead in Sitka landslide, Walker to visit: KTOO Public Media, August 18, 2015. https://www.ktoo.org/2015/08/18/gov-walker-visit-sitka-devastating-landslides/

Weather Spark, 2023: Climate and average weather year round in Haines, Alaska, United States. https://weatherspark.com/y/286/Average-Weather-in-Haines-Alaska-United-States-Year-Round#:~:text=The%20windier%20part%20of%20the,of%208.4%20miles%20per%20hour. [accessed March 23 2023]

Zechmann, J., in press, High-resolution lidar data for Haines, Southcentral Alaska, 24 October 2021-4 October 2022: Alaska Division of Geological and Geophysical Surveys Raw Data File.

Ziemer, R.R., 1981, The role of vegetation in the stability of forested slopes, Proceedings of the International Union of Forestry Research Organizations, XVII World Congress, 6-17 September 1981, Kyoto, Japan, v. 1, p. 297-308.

APPENDIX A: 2021 SEVEN COLUMN SHEETS

PROJECT NAME: Haines, AK Landslide DECEMBER 2020
LOCATION: Haines Borough, AK
SAMPLED BY: V. Nelson, M. Darrow
DATE: 6/16/2021 - 6/26/2021

SAMPLE NO.		21-01	21-02	21-03	21-04	21-05	21-06	21-07
UTM COORDINATES		Z8 476236 6564663	Z8 476236 6564663	Z8 468559 6576320	Z8 468559 6576320	Z8 472268 6572107	Z8 472268 6572107	Z8 469757 6573833
BAG OR TIN		BAG	TIN	TIN	BAG	TIN	BAG	TIN
DATE SAMPLED		6/17/21	6/17/21	6/17/21	6/17/21	6/18/21	6/18/21	6/21/21
% Passing	2"	100			100		100	
	1.5"	100			100		100	
	1"	97			96		100	
Gravel	3/4"	96			87		100	
	1/2"	92			85		97	
	3/8"	89			82		95	
	#4	81			76		90	
	#10	68			68		79	
	#20	53			53		66	
Sand	#40	38			30		58	
	#60	26			15		49	
	#100	17			6		41	
Silt/Clay	#200	9.4			1.5		30.6	
	0.02	3.9					15.2	
Hydro	0.005	1.5					6.1	
	0.002	1.0					4.2	
LIQUID LIMIT		NV					24.1	
PLASTIC INDEX		NP					5.1	
SOIL CLASSIFICATION		SP-SM			SP		SC-SM	
SOIL DESCRIPTION		PG Sa w/ Si, Gr	PG Sa w/ Si, Gr	PG Sa w/ Gr	PG Sa w/ Gr	Si Cl Sa	Si Cl Sa	Si Cl Sa
NATURAL MOISTURE			24.98	5.55		12.36		16.48
ORGANICS			4.78			0.6		0.26
SP. GR. (FINE)							2.94	

PROJECT NAME:	Haines, AK Landslide DECEMBER 2020
LOCATION:	Haines Borough, AK
SAMPLED BY:	V. Nelson, M. Darrow
DATE:	6/16/2021 - 6/26/2021

SAMPLE NO.		21-08	21-09	21-10	21-11	21-12	21-13	21-14
UTM COORDINATES		Z8 469757 6573833	Z8 469702 6573889	Z8 469702 6573889	Z8 469239 6576407	Z8 469239 6576407	Z8 469236 6576369	Z8 469236 6576369
BAG OR TIN		BAG	BAG	TIN	BAG	TIN	TIN	BAG
DATE SAMPLED		6/21/21	6/21/21	6/21/21	6/21/21	6/21/21	6/21/21	6/21/21
% Passing	2"	100	100		100			100
	1.5"	92	97		100			100
	1"	85	97		100			100
Gravel	3/4"	81	92		100			100
	1/2"	80	87		99			100
	3/8"	76	86		98			96
	#4	69	83		96			91
	#10	63	78		93			82
	#20	56	70		88			62
Sand	#40	48	63		72			31
	#60	40	55		45			12
	#100	30	44		14			3
Silt/Clay	#200	17.5	25.4		1.7			0.8
	0.02	8.0	12.1					
Hydro	0.005	2.8	4.0					
	0.002	2.1	3.0					
LIQUID LIMIT		NV	21.9					
PLASTIC INDEX		NP	NP					
SOIL CLASSIFICATION		SM	SM		SP			SP
SOIL DESCRIPTION		Si Sa w/ Gr	Si Sa w/ Gr	Si Sa w/ Gr	PG Sa	PG Sa	PG Sa	PG Sa
NATURAL MOISTURE				14.25		8.01	4.71	
ORGANICS								
SP. GR. (FINE)		2.58	2.92					

PROJECT NAME: Haines, AK Landslide DECEMBER 2020
LOCATION: Haines Borough, AK
SAMPLED BY: V. Nelson, M. Darrow
DATE: 6/16/2021 - 6/26/2021

SAMPLE NO.		21-15	21-16	21-17	21-18	21-19	21-20	21-21
UTM COORDINATES		Z8 469285 6576400	Z8 469285 6576400	Z8 469299 6576410	Z8 469299 6576410	Z8 476504 6564421	Z8 476504 6564421	Z8 476504 6564421
BAG OR TIN		TIN	BAG	TIN	BAG	BAG	TIN	BAG
DATE SAMPLED		6/21/21	6/21/21	6/21/21	6/21/21	6/22/21	6/22/21	6/22/21
% Passing	2"		100		100	100		100
	1.5"		90		100	100		100
	1"		79		100	94		100
Gravel	3/4"		77		100	91		100
	1/2"		74		100	87		97
	3/8"		72		100	85		91
	#4		68		97	79		83
	#10		62		92	70		74
	#20		48		80	55		61
Sand	#40		25		53	43		49
	#60		9		20	36		41
	#100		3		4	30		34
Silt/Clay	#200		0.7		0.5	25.0		26.2
	0.02					10.7		15.1
Hydro	0.005					2.5		5.7
	0.002					1.7		3.6
LIQUID LIMIT						NV		NV
PLASTIC INDEX						NP		NP
SOIL CLASSIFICATION			SP		SP	SM		SM
SOIL DESCRIPTION		PG Sa w/ Gr	PG Sa w/ Gr	PG Sa	PG Sa	Si Sa w/ Gr	Si Sa w/ Gr	Si Sa w/ Gr
NATURAL MOISTURE		3.63		4.99			15.03	
ORGANICS								
SP. GR. (FINE)						2.99		3.17

PROJECT NAME: Haines, AK Landslide DECEMBER 2020
LOCATION: Haines Borough, AK
SAMPLED BY: V. Nelson, M. Darrow
DATE: 6/16/2021 - 6/26/2021

SAMPLE NO.		21-22	21-23	21-24	21-25	21-26	21-27	21-28
UTM COORDINATES		Z8 477324 6564623	Z8 477324 6564623	Z8 476465 6564956	Z8 476465 6564956	Z8 476520 6564920	Z8 476520 6564920	Z8 470968 6573056
BAG OR TIN		BAG	TIN	BAG	TIN	BAG	TIN	TIN
DATE SAMPLED		6/22/21	6/22/21	6/22/21	6/22/21	6/22/21	6/22/21	6/23/21
% Passing	2"	100		100		100		
	1.5"	89		80		100		
	1"	76		74		92		
Gravel	3/4"	64		73		84		
	1/2"	46		64		76		
	3/8"	40		62		71		
	#4	32		56		56		
	#10	25		46		39		
	#20	19		34		27		
Sand	#40	17		24		20		
	#60	15		18		14		
	#100	12		13		9		
Silt/Clay	#200	9.4		8.4		4.7		
	0.02	5.1		4.2		2.3		
Hydro	0.005	1.0		1.5		0.8		
	0.002	0.6		1.2		0.6		
LIQUID LIMIT		NV		NV		NV		
PLASTIC INDEX		NP		NP		NP		
SOIL CLASSIFICATION		GP-GM		SP-SM		SW		
SOIL DESCRIPTION		PG Gr w/ Si, Sa	PG Gr w/ Si, Sa	PG Sa w/ Si, Gr	PG Sa w/ Si, Gr	WG Sa w/ Gr	WG Sa w/ Gr	PG Gr w/ Sa
NATURAL MOISTURE			24.47		14.24		9.00	4.10
ORGANICS								
SP. GR. (FINE)		2.48		3.39		3.12		

PROJECT NAME: Haines, AK Landslide DECEMBER 2020
LOCATION: Haines Borough, AK
SAMPLED BY: V. Nelson, M. Darrow
DATE: 6/16/2021 - 6/26/2021

SAMPLE NO.		21-29	21-30	21-31	21-32	21-33	21-34	21-35
UTM COORDINATES		Z8 470968 6573056	Z8 475051 6566978	Z8 475051 6566978	Z8 475035 6566934	Z8 475035 6566934	Z8 474613 6569265	Z8 474613 6569265
BAG OR TIN		BAG	BAG	TIN	TIN	BAG	TIN	BAG
DATE SAMPLED		6/23/21	6/24/21	6/24/21	6/24/21	6/24/21	6/25/21	6/25/21
% Passing	2"	83	100			100		100
	1.5"	76	85			100		100
	1"	66	73			100		89
Gravel	3/4"	61	59			100		83
	1/2"	58	49			100		75
	3/8"	55	43			100		67
	#4	49	31			97		51
	#10	40	17			96		33
	#20	26	11			95		20
Sand	#40	13	8			93		12
	#60	5	6			91		9
	#100	2	4			87		6
Silt/Clay	#200	1.0	2.9			78.9		4.3
	0.02					56.9		2.2
Hydro	0.005					35.0		0.6
	0.002					22.5		0.3
LIQUID LIMIT						30.0		NV
PLASTIC INDEX						8.6		NP
SOIL CLASSIFICATION		GP	GW			CL		GW
SOIL DESCRIPTION		PG Gr w/ Sa	PG Gr w/ Sa	PG Gr w/ Sa	Cl w/ Sa	Cl w/ Sa	WG Gr w/ Sa	WG Gr w/ Sa
NATURAL MOISTURE				18.12	25.12		16.09	
ORGANICS				5.24	1.11			
SP. GR. (FINE)						2.62		2.75

PROJECT NAME:	Haines, AK Landslide DECEMBER 2020
LOCATION:	Haines Borough, AK
SAMPLED BY:	V. Nelson, M. Darrow
DATE:	6/16/2021 - 6/26/2021

SAMPLE NO.		21-36	21-37					
UTM COORDINATES		Z8 474104 6571216	Z8 474104 6571216					
BAG OR TIN		TIN	BAG					
DATE SAMPLED		6/25/21	6/25/21					
% Passing	2"		77					
	1.5"		74					
	1"		70					
Gravel	3/4"		66					
	1/2"		59					
	3/8"		54					
	#4		40					
	#10		23					
	#20		17					
Sand	#40		15					
	#60		12					
	#100		7					
Silt/Clay	#200		3.4					
	0.02							
Hydro	0.005							
	0.002							
LIQUID LIMIT								
PLASTIC INDEX								
SOIL CLASSIFICATION			GW					
SOIL DESCRIPTION		WG Gr w/ Sa	WG Gr w/ Sa					
NATURAL MOISTURE		6.48						
ORGANICS								
SP. GR. (FINE)								

APPENDIX B: 2022 SEVEN COLUMN SHEETS

PROJECT NAME: Haines, AK Landslide DECEMBER 2020
LOCATION: Haines Borough, AK
SAMPLED BY: V. Nelson, M. Darrow
DATE: 7/14/2022 - 7/27/2022

SAMPLE NO.		22-01	22-03	22-04	22-05	22-06	22-07	22-08
UTM COORDINATES		Z8 477139 6564419	Z8 477305 6564456	Z8 477443 6564417	Z8 473436 6571430	Z8 473436 6571430	Z8 473425 6571432	Z8 473425 6571432
BAG OR TIN		BAG	BAG	BAG	BAG	TIN	BAG	TIN
DATE SAMPLED		7/17/22	7/17/22	7/17/22	7/19/22	7/19/22	7/19/22	7/19/22
% Passing	2"	100	100	100	100		100	
	1.5"	100	100	100	100		94	
	1"	100	100	100	95		91	
Gravel	3/4"	98	100	100	91		86	
	1/2"	95	100	100	86		77	
	3/8"	93	100	100	78		71	
	#4	89	100	95	67		55	
	#10	78	99	89	56		39	
	#20	60	95	84	48		27	
Sand	#40	45	85	75	44		17	
	#60	35	71	64	40		12	
	#100	25	49	61	28		9	
Silt/Clay	#200	13.7	32.6	47.7	14.8		7.0	
	0.02	2.1	19.0	32.6	4.5		2.9	
Hydro	0.005	0.5	4.7	9.2	1.7		1.0	
	0.002	0.3	2.5	6.1	0.8		0.7	
LIQUID LIMIT		NV	NV	NV	NV			
PLASTIC INDEX		NP	NP	NP	NP			
SOIL CLASSIFICATION		SM	SM	SM	SM		SW-SM	
SOIL DESCRIPTION		Si Sa	Si Sa	Si Sa	Si Sa w/ Gr	Si Sa w/ Gr	WG Sa w/ Si, Gr	WG Sa w/ Si, Gr
NATURAL MOISTURE						13.22		8.04
ORGANICS								
SP. GR. (FINE)		3.20	2.80	2.41	3.24		2.93	

PROJECT NAME: Haines, AK Landslide DECEMBER 2020
LOCATION: Haines Borough, AK
SAMPLED BY: V. Nelson, M. Darrow
DATE: 7/14/2022 - 7/27/2022

SAMPLE NO.		22-10	22-11	22-12	22-13	22-14	22-15	22-16
UTM COORDINATES		Z8 473615 6571175	Z8 473615 6571175	Z8 473225 6571144	Z8 473225 6571144	Z8 470857 6572525	Z8 470870 6572565	Z8 470870 6572565
BAG OR TIN		BAG	TIN	BAG	TIN	BAG	TIN	BAG
DATE SAMPLED		7/19/22	7/19/22	7/19/22	7/19/22	7/20/22	7/20/22	7/21/22
% Passing	2"	100		100		100		100
	1.5"	100		100		100		100
	1"	81		95		100		100
Gravel	3/4"	72		93		100		100
	1/2"	58		89		100		100
	3/8"	52		88		100		100
	#4	44		80		93		100
	#10	37		69		73		99
	#20	31		60		48		96
Sand	#40	27		47		28		90
	#60	20		38		16		72
	#100	13		29		10		53
Silt/Clay	#200	6.3		22.9		4.9		40.9
	0.02	1.4		4.9				16.0
Hydro	0.005	0.6		2.0				3.4
	0.002	0.4		2.0				2.9
LIQUID LIMIT								
PLASTIC INDEX								
SOIL CLASSIFICATION		GP-GM		SM		SP		SM
SOIL DESCRIPTION		PG Gr w/ Si, Sa	PG Gr w/ Si, Sa	Si Sa w/ Gr	Si Sa w/ Gr	PG Sa	Sa Si	Si Sa
NATURAL MOISTURE			23.68		35.95		8.45	
ORGANICS					5.61			
SP. GR. (FINE)		2.87		2.95				2.57

PROJECT NAME:	Haines, AK Landslide DECEMBER 2020
LOCATION:	Haines Borough, AK
SAMPLED BY:	V. Nelson, M. Darrow
DATE:	7/14/2022 - 7/27/2022

SAMPLE NO.		22-17	22-18	22-19	22-20	22-24	22-25	22-28A
UTM COORDINATES		Z8 477190 6564473	Z8 477181 6564453	Z8 477112 6564491	Z8 477112 6564491	Z8 477023 6564509	Z8 477387 6564667	Z8 474104 6571203
BAG OR TIN		BAG	TIN	BAG	TIN	TIN	BAG	BAG
DATE SAMPLED		7/21/22	7/21/22	7/21/22	7/21/22	7/21/22	7/21/22	7/22/22
% Passing	2"	100		72			86	100
	1.5"	84		67			82	100
	1"	70		54			45	100
Gravel	3/4"	68		51			28	100
	1/2"	63		46			14	100
	3/8"	62		44			12	100
	#4	61		40			10	100
	#10	58		35			8	100
	#20	51		26			7	99
Sand	#40	39		18			6	98
	#60	28		11			3	95
	#100	16		6			2	82
Silt/Clay	#200	6.7		2.8			1.6	70.1
	0.02	1.2						59.0
Hydro	0.005	0.3						37.3
	0.002	0.2						25.6
LIQUID LIMIT								34.4
PLASTIC INDEX								5.2
SOIL CLASSIFICATION		SP-SM		GP			GP	ML
SOIL DESCRIPTION		PG Sa w/ Si, Gr	PG Sa w/ Si, Gr	PG Gr w/ Sa	PG Gr w/ Sa	Sa Si	PG Gr	Si Sa
NATURAL MOISTURE			207.82		20.02			
ORGANICS			44.7		4.36	5.26		
SP. GR. (FINE)		3.11						2.82

PROJECT NAME: Haines, AK Landslide DECEMBER 2020
LOCATION: Haines Borough, AK
SAMPLED BY: V. Nelson, M. Darrow
DATE: 7/14/2022 - 7/27/2022

SAMPLE NO.		22-28B	22-28C	22-29	22-30	22-31	22-32	22-33
UTM COORDINATES		Z8 474104 6571203	Z8 474104 6571203	Z8 468662 6576363	Z8 468662 6576363	Z8 468662 6576363	Z8 468662 6576363	Z8 468662 6576363
BAG OR TIN		TIN	TIN	BAG	BAG	BAG	TIN	TIN
DATE SAMPLED		7/22/22	7/22/22	7/22/22	7/22/22	7/22/22	7/22/22	7/22/22
% Passing	2"			100	100	100		
	1.5"			100	100	100		
	1"			100	100	100		
Gravel	3/4"			100	100	100		
	1/2"			100	100	100		
	3/8"			97	96	98		
	#4			93	93	95		
	#10			87	89	91		
	#20			68	80	79		
Sand	#40			30	51	56		
	#60			8	21	32		
	#100			1	7	12		
Silt/Clay	#200			0.3	1.9	2.8		
	0.02							
Hydro	0.005							
	0.002							
LIQUID LIMIT								
PLASTIC INDEX								
SOIL CLASSIFICATION				SP	SP	SP		
SOIL DESCRIPTION		Si Sa	Si Sa	PG Sa	PG Sa	PG Sa	PG Sa	PG Sa
NATURAL MOISTURE		31.25	23.93				0.92	6.64
ORGANICS								
SP. GR. (FINE)								

PROJECT NAME: Haines, AK Landslide DECEMBER 2020
LOCATION: Haines Borough, AK
SAMPLED BY: V. Nelson, M. Darrow
DATE: 7/14/2022 - 7/27/2022

SAMPLE NO.		22-34	22-35	22-36	22-39	22-42	22-43	22-44
UTM COORDINATES		Z8 468662 6576363	Z8 468662 6576363	Z8 468662 6576363	Z8 476170 6562876	Z8 475647 6562919	Z8 475647 6562919	Z8 469465 6574158
BAG OR TIN		BAG	BAG	BAG	BAG	TIN	TIN	BAG
DATE SAMPLED		7/22/22	7/22/22	7/22/22	7/23/22	7/23/22	7/23/22	7/25/22
% Passing	2"	100	100	100	100			83
	1.5"	100	100	90	100			71
	1"	97	100	82	86			61
Gravel	3/4"	94	98	76	75			55
	1/2"	89	96	71	57			47
	3/8"	88	94	69	49			41
	#4	85	92	66	35			33
	#10	78	85	61	25			26
	#20	58	68	47	16			17
Sand	#40	30	46	26	12			10
	#60	14	28	10	9			6
	#100	4	11	3	8			4
Silt/Clay	#200	1.0	2.9	0.7	7.3			1.6
	0.02				2.9			
Hydro	0.005				0.7			
	0.002				0.5			
LIQUID LIMIT					NV			
PLASTIC INDEX					NP			
SOIL CLASSIFICATION		SP	SP	SP	GW-GM			GW
SOIL DESCRIPTION		PG Sa	PG Sa	PG Sa w/ Gr	WG Gr w/ Si, Sa			WG Gr w/ Sa
NATURAL MOISTURE								
ORGANICS						18.02	17.67	
SP. GR. (FINE)					2.64			

PROJECT NAME:	Haines, AK Landslide DECEMBER 2020
LOCATION:	Haines Borough, AK
SAMPLED BY:	V. Nelson, M. Darrow
DATE:	7/14/2022 - 7/27/2022

SAMPLE NO.		22-45	22-46	22-47				
UTM COORDINATES		Z8 469465 6574158	Z8 476369 6573030	Z8 476369 6573030				
BAG OR TIN		TIN	BAG	TIN				
DATE SAMPLED		7/25/22	7/26/22	7/26/22				
% Passing	2"		95					
	1.5"		95					
	1"		90					
Gravel	3/4"		81					
	1/2"		72					
	3/8"		70					
	#4		65					
	#10		59					
	#20		49					
Sand	#40		36					
	#60		22					
	#100		11					
Silt/Clay	#200		4.5					
	0.02							
Hydro	0.005							
	0.002							
LIQUID LIMIT								
PLASTIC INDEX								
SOIL CLASSIFICATION			SP					
SOIL DESCRIPTION		WG Gr w/ Sa	PG Sa w/ Gr	PG Sa w/ Gr				
NATURAL MOISTURE		6.17		3.94				
ORGANICS				2.62				
SP. GR. (FINE)								